Biomaterials 258 (2020) 120297

Contents lists available at ScienceDirect

Biomaterials

journal homepage: www.elsevier.com/locate/biomaterials

Review

Nanomedicine progress in thrombolytic therapy

Alina Zenych, Louise Fournier, Cédric Chauvierre *

Université de Paris, Université Sorbonne Paris Nord, UMRS1148, INSERM, F-75018, Paris, France

ARTICLE INFO

Keywords:
Thrombolytics
Targeted thrombolysis
Thrombolytic therapy
Nanomedicine
Nanoparticles
Microbubbles

ABSTRACT

Thrombotic occlusions of blood vessels are responsible for life-threatening cardiovascular disorders such as myocardial infarction, ischemic stroke, and venous thromboembolism. Current thrombolytic therapy, the injection of Plasminogen Activators (PA), is yet limited by a narrow therapeutic window, rapid drug elimination, and risks of hemorrhagic complications. Nanomedicine-based vectorization of PA protects the drug from the enzymatic degradation, improves the therapeutic outcomes, and diminishes adverse effects in preclinical models. Herein, we review the pathophysiology of arterial and venous thrombosis and summarize clinically approved PA for the treatment of acute thrombotic diseases. We examine current challenges and perspectives in the recent key research on various (lipid, polymeric, inorganic, biological) targeted nanocarriers intended for the site-specific delivery of PA. Microbubbles and ultrasound-assisted sonothrombolysis that demonstrate thrombolysis enhancement in clinical trials are further discussed. Moreover, this review features strategies for the rational design of nanocarriers for targeted thrombolysis and effective PA encapsulation in view of interactions between nanomaterials and biological systems. Overall, nanomedicine represents a valued approach for the precise treatment of acute thrombotic pathologies.

1. Introduction

Cardiovascular diseases (CVD), the major global health threat, are associated with high morbidity and mortality that account for an estimated 17.9 million lives each year (31% of all deaths worldwide) [1], and this figure is expected to rise to >23.6 million annual deaths by 2030 [2]. CVD are a group of disorders of the heart (e.g., heart failure, rheumatic heart disease, abnormal heart rhythms, inflammatory heart diseases, cardiomyopathy) and blood vessels (coronary artery disease, cerebrovascular disease, aortic aneurysms, peripheral artery disease, etc.). CVD affect almost equally men as women, however, the disease develops about seven to ten years later in women as compared to men [3]. Furthermore, CVD are associated with substantial health-care costs, which are estimated at $329.7 billion annually in the United States [2] and nearly €200 billion in the European Union [4].

A large number of CVD may be prevented by addressing major risk factors through lifestyle interventions and pharmaceutical treatment where necessary [1]. Nevertheless, hypertension, the leading cardiovascular risk factor, is attributed to ~13% of global deaths (7.5 million deaths), followed by tobacco use 9%, diabetes 6%, physical inactivity 6%, obesity 5%, and high cholesterol level 4.5% [3].

Three major cardiovascular disorders – myocardial infarction (heart attack), ischemic stroke, and venous thromboembolism defined as deep vein thrombosis and/or pulmonary embolism – are severe complications of thrombosis, the formation of a blood clot in the vessels (Fig. 1). Within all deaths from CVD, 85% are caused by heart attacks and strokes, one-third of them in people under the age of 70 years [1]. To improve human survival and quality of life, early detections and effective treatments are principal.

Thrombolytic drugs are administered to dissolve a thrombus and restore the blood flow in acute thrombotic events, however, they are rapidly inactivated in the blood and trigger hemorrhagic complications, as we explain below. Paradoxically, while rapid reperfusion is the standard of care to minimize the infarct size, the restoration of blood flow itself may provoke irreversible tissue damage in a process called reperfusion injury [5]. Therefore, the pursuit of innovative solutions for the management of thrombotic diseases remains an open field of research, where nanomedicine is emerging to be a promising strategy to improve both the efficacy and safety of thrombolytic therapy.

This review delves into the preclinical research on nano- or microparticles of various composition for delivering fibrinolytic agents, reported during the last 10 years. Ultrasound (US)-responsive microbubbles with thrombolytics are highlighted as a potential theranostic system for both US visualization of the pathologic thrombi and

* Corresponding author.
E-mail address: cedric.chauvierre@inserm.fr (C. Chauvierre).

https://doi.org/10.1016/j.biomaterials.2020.120297
Received 22 January 2020; Received in revised form 10 July 2020; Accepted 1 August 2020
Available online 6 August 2020

their destruction by a combination of mechanical stress with increased penetration and drug potency.

The database searched included MEDLINE/PubMed and Science Direct for research articles published in English from 2010 to present, using the combinations of the keywords “nanomedicine”, “nanoparticles”, “microbubbles”, “liposomes”, “streptokinase”, “urokinase”, “tissue plasminogen activator”, “nanothrombolysis”, “thrombolytic therapy”, “drug delivery systems”, “thrombolysis”, “targeted thrombolysis”, etc.

1.1. Pathophysiology of arterial and venous thrombosis

Atherosclerosis is the key precursor of cardiovascular pathologies and it starts in adolescence. Atherosclerosis is a complex immune-inflammatory disorder whose progression involves multiple biological pathways that are influenced by genetic and environmental factors. Elevated plasma cholesterol level, hypertension, diabetes, tobacco smoking, male gender, and some inflammatory markers are among the proatherogenic risk factors of atherosclerosis, while physical exercise, a healthy diet, and high High-Density Lipoproteins (HDL) counts have an atheroprotective role [6].

Atherosclerotic lesions are initiated when the endothelium is activated by atherogenic and pro-inflammatory stimuli, such as primarily Vascular Cell Adhesion Molecule-1 (VCAM-1), intercellular adhesion molecule-1, E-selectin, and P-selectin [7]. It has been demonstrated a direct hemodynamic role in atherogenesis, notably by endothelial cells as their numerous signaling pathways are dependent on the hemodynamic patterns [8,9]. Low shear stress and turbulent flow at arterial curvature and branch points are major drivers of plaque development and instability. Plasma molecules and Low-Density Lipoproteins (LDL) penetrate dysfunctional endothelium into the subendothelial space where atherogenic lipoproteins are oxidized, mediated by myeloperoxidase, 15-lipoxygenase, and/or Nitric Oxide Synthase (NOS) [7]. Low-grade inflammation contributes to the disease progression due to the focal recruitment of circulating monocytes and T-lymphocytes [10]. Modulated by chemotactic cytokines, such as oxidized LDL and Monocyte Chemoattractant Protein-1 (MCP-1) [11], monocytes infiltrate arterial intima through transendothelial migration and differentiate into macrophages by internalizing the atherogenic lipoproteins via scavenger receptors. The incidence of the foam cells (lipid-laden macrophages) and their death by apoptosis and necrosis contribute to the formation of destabilizing atheromatous lipid-rich core within the plaque. Moreover, the foam cells express an array of inflammatory factors and produce proteolytic enzymes, such as Matrix MetalloProteinases (MMPs) [11], that are implicated in matrix degradation and plaque disruption [12]. To insulate the thrombogenic lipid-rich core of the atheroma from the bloodstream, the fibrous cap develops at the lesion site as a fibroproliferative response mediated by intimal smooth muscle cells. The recruitment of the smooth muscle cells and the production of the collagen-rich matrix are considered as beneficial since they protect

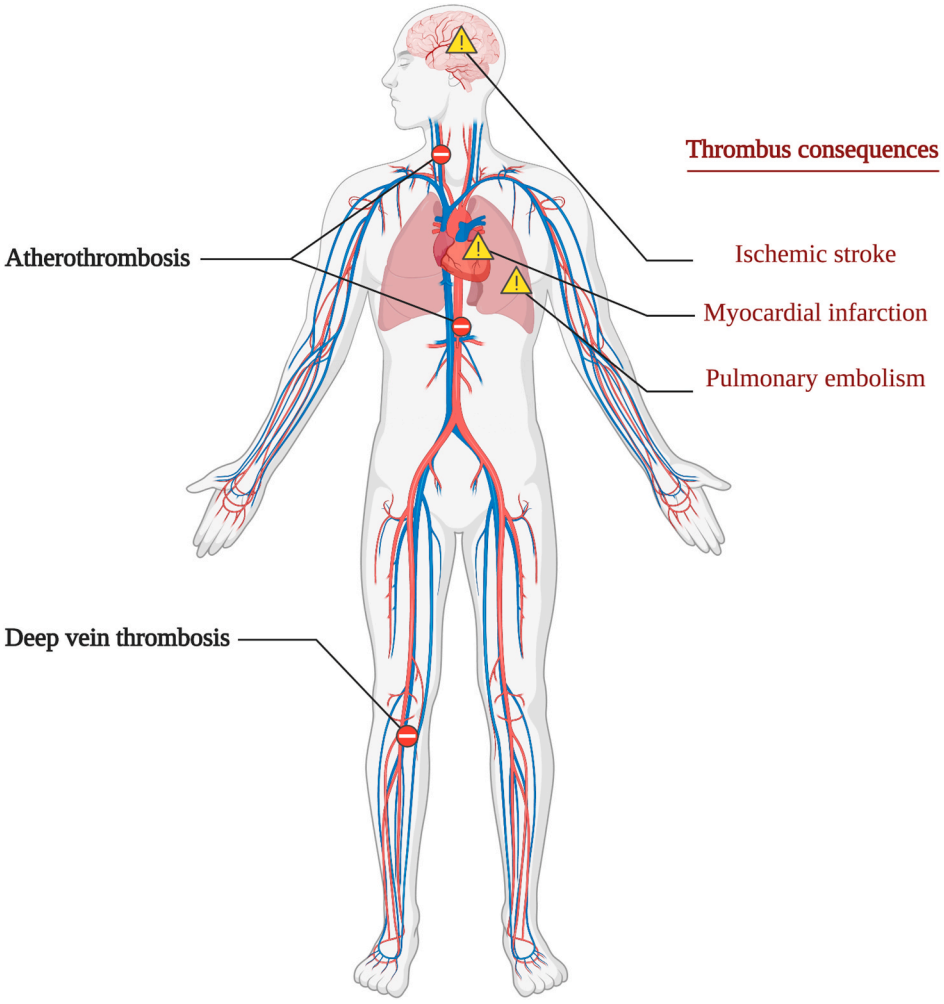

Fig. 1. Schematic of thrombotic diseases. Blot clot formation both in arteries (atherothrombosis) and veins (deep vein thrombosis) are influenced by congenital diseases and environmental factors. When the clot obstructs blood vessels in the brain, lungs, or heart, it may induce life-threatening consequences such as ischemic stroke, pulmonary embolism, or myocardial infarction.

the plaques against rupture and subsequent thrombosis. Conversely, the disintegration of foam cells and loss of smooth muscle cells may have detrimental consequences, leading to the formation of a destabilizing lipid-rich core and a fragile and rupture-prone fibrous cap. Atherosclerotic plaque calcification is an inflammation-driven process that manifests in all stages of the disease and should be defined as a two-phase process: microcalcification, the early stage of intimal calcium formation, and the end-stage of macrocalcification. While coronary Computed Tomography (CT)-detected macroscopic calcification in artery plaque acts as a biomarker of the overall disease progression, it is believed to stabilize the plaque and prevent acute events [13]. On the contrary, microcalcification, which can be identified by Positron Emission Tomography (PET)/CT imaging with ^{18}F-sodium fluoride, is associated with plaque vulnerability and an increased risk of rupture, since it aggravates plaque inflammation and augments mechanical stress in the fibrous cap [14].

Injury of the fibrous cap of atherosclerotic plaque is a primary trigger for arterial thrombosis, promoting hemorrhage and luminal prothrombotic response [15]. For initial flow obstruction, the blood coagulation cascade activates the platelets that are rapidly recruited to the site and aggregate, resulting in rapid thrombus growth [16] (Fig. 2A). Fibrin network then develops for the stabilization of platelet-rich thrombosis. Although most episodes of the ruptured fibrous cap occur silently without clinical symptoms, plague rupture with subsequent thrombosis often culminates in devastating clinical events such as myocardial infarction (MI) or ischemic stroke [15].

Contrary to atherothrombosis, the pathogenesis of Venous Thrombosis (VT) is only partially understood. The main components of the venous thrombi are fibrin and erythrocytes, and less activated platelets [17] (Fig. 2B). VT is initiated at the venous valves where stasis may occur under low shear blood flow [18]. Valvular sinus stasis aggravates hypoxia, promoting activation of the endothelium and leukocytes via mainly Hypoxia-Inducible Factor-1 (HIF-1) and Early Growth Response 1 (EGR-1) pathways. Besides, hypoxia condition modulates hypercoagulability. HIF-1 and EGR-1 pathways up-regulate the expression of P-selectin on endothelium, prompting monocytes to release microvesicles bearing tissue factor, which initiates thrombin production and fibrin deposition around the intact endothelial wall [19]. Both inherited and environmental factors raise the likelihood of the occurrence of venous thrombotic diseases, such as an imbalance of pro-vs. anti--coagulation proteins, as well as cancer, obesity, and major surgery [16].

1.2. Clinical treatment of acute thrombotic diseases

For the treatment of acute arterial or venous thrombotic events, fibrinolytic drugs can be administered in order to proteolytically disrupt blood clots and restore blood flow. Fibrinolytic, or thrombolytic, agents are Plasminogen Activators (PA) that activate the proenzyme

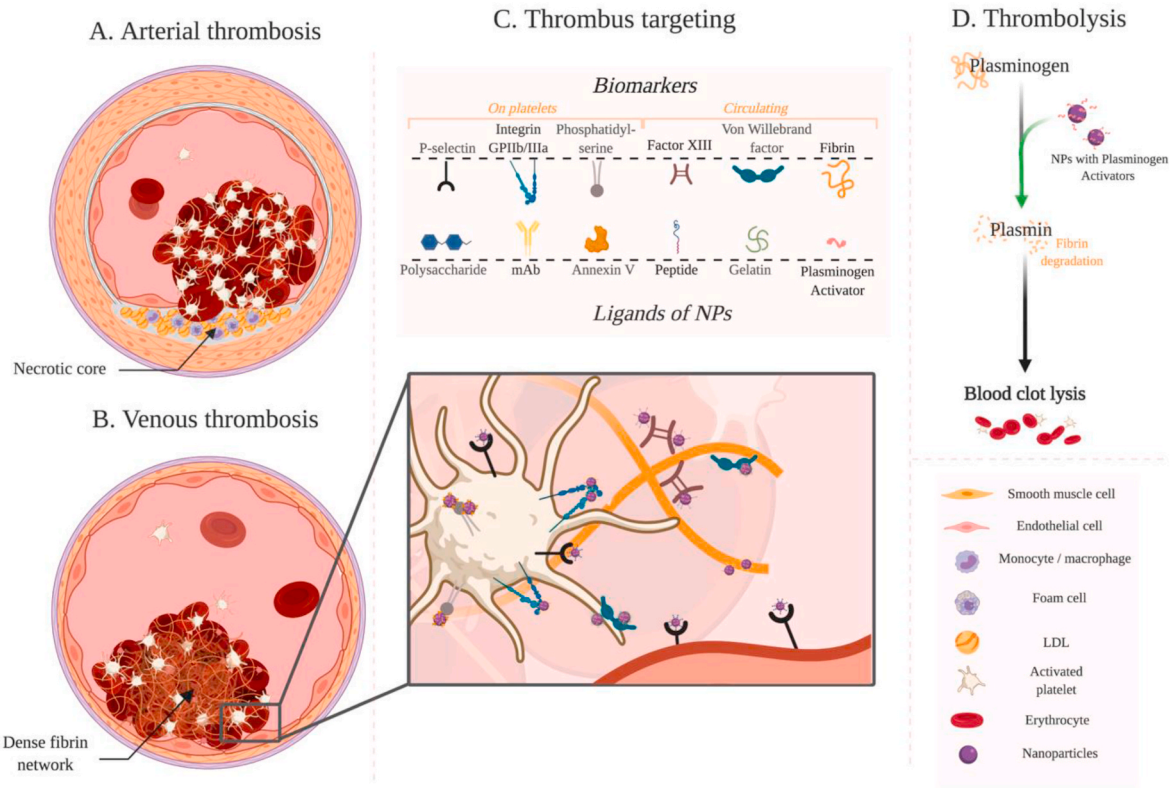

Fig. 2. Comparison of the arterial (A) and venous (B) thrombosis. Arterial clots (A) are composed of a high platelet ratio and are so-called "white thrombi". They are mostly the result of atherosclerosis. Multiple cellular pathways that initiate the activation of the endothelial cells are involved in thrombus formation. LDL penetrate the tissue, causing local inflammation and recruitment of circulating inflammatory cells. The disruption of the atherosclerotic plaque triggers the recruitment of smooth muscle cells to prevent wall rupture. Eventually, platelets aggregate on the impaired vessel wall with a consecutive formation of a fibrin network. On the other hand, venous clots (B), "red thrombi", contain erythrocytes and a denser fibrin network with fewer platelets. The thrombus formation is responsive to the following triggers: a vessel wall injury, a stasis of the blood flow, and hypercoagulability of the blood. C. Thrombus targeting with functionalized nano-/microparticles. Thrombi express a variety of cellular and molecular components – the surface of activated platelets (P-selectin, integrin GPIIb/IIIa, phosphatidylserine) or circulating proteins (Factor XIII, vWF, or fibrin) – that can be employed for specific targeting. NPs are designed with different ligands to these biomarkers: polysaccharide fucoidan, peptides, monoclonal antibodies, etc. D. Thrombolysis with PA-bearing and targeted to the thrombi NPs. The PA convert plasminogen into plasmin that breaks down the fibrin network and releases the components of the blood clot. Abbreviations: *LDL*, low-density lipoproteins; *vWF*, von Willebrand factor; *mAb*, monoclonal antibodies; *NPs*, nanoparticles; *PA*, plasminogen activators. (For interpretation of the references to color in this figure legend, the reader is referred to the Web version of this article.)

plasminogen to plasmin that then cleaves fibrin network into soluble degradation products. This activation of the fibrinolytic system destabilizes the structure of a thrombus [20]. Thrombolytic therapy is thereby used in patients with such pathologies as acute MI, acute ischemic stroke, peripheral arterial disease, deep vein thrombosis, and massive pulmonary embolism [21].

U.S. Food and Drug Administration (FDA)-approved "clot busters" drugs for use in thrombotic diseases are recombinant-based PA (e.g., alteplase – rtPA, reteplase – rPA, and tenecteplase – TNK), streptokinase (SK), and urokinase (uPA). The main differences between them relate to their antigenicity, half-life, lytic potential, fibrin specificity, and hemorrhagic risks [22]. First-generation thrombolytic drugs (urokinase, streptokinase) are non-fibrin specific when second and third-generation (alteplase and its variants) overcome this issue. Generally, human protein-derived PA (urokinase, alteplase, reteplase, tenecteplase) are nonantigenic, contrary to those derived from a bacterial species (streptokinase) [23]. The half-life of each PA determines their mode of administration (a bolus injection, short infusion, or continuous intravenous infusion). A comparison of different FDA-approved PA with their clinical indications is summarized in Table 1.

The leading drawbacks of fibrinolytic therapy include treatment failures such as ineffectiveness, re-thrombosis as a result of a persistent vascular lesion and plasma hypercoagulability, and a high risk of bleeding complications, with intracerebral hemorrhages occurring in 1–7% of treated patients [21]. Moreover, PA are physiologically inhibited by Plasminogen Activator Inhibitors (PAI) such as PAI-1 and PAI-2 while alpha 2-antiplasmin and alpha 2-macroglobulin inactivate plasmin, thereby reducing the treatment efficacy [24]. In view of these limitations, the constant development of novel molecules aims to address the problems associated with available thrombolytics. The novel candidates that are mutants of available PA or might be produced from the microbial, plant, and animal origin are discussed in the review [25].

The association of thrombolytic drugs with endovascular methods significantly improved interventional management of acute thrombotic events. The percutaneous coronary intervention has become more common for reperfusion, improving survival rates in patients with MI [26,27]. When available, this catheter-based procedure that is performed by an interventional cardiologist has to be offered promptly after/or in place of initial thrombolytic therapy. Since 2015, mechanical thrombectomy (MT) using a stent retriever is recommended as a complementary treatment to fibrinolytic therapy for ischemic stroke related to large vessel occlusions in the anterior circulation such as in the internal carotid artery and proximal middle cerebral artery [28,29] after multiple positive randomized control trials [30,31]. Yet, since MT needs to be performed by a qualified neurointerventionist at comprehensive stroke centers, access to them often remains difficult. In France, in particular, out of 135 nationwide neurovascular centers, only 40 are capable of performing thrombectomy to date [32]. Therefore, there is still a dire need for a safe and non-invasive solution.

With the advent of the field of nanotechnology, there has been considerable interest in integrating nanomedicine and thrombolytic therapy for the treatment of acute thrombotic events. Nanomedical approaches for targeted fibrinolysis could advance clinical outcomes by improving current pharmaceutical methods when interventional catheter-based strategies are not available or not recommended (as, for example, in ischemic stroke due to occlusions in smaller vessels or posterior circulation). By acting locally at the thrombus site, there is a promise that nanomedicine-delivered "clot-busting" agents deliver superior recanalization rates and attenuate life-threatening bleeding complications associated with their intravenous administration. One may also expect the chance to replace intravenous infusion by bolus injection of the first- and second-generation PA due to the extended drug half-life. In the ideal treatment settings, the synergic combination of endovascular and nanotherapeutic methods would represent a more precise approach to manage thrombotic pathologies.

2. Nanomedicine for targeted drug delivery

Nanomedicine, a medical application of nanotechnology, combines a powerful set of nano-engineered devices for diagnostic and/or therapeutic applications. Nanoparticle (NP)-based drug delivery can increase drug circulation time, improve therapeutic efficacy, and reduce unwanted off-target effects by delivering an active molecule to the injury site [33]. The liposomal formulation of doxorubicin – Doxil® – was the first clinically approved nanomedicine therapy by the FDA in 1995 for the Kaposi's sarcoma and other cancers that reduced cardiotoxicity compared with a conventional formulation [34]. Other NP formulations are approved for the treatment of distinct pathologies, such as cancers, fungal infections, iron-deficient anemia, macular degeneration, as well as vaccines for hepatitis A and influenza [35,36].

Different nano- or microcarriers (e.g., liposomes, polymeric, magnetic nano- & microparticles, quantum dots, nanotubes, dendrimers) are similarly researched in the therapeutic area of CVD [37]. Nanotechnology plays a role for wide-ranging cardiovascular applications, such as hypertension [38], atherosclerosis [39], prevention of restenosis following interventional cardiology [40], ablation for atrial fibrillation [41], cardiac tissue engineering [42], but also in the management of aneurysms [43] as well as CVD prevention [44].

Table 1
Thrombolytic agents approved by the FDA.

Agent	Abbreviation	Source	Safety [immunogenicity, fibrin specificity]	Half-life, min	Regimen	Total Dose	Metabolism	Indication
First-generation								
Streptokinase	SK	β-hemolytic streptococcus	Immunogenic Non-fibrin specific	20	Infusion	1.5×10^6 IU	Renal	PE Acute MI PAO, DVT
Urokinase	uPA	Human urine & kidney cell culture	Non-fibrin specific	15	Infusion	$2.25–6.25 \times 10^6$ IU	Renal	PE Acute MI PAO, DVT
Second-generation								
Alteplase	rtPA	Recombinant DNA technology	Fibrin specific (++)	4–8	Infusion	MI: 50–100 mg IS: 0.9 mg/kg PE: 100 mg	Hepatic	Acute MI Acute IS PE
Third-generation								
Reteplase	rPA	Recombinant DNA technology	Fibrin specific (+)	14–18	Double bolus	20 IU	Renal	Acute MI PAO
Tenecteplase	TNK		Fibrin specific (+++)	11–20	Bolus	30–50 mg	Renal	Acute MI

Abbreviations: *DVT*, Deep Vein Thrombosis; *MI*, Myocardial Infarction, *PAO*, Peripheral Arterial Occlusion; *PE*, Pulmonary Embolism; *IS*, Ischemic Stroke; *IU*, International Units.

2.1. Evolution and milestones in the progress of nanomedicine for fibrinolytic therapy

The field of nanomedicine in fibrinolytic therapy is evolving vibrantly, as evidenced by the expanding list of preclinical concepts of nanomaterial complexation with PA. An ideal vehicle for thrombolytic drug delivery should be biocompatible, non-toxic, non-immunogenic, biodegradable, and should avoid rapid clearance by the immune system [45]. The benefits of utilization of the nanoparticles (NPs) are attributed to their high surface-volume ratio, multifunctionality, high bioavailability, and possible control of therapeutic agent release. Control drug release facilitates the release of the payload from the NPs at the thrombus site upon internal or external stimuli such as temperature [46,47], pH [48], US [49], or magnetic field [46], etc. Specific thrombus targeting can be achieved by modifying the surface of nanocarriers with targeting moieties (antibodies, aptamers, polysaccharides, peptides, and small molecules) and/or application of magnetic energy, enhancing the therapeutic effect due to accumulation of thrombolytic drug at the clot surface [50] (Fig. 2C and D). Furthermore, encapsulation of the fibrinolytic drug onto the NPs can protect it from inactivation by PAI-1 in the bloodstream [51] and prolong its blood circulation time [48,52,53], thus achieving safe and effective thrombolysis at a lower dose [54,55]. Nanocarrier protection may further limit drug leakage during circulation, reducing the risk of hemorrhagic complications [56,57] such as cerebral hemorrhages that often accompany the injection of free plasminogen activators.

The timeline shown in Fig. 3 depicts evolution and milestones in the conceptual advances of nanomedicine-facilitated thrombolysis.

The story begins in the late '80s when dextran-coated iron oxide microparticles loaded with SK were utilized for magnetically driven thrombolysis of the carotid arteries in dogs [58]. Around the same time, SK-bearing liposomes entered the field by accelerating reperfusion in acute MI [59]. The first reported microbubbles for sonothrombolysis in 1996 were initially composed of denatured albumin shells, however, this formulation is no longer used due to stability/immunogenicity issues [60]. Polymeric platforms in thrombolytic therapy started to emerge a decade later in order to improve a stability profile of the liposomes in biological fluids. In 2004, first-reported polymer microparticles were designed from Polyethylene Glycol (PEG) and loaded with SK to tackle coronary thrombosis in a canine model [61]. The early success of the rtPA-conjugated erythrocytes in thromboprophylaxis in 2003 led to the further investigation and development of diverse bio-inspired nano solutions [62]. These initial studies evidenced an undoubtable potential of nanomedicine to boost thrombolytic therapy in animal models, however, they often lacked a complete analysis in terms of particle physico-chemistry and safety, drug loading efficiency/release, targeting and thrombolytic efficacy in appropriate *in vitro* and subsequently *in vivo* models, which is currently recognized and adopted [63]. The evolution of nanomedicine-based fibrinolysis continued with the development of surface-coated, mostly nanosized particles that exhibit considerably longer circulation half-life *in vivo* and superior safety profiles than uncoated microparticles. Notable examples from late 00′ are the PA-bearing polymer NPs that were coated with chitosan and cRGD peptide, a prototype of the utilization of a popular targeting ligand of GPIIb/IIIa [64], as well as magnetic NPs coated with dextran [65] and polyacrylic acid [66] for magnetically guided thrombolysis.

The last decade, which we review in this paper, was fruitful for progress in nanomedicine-assisted thrombolysis. During these years, researchers commonly used active targeting strategies. Apart from magnetic targeting of iron oxide NPs, the utilization of monoclonal antibodies (mAb) and peptides that recognize biomarkers associated with thrombotic pathologies have allowed the development of more selective nanosystems that advanced into the multivalent design in 2017 [57]. In 2018, polymeric NPs were functionalized with fucoidan, affordable high-quality P-selectin ligand for site-specific fibrinolytic activity [67] as an alternative to costly mAb and peptides. From 2012, theranostic hybrid approaches emerge: inorganic nanocarriers that serve for thrombolysis and optical imaging [68] or MRI [69]. Echogenic liposomes are widely studied with the *in vitro* clot model for sonothrombolysis due to tunable designs like targeting and/or rtPA loading [70]. Recently, targeting nanobubbles were published that complemented PA with sonothrombolysis, as they penetrate deeper into the clots comparing to microbubbles [71]. The nanoformulations with controlled release start appearing more frequently: via hemodynamic phenomena – increased shear stress in the stenotic arteries [72] and

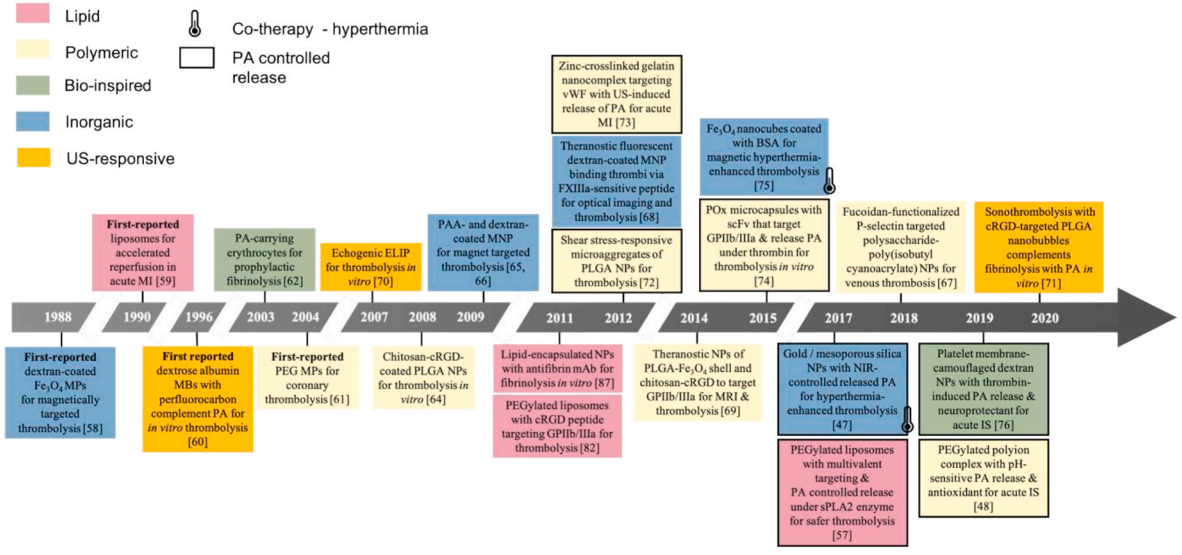

Fig. 3. The timeline of evolution and milestones in the progress of nanomedicine for fibrinolytic therapy: history and current trends. This figure mostly comprises the PA-loaded platforms tested with *in vivo* experiments; however, we also included several remarkable *in vitro* concepts. Abbreviations: *PA*, plasminogen activator; *MI*, myocardial infarction; *IS*, ischemic stroke; *PEG*, polyethylene glycol; *PLGA*, poly(lactic-co-glycolic acid); *PAA*, poly (acrylic acid); *BSA*, bovine serum albumin; *POx*, poly(2-oxazoline); *vWF*, von Willebrand Factor; *FXIIIa*, activated factor XIII; *$sPLA_2$*, secreted phospholipase A2 enzyme; *MNP*, magnetic nanoparticles; *MPs*, microparticles; *NPs*, nanoparticles; *MBs*, microbubbles; *ELIP*, echogenic liposomes; *mAb*, monoclonal antibodies; *scFv*, single-chain antibody; *MRI*, magnetic resonance imaging; *US*, ultrasound; *NIR*, near-infrared.

US-induced [73] in 2012, upon enzyme exposure since 2015 [74], elevated temperature since 2017 [47], and low pH in 2019 [48]. To enhance thrombolysis, adjuvant therapy in the form of local hyperthermia by a magnetic field [75] or near-infrared (NIR) light [47] was used in the late 10's.

Nowadays, the trend is to create complex multifunctional but, at the same time, biocompatible and biodegradable nanocarriers. Application of novel biomaterials, hybrid NPs with biomimetic surfaces, incorporating active targeting molecules, and the ability to modulate the release spatially and temporally is being widely researched. The researchers also commenced investigating the solution to complement nanomedicine-based fibrinolysis by counteracting the pathological processes related to ischemia with an antioxidant [48] and neuroprotection [76] approach for ischemic stroke in 2019.

In the next chapters, we are going to describe in detail the complexation of PA with different types of nanocarriers, which are summarized in Fig. 4, and their corresponding therapeutic effects in preclinical studies.

3. Lipid drug delivery

3.1. Liposomal drug delivery

Liposomes, first described in the mid-'60s, are defined as spherical vehicles made of an aqueous core surrounded by phospholipid bilayers. Since then, because of their excellent biocompatibility, low toxicity, and easy preparation methods, liposomes are considered as one of the most promising tools for drug delivery in medical fields of principally small molecules (e.g., chemotherapeutics) with some being clinically approved [77], but also proteins, DNA, RNA, and imaging probes [78].

Liposomes are generally fabricated by thin-film hydration, which consists of dissolving lipid components in an organic solvent, drying down by rotary evaporation, and rehydrating in water, as well as by freeze-drying, reverse-phase evaporation, or injection of ethanol with phospholipids into an aqueous phase. Membrane extrusion, sonication, and/or freeze-thawing are further employed to modulate the particle size [79]. In terms of the size and number of bilayers, different types of liposomes can be produced, such as small unilamellar vesicles (single phospholipid bilayer sphere), large unilamellar vesicles, and multilamellar vesicles (an onion structure of bilayers) [78]. The amphiphilic properties of liposomes allow them to internalize both hydrophilic and hydrophobic compounds.

Liposomal encapsulation of plasminogen activators for thrombus-specific drug delivery is frequently exploited to improve the drug half-life and reduce hemorrhagic side effects. Given that the conventional liposomes aggregate *in vivo* and undergo rapid systemic clearance via Mononuclear Phagocyte System (MPS) after contact with plasma proteins, decoration with FDA-approved PEG has been adopted to provide steric stabilization and reduce liposomal opsonization, and, therefore, to improve the pharmacokinetics of PA in blood [79].

The liposomal surface modification strategies by site-directed target ligands, such as antibodies, peptides, or stimuli-responsive drug release (thermo- or pH-sensitive liposomes) have been tested in the preclinical development. Most targeting approaches are directed towards Glyco-Protein IIb/IIIa (GPIIb/IIIa). GPIIb/IIIa is an integrin complex on the platelet membrane that mediates platelet adhesion and aggregation during hemostasis. Normally present in its inactive state on resting platelets, it undergoes conformational changes to allow the platelets to bind to fibrin upon platelet stimulation by physiologic ligands such as thrombin or collagen [80]. Thrombolytics are generally incorporated into the inner aqueous core of the liposomes during the synthesis process, however, they can also be adsorbed onto the surface or covalently grafted to the PEGylated liposomes [81].

In the study of Vaidya et al., long circulatory PEGylated liposomes were coupled with a cyclic Arg-Gly-Asp (cRGD) [CNPRGDY(OEt)RC] and targeted GPIIb/IIIa receptor both *in vitro* and *in vivo* [82]. Despite a low level of streptokinase release (12.20 ± 0.94%) over the course of 35 h, the study reported the improved thrombolysis rate of cRGD-targeting liposomal SK compared with free SK after 1 h in rats (34% vs. 22%). When rtPA was loaded onto both non-PEGylated and PEGylated GPIIb/IIIa-targeting liposomes, a favorable rtPA release profile from PEGylated ones was demonstrated in the work [52], with a substantial

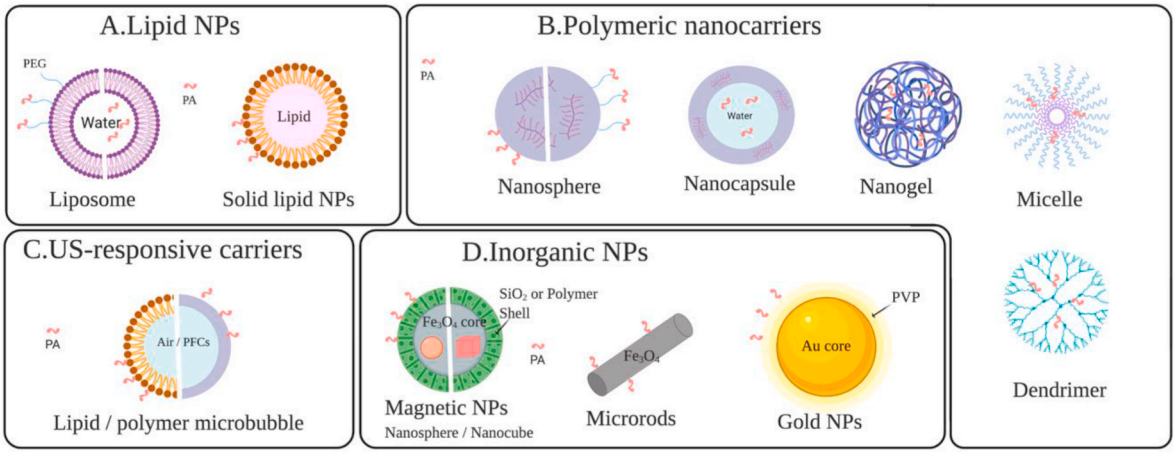

Fig. 4. Nanomedicine-based platforms with Plasminogen Activators. A. Lipid nanocarriers. In liposomes, PA may be embodied into the aqueous core or adsorbed/covalently conjugated onto the PEGylated phospholipid shell. In solid lipid NPs, PA is covalently grafted to their surface. B. Polymer-based nanoplatforms. PA are typically entrapped inside amphiphilic micelles and self-assembled gelatin or chitosan nanogels due to electrostatic interactions, incorporated into the aqueous core of nanocapsules, or covalently attached to the surface of the nanospheres and dendrimers via EDC/NHS chemistry. Surface decoration with PEGylation or polysaccharides is common for better stealth effects, particularly significant for the NPs from hydrophobic synthetic polymers. C. Ultrasound-responsive carriers. Microbubbles are microspheres filled with gas (e.g., C_4F_{10}, N_2, C_4F_8) or air, mostly coated with phospholipids or polymers that bind PA onto the outer layer via covalent interactions. Upon exposure to low-frequency ultrasound, microbubbles can burst to realize sonothrombolysis. D. Inorganic nanoparticles. In magnetic NPs, inner core – in the shape of nanospheres or nanocubes – is mostly iron oxide (Fe_3O_4), and the surface is decorated with organic (e.g., dextran, chitosan, polyacrylic acid) or inorganic (SiO_2) shell. PA is conjugated to the surface via EDC/NHS or simple adsorption. Uncoated iron oxide microrods may load PA via glutaraldehyde. Gold NPs immobilized PA via bio-affinity ligation. Abbreviations: *PEG*, Polyethylene glycol; *PA*, plasminogen activator; *NPs*, nanoparticles; *US*, ultrasound; *PVP*, polyvinyl pyrrolidone; *PFCs*, perfluorocarbons. (For interpretation of the references to color in this figure legend, the reader is referred to the Web version of this article.)

amount of drug released within 30 min after administration followed by a slow continuous release over 24 h. This strategy intends to achieve reperfusion and prevent re-thrombosis. The half-life of rtPA in plasma was prolonged from 7 min for native rtPA to 103 and 141 min for non-PEGylated and PEGylated liposomes. Besides, rtPA-loaded liposomes were 35% more potent than native rtPA for vessel recanalization but produced a 4.3-fold less depletion of circulating fibrinogen, potentially reducing hemorrhagic risks, in $FeCl_3$-rat venous thrombosis model.

Huang et al. exploited the targeted delivery and controlled release of rtPA incorporated into PEGylated liposomes coated with cRGD peptide [83]. Membrane fusion attributed to interactions between cRGD peptides on liposomes and GPIIb/IIIa integrins on activated platelets caused liposomal membrane destabilization and rtPA release. Due to this, over 90% of the entrapped rtPA was released within 1 h in targeted liposomes compared to <10% after 6 h in untargeted ones, and this release profile could be adjusted by altering the concentration of activated platelets. Zhang et al. [56] combined the active thrombus targeting with cRGD and gradual release of the drug from the liposomes without burst effect over 5 h. They improved the *in vivo* thrombolytic efficacy by ~4-fold over free uPA, at the same time shortening bleeding time of the tail bleeding assay of hemostasis, thereby potentially reducing the side effects of uPA.

In the elegant study [57], Pawlowski et al. took inspiration from platelet-derived microparticles that are plasma membrane vehicles shed from platelets that are undergoing activation, stress, or apoptosis (Fig. 5A) [84]. They designed a liposomal system with a multivalent targeting strategy towards both GPIIb/IIIa and P-selectin on activated platelets using the peptides CGSSSG*RGD*SPA and CDA*EWVDV*S, respectively (Fig. 5B and C). As the constructs could be degraded under secreted phospholipase A2 ($sPLA_2$) enzyme, secreted from leukocytes and active platelets in the thrombus, it could so release encapsulated SK (Fig. 5D and E). While thrombolytic efficacy of the targeted liposomes was comparable to free SK in $FeCl_3$-induced carotid artery thrombosis model, hemostatic capability for liposome-encapsulated SK was improved as measured by mouse tail bleeding time.

Hsu et al. [85] synthesized a hybrid NP-system, PEGylated thermosensitive magnetic liposomes (TMLs), encapsulating Fe_3O_4 NPs within liposomes, via solvent evaporation/sonication and freeze-thaw method.

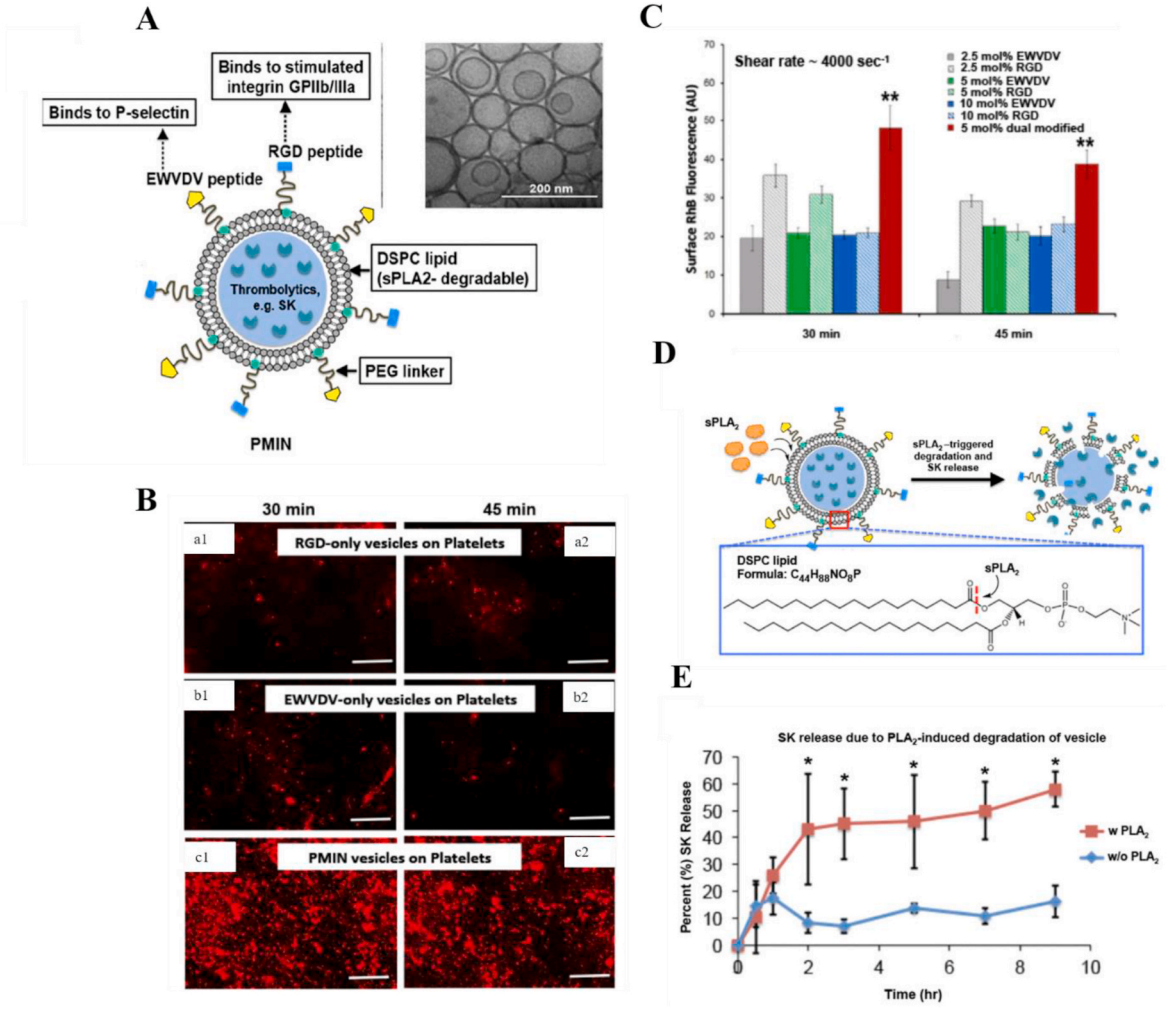

Fig. 5. A. Schematic representation of platelet-derived microparticles-inspired nanovesicle (PMIN) with dual-targeting strategy and controlled release of the thrombolytic upon sPLA2 enzyme exposure, with a representative cryo-TEM image of PMINs. B. Representative fluorescent images of particle binding show that RGD-decorated vesicles (a1, a2) and EWVDV-decorated vesicles (b1, b2) have a reasonable extent of binding and retention on the platelet-rich thrombus surface. However, the level of binding and retention levels are enhanced for dual modified PMINs (c1, c2). C. Quantitative analysis of fluorescence intensity shows that PMINs have significantly higher binding and retention capabilities compared to singly modified vesicles even when the mol% composition of single peptide modification is to twice (10 mol%) that of dual peptide modification (5 mol%) at high shear rate flow conditions. D. Schematic mechanism of sPLA2-induced membrane degradation due to cleavage of sn-2 acyl group of the phosphatidylcholine lipids. E. Release kinetics assessment of SK from PMINs shows that upon sPLA2 exposure, the percent (%) release of SK from PMINs is enhanced (~4 fold) compared to passive release without sPLA2 exposure. Adapted with permission from Ref. [57]. Copyright 2017 Elsevier Ltd.

Thrombolytic activity *in vitro* of rtPA-loaded TMLs at 43 °C was augmented as compared to at 37 °C due to enhanced drug release and higher enzyme activity at higher temperature. In addition to magnetic targeting, TMLs demonstrated a first-ever reported dual control mechanism of the drug release in serum: temperature- and magnet-sensitive, increasing at 43 °C and retarding with external magnetic force at 0.5 T in the follow-up work [46]. This technique could allow the liposomes to be magnetically guided toward the thrombus, preventing premature drug release. With appropriate biocompatibility of the nanocarriers, TML@rtPA restored arterial blood flow, iliac blood flow, and hind-limb perfusion, whereas the same dose of rtPA exerted no benefit in rat embolic model at 0.2 rtPA mg/kg under magnetic force at 43 °C.

3.2. Solid lipid nanoparticles

Solid Lipid Nanoparticles (SLNs) is an alternative drug delivery system. Contrary to conventional liposomes, which contain a lipid bilayer with an aqueous core, SLNs consist of lipid monolayer enclosing a solid lipid core stabilized by a surfactant, reaching a higher drug entrapment rate for a hydrophobic drug. Different preparation methods of SLNs include hot or cold homogenization, solvent emulsification/diffusion, or microemulsion [86]. Marsh et al. [87] prepared perfluorooctylbromide lipid-encapsulated NPs that can be assimilated to SLNs with a size 250 nm by emulsification/sonication method. Anti-fibrin mAb on the surface of the SLNs specifically targeted fibrin network in a canine model of the electrode-induced arterial thrombosis. Sulfhydryl functionalized uPA was covalently coupled to these SLNs and retained its fibrinolytic activity *in vitro*.

Overall, cRGD peptide-decorated PEGylated liposomes became a standard engineering approach in thrombolytic research owing to their cyto- and hemocompatibility [56] with a high potential for clinical translation, which might, in contrast, take longer for complex hybrid systems.

4. Polymeric drug delivery

Depending on the preparation method, polymeric NPs can have nanosphere or nanocapsule structures. Both naturally occurring hydrophilic polymers and synthetic biocompatible polymers are used in the NP fabrication and offer simple surface modification and functionalization [88]. Natural polymers such as polysaccharides (hyaluronan, alginate, and chitosan) and proteins (gelatin and albumin) are common [89]. Synthetic polymers come either in prepolymerized forms, such as polyesters like polycaprolactone (PCL), polylactic acid (PLA), or polymerized from the monomers, e.g., poly (methyl methacrylate), poly (alkyl cyanoacrylate) (PACA), poly (acrylic acid) (PAA), poly(lactic--*co*-glycolic acid) (PLGA), poly(2-oxazoline) (POx), and poly(amidoamine) (PAMAM). Synthetic polymers benefit from high purity and reproducibility over natural polymers; the latter, however, represent a significant interest due to their safety, abundance in nature, and low cost. Polymeric nanoparticles are conventionally fabricated by two methods: the dispersion of preformed polymers or the polymerization of monomers [90]. The plasminogen activators are typically dissolved and entrapped, or covalently attached to the surface of the NPs prepared from some of the above-mentioned polymers.

Chitosan (Cs), as well as its chemical derivatives, has been widely used because of its biocompatibility and biodegradability, low toxicity, and low immunogenicity in thrombolytic drug delivery. Chitosan is a cationic hydrophilic polysaccharide, derived from chitins, able to form polyelectrolyte complexes with negatively charged molecules [91].

Self-assembled chitosan NPs were produced via the ionic crosslinking with sodium tripolyphosphate, possessing a size 236 nm, and further loaded with uPA with encapsulation efficiency ~95% [92]. Both intravenous injection and catheter-driven drug delivery were tested in a thrombin-induced rabbit venous thrombosis, pointing out superior thrombolytic efficacy for the latter comparing with free uPA. Another group [93] elaborated a chitosan-based NPs/SK drug complexation via non-covalent interactions. Synthesis conditions such as pH and Cs concentration were optimized using a computational model. The team of Shamsi et al. reported the synthesis of uniform and spherical SK-entrapped chitosan NPs with a diameter 67 ± 13 nm and a narrow polydispersity by microfluidics [94]. A steady and sustained SK release was achieved during 48 h *in vitro* in addition to higher SK amidolytic activity in plasma in rats, comparing with free SK. Given that quaternized derivative of chitosan - N,N,N-Trimethyl Chitosan (TMC) has superior solubility and increased charge density, Liao et al. covalently grafted TMC with cRGD to target GPIIb/IIIa receptors [95]. The resulted cRGD-LK-NPs were formed with lumbrokinase (LK) via ionic gelation using sodium tripolyphosphate and could effectively accelerate thrombolysis in clot-occluded tubes and $FeCl_3$ rat carotid artery model at 90, 000 U/kg of LK.

Jin et al. prepared PEG crosslinked glycol chitosan hollow nanogels by an ultrasonic spray technique and loaded uPA with 80% loading efficiency. Such NP design improved uPA half-life in rats from 18 min to 40 min without causing biotoxicity. The application of diagnostic US at 2 MHz accelerated uPA release from the nanogels (90% of uPA released within 1 h vs. 80% within 6 h without the US) [53]. While the hollow cavity of the nanogels did not contain gas, they were responsive to the US due to the vibration of the polymer shell. The ultrasonic stimulation enhanced the thrombolysis *in vitro* for both free uPA and the uPA-loaded nanogels [53]. Notably, the nanogels allowed the delivery of uPA with no signs of a stroke or blood-brain barrier permeability damage after 24 h *in vivo* [96].

Gelatin, a protein obtained from the collagen hydrolysis, is an attractive natural macromolecule for a thrombolytic nanocarrier owing to its biocompatibility and biodegradability, and wide availability at low cost [97]. Gelatin-based NPs require crosslinking with glutaraldehyde or another bifunctional cross-linker during preparation, and their surface can be tuned with site-specific ligands, cationized with amine derivatives, or PEGylated.

Polyelectrolyte complex of cationized gelatin and anionic PEGylated gelatin with rtPA mutant (monteplase) fabricated a 200 nm thrombolytic delivery system [98]. While fibrinolytic activity *in vitro* was suppressed to 45% due to nanocomplexation, it was fully recovered under US stimulation (1 MHz, intensity 0.75 W/cm^2), demonstrating an ultrasound-responsive rtPA release. US control drug release can be explained by the production of the stable cavitation state and shear stress on the surrounding tissues [49]. In a rabbit thrombosis model, a combination of the US with rtPA-NPs allowed full vessel recanalization for all treated animals after 30 min, which was superior to free rtPA (10% recanalization after 60 min) and free rtPA + US (90% recanalization after 30 min).

Uesugi et al. further developed a zinc-crosslinked gelatin complex with monteplase [73], which restored its rtPA fibrinolytic activity upon US exposure *in vitro* [73] and *in vivo* to the level of free rtPA [54]. Monteplase-loaded NPs increased thrombus affinity 3-fold as a result of interactions of the gelatin with von Willebrand Factor (vWF), a blood glycoprotein that is a crucial component of platelet-rich thrombi. In a swine model of acute myocardial infarction, treatment with rtPA alone dissolved only 30% of occluded coronary thrombi at a dose of 55,000 IU/kg and no thrombi at 27,500 IU/kg within 60 min, while NPs carrying 55,000 IU/kg rtPA achieved recanalization of 90% thrombi within 30 min comparing to 60% of cases in 60 min at a dose of 27,500 IU/kg, under continuous-wave US field (1 MHz, 1 W/cm^2) [54].

Poly(d,l-lactic-co-glycolic acid) (PLGA), a synthetic biodegradable polymer that is relatively hydrophobic, has the FDA and the European Medicine Agency (EMA) approval for drug delivery systems. The PLGA micro- or nanoparticles are mostly synthesized by a double emulsion solvent evaporation system with poly(vinyl alcohol) (PVA) as an emulsion stabilizer [99].

In order to establish slow and controlled thrombolysis and prevent abdominal aortic aneurysm rupture, Sivaraman et al. produced PLGA

NPs with 10 μg rtPA using didodecyldimethylammonium bromide (DMAB) or PVA as a surfactant [100]. DMAB-stabilized NPs demonstrated gradual clot lysis and higher binding to the fibrin clots. Nano-delivery system overall improved the proliferation of the aneurysmal smooth muscle cells (EaRASMC) exposed to the clot lysis byproducts, attenuated the elastic matrix degradation and proteolytic enzyme activities within EaRASMC cultures.

Surface PEGylation of PLGA NPs plays a favorable role in biocompatibility and improves pharmacokinetics by preventing opsonization. Colasuonno et al. formulated discoidal porous nanoconstructs (DPNs) with a mixture of PLGA and PEG and loaded rtPA with efficiency ~100% via EDC/NHS reaction [101]. Despite the absence of active targeting, a high thrombolytic potential of these NPs might be attributed to their erythrocyte-mimicking shape and deformability, leading to efficient circulation profiles and accumulation of rtPA-DPNs at the clot site. A hybrid theranostic system was developed by Zhou et al., when rtPA was encapsulated into a shell of PLGA and Fe_3O_4, and a chitosan-cRGD peptide was grafted on the surface to target GPIIb/IIIa [69]. Such design addressed a dual function: the early detection of a thrombus and the dynamic monitoring of thrombolytic efficiency using a Magnetic Resonance Imaging (MRI) scanner. The obtained NPs showed a sustainable release profile: a slow-release during the first 15 min and a fast release until 60 min. MRI contrast enhancement was illustrated in the murine thrombus model; effective thrombolysis was performed in the *in vitro* blood clot.

Inspired by pathophysiological mechanisms [72], the microaggregates of multiple PLGA NPs dissociated into rtPA-bearing NPs when exposed to abnormally high hemodynamic shear stress (≥100 dyne/cm^2) in the vascular occlusions. The obtained Shear-Activated NanoTherapeutics with rtPA (rtPA-SA-NTs) performed effective thrombolysis in multiple preclinical models, as they delayed the time to full vessel occlusion in a $FeCl_3$ mouse arterial thrombus model, reversed the debilitating hemodynamic changes of acute pulmonary embolism *ex vivo* at a concentration 100-times lower of native rtPA, and increased survival in an otherwise fatal mouse pulmonary embolism model *in vivo*.

Poly(alkyl cyanoacrylate) (PACA) is an alternative to PLGA

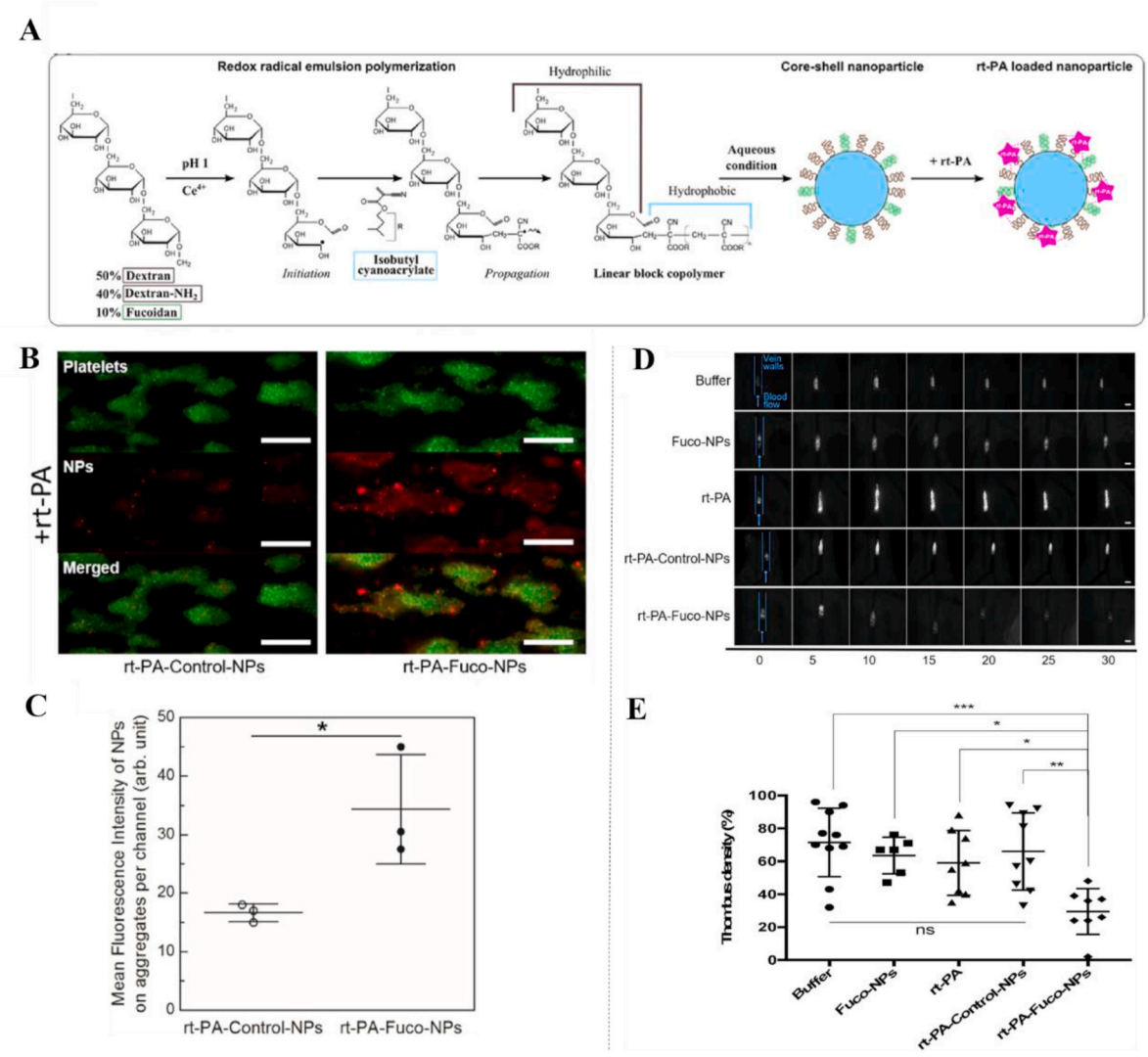

Fig. 6. A. Formulation of fucoidan-functionalized NPs with rtPA. Cerium (IV) ions oxidize polysaccharide chains. The free radical initiates the radical emulsion polymerization of isobutyl cyanoacrylate monomers and create amphiphilic linear blocks copolymers that assemble into core-shell NPs in water. rt-PA interacts with the NPs by electrostatic interactions. B. The fluorescence image shows that rtPA-loaded NPs (in red) with fucoidan adhere notably more onto activated platelet aggregates (in green) than the particles without fucoidan under flow conditions (scale bar = 50 μm). C. Corresponding quantitative analysis of rt-PA-loaded NPs on platelet aggregates. D. Evaluation of thrombolysis efficiency in a mouse model of venous thrombosis at the rtPA dose of 2.5 mg/kg. Fluorescence images of thrombus evolution after treatment injection as determined by platelet accumulation at different times (scale bar = 200 μm). E. Corresponding quantitative analysis of the thrombus density at 30 min after injection. Adapted with permission from Ref. [67]. Copyright 2017 Elsevier Ltd. (For interpretation of the references to color in this figure legend, the reader is referred to the Web version of this article.)

biodegradable polymer that was initially developed and approved as a surgical glue [102]. Juenet et al. prepared hydrophilic polysaccharide-decorated poly(isobutyl cyanoacrylate) core-shell NPs with a mean size of 130 nm by redox radical emulsion polymerization and loaded rtPA by adsorption [67] (Fig. 6A). Functionalization of the NPs with an algae-derived abundant and cost-effective sulfated polysaccharide fucoidan (Fuco) [103] allowed binding P-selectin on activated platelets under arterial or venous shear stress conditions (Fig. 6B and C). Fucoidan, as a targeting ligand for P-Selectin overexpression in cardiovascular pathologies, was prior validated on microscale particles, including polysaccharide microparticles with iron oxide for MRI imaging [104] and polymer microcapsules [105]. Thrombolytic efficacy was 2-fold enhanced for rtPA-loaded Fuco-NPs comparing with rtPA-Control-NPs and free rtPA in $FeCl_3$ murine model of venous thrombosis at the rtPA dose of 2.5 mg/kg [67], which is 4 times lower than the appropriate therapeutic dose in mice [106] (Fig. 6D and E).

Polycaprolactone (PCL). PCL is a non-toxic biodegradable hydrophobic polyester that is approved by the FDA for several medical applications, including for targeted drug delivery. Its slow degradation profile under physiological conditions (from months to years) makes it attractive for long-term drug delivery devices or implants [107].

Deng et al. synthesized the PEG-PCL NPs by single emulsion and solvent evaporation method and conjugated with rtPA via EDC/NHS [108]. rtPA preserved its amidolytic activity *in vitro* and remained active *in vivo* up to 3 h. Despite some reduction in lytic activity in the *in vitro* blood clot test, rtPA-loaded NPs reduced the infarct volume in the brain by ~70% comparing with free rtPA at 1 mg/kg.

Pan et al. produced cationic micelles with a mean size of ~190 nm [109]. Polymeric micelles are a frequently employed class of NPs with a distinct core-shell structure that are self-assembled from amphiphilic components in an aqueous solvent. They were prepared with a mixture of polymers: polycaprolactone-block-poly(2-(dimethylamino) ethylmethacrylate) (PCL-PDMAEMA) – to form NP core, methoxy-PEG-PCL – to enhance the colloidal stability and biocompatibility, and PCL-PEG conjugated with RGDfk peptide – to target GPIIb/IIIa. The micelles adsorbed anionic LM via electrostatic interactions [109]. They could target thrombus and exhibited thrombolytic potential *in vivo* with almost 2-fold reduced bleeding time vs. free LM, thus, mitigating hemorrhagic risks. Two years earlier, the same team published a work similarly dealing with LM-adsorbed micelles from triblock polymer – polycaprolactone-block-poly(2-(dimethylamino) ethyl methacrylate)-block-poly(2-hydroxyethyl methacrylate) (PCL-PDMAEMA-PHEMA) [110]. In a less common targeting strategy, Annexin V, a human phospholipid-binding protein that binds phosphatidylserine on the surface of activated platelets in a calcium-dependent manner and is proposed to play a role in the inhibition of blood coagulation [111], was conjugated to the micelles to target thrombi in a murine $FeCl_3$-induced model and perform the *in vivo* thrombolytic activity.

Poly(2-oxazoline) (POx). This hydrophilic biocompatible but non-biodegradable synthetic polymer features a stealth effect similar to PEG [107]. Gunawan et al. synthesized smart multifunctional polymer microcapsules based on a brushlike POx with alkyne functional groups (B-PEtOx$_{Alk}$) polymer via layer-by-layer assembly on removable mesoporous silica templates [74]. uPA was encapsulated onto these microcapsules via electrostatic interactions (6.4×10^{-15} g uPA per capsule) and could be released upon exposure to thrombin owing to the thrombin-sensitive cross-linker peptide (ELTPRGWRLE). The NP surface-functionalization with a single-chain antibody (scFv) enabled a high affinity toward the GPIIb/IIIa on activated platelets in microfluidic flow channels.

Poly(acrylic acid) (PAA) is an anionic polyelectrolyte, which is a synthetic polymer of acrylic acid. PAA is not biodegradable, although it displays excellent biocompatibility and low toxicity [107].

Mei et al. successfully combined the thrombolytic and antioxidant strategy, incorporating 4-amino-2,2,6,6-tetramethylpiperidine-1-oxyl (4-amino-TEMPO) antioxidant into polyion complex NPs as to eliminate Reactive Oxygen Species (ROS) after ischemia-reperfusion injury [48] (Fig. 7A). Self-assembled NPs were composed of anionic PAA, cationic poly(ethylene glycol)-b-poly[4-(2,2,6,6-tetra-methylpiperidine-1-oxyl) aminomethylstyrene] (PEG-b-PMNT) diblock amphiphilic copolymers, and rtPA. The NPs were colloidally stable due to the hydrophobic nature of the core-forming polycationic PMNT segment. Nanocomplexation extended the *in vivo* half-life of rtPA from 8.2 min to 71.2 min. The complex dissociation in the acidic pH, typical for the ischemia, released the drug. At rtPA dose 1 mg/kg, antioxidant-containing NPs improved neurological deficit, reduced cerebral infarct volume, decreased cerebral superoxide ROS and lipid peroxidation levels as well as subarachnoid hemorrhage, contrary to free rtPA and antioxidant-free nanocomplex (Fig. 7B–G).

Poly(amidoamine) (PAMAM) is a class of dendrimers – nano-sized, radially symmetric artificial macromolecules with highly branched three-dimensional polymeric structure. Due to the multiple functional surface groups, they are commonly exploited for conjugation with pharmaceutical compounds. Mukhametova et al. developed PAMAM dendrimers, containing ethylenediamine core with amidoamine internal structure and a primary amine terminal surface [112]. They were covalently grafted with SK by EDC/sulfo-NHS chemistry and preserved up to 85% of thrombolytic activity *in vitro* compared with free SK [112]. Nonetheless, the clinical use of the dendrimers is limited because of high toxicity, unknown biocompatibility, biodistribution, biodegradation, and pharmacokinetic profile, and high cost of production [113].

To sum up, multiple excellent papers reported superior thrombolytic potential and favorable therapeutic outcomes with PA-loaded polymeric nanocarriers. These NPs are expected to prevail in thrombolysis research, considering their benefits: simple surface modification & functionalization, "smart" nanoparticulate design with controlled drug release, FDA-approval of some polymers that are both biodegradable and biocompatible.

5. Inorganic nanoparticles

5.1. Magnetic nanoparticles

Magnetic nanoparticles (MNP) are of great interest in thrombolytic drug delivery due to their large surface area, small particle size (1–100 nm), strong superparamagnetic properties that permit their detection by MRI, excellent biocompatibility with low toxicity. Initially, MNP were introduced to the MRI field to overcome the low sensitivity of the standard imaging method. The assumption was to avoid the proton relaxation effect of MRI imaging with direct visualization of NPs containing iron oxide nanocrystals [114]. The system was functionalized with a fibrin-binding peptide that indicated promising results for MRI visualization of *in vitro* blood clots. MNP are usually composed of a metal core of magnetite Fe_3O_4 or maghemite γ-Fe_2O_3 and a functionalized shell. Co-precipitation and thermal decomposition are among the most widely studied synthesis methods for magnetic NPs. Aside from the typically used iron oxide, other magnetic elements such as Ni, Co, and their oxides can also be applied for NP manufacture. Cheng et al. [115] fabricated magnetic Ni nanorods via the oblique angle deposition method (physical vapor deposition technique). Hydrodynamic flows, induced by rotating nanorods suspension with rtPA by a pair of permanent magnets, enhanced rtPA mass transport and accelerated thrombolysis. Nevertheless, due to nickel toxicity, this technology cannot be translated into clinical settings.

Fibrinolytic drug-loaded MNPs can be concentrated at the thrombus under the external high-gradient magnetic field for targeted thrombolysis. Hu et al. [55] employed enzymatical (rtPA reaction) and mechanical clot lysis with rtPA-loaded rotating Fe_3O_4–C microrods (MRs) under an external magnetic field. These MRs were assembled from smaller particles with nanometric pores and possessed an average length L = 1.3 μm and a diameter D = 0.5 μm rtPA-MRs under magnetic field recanalized occluded cerebral artery faster and at a lower dose

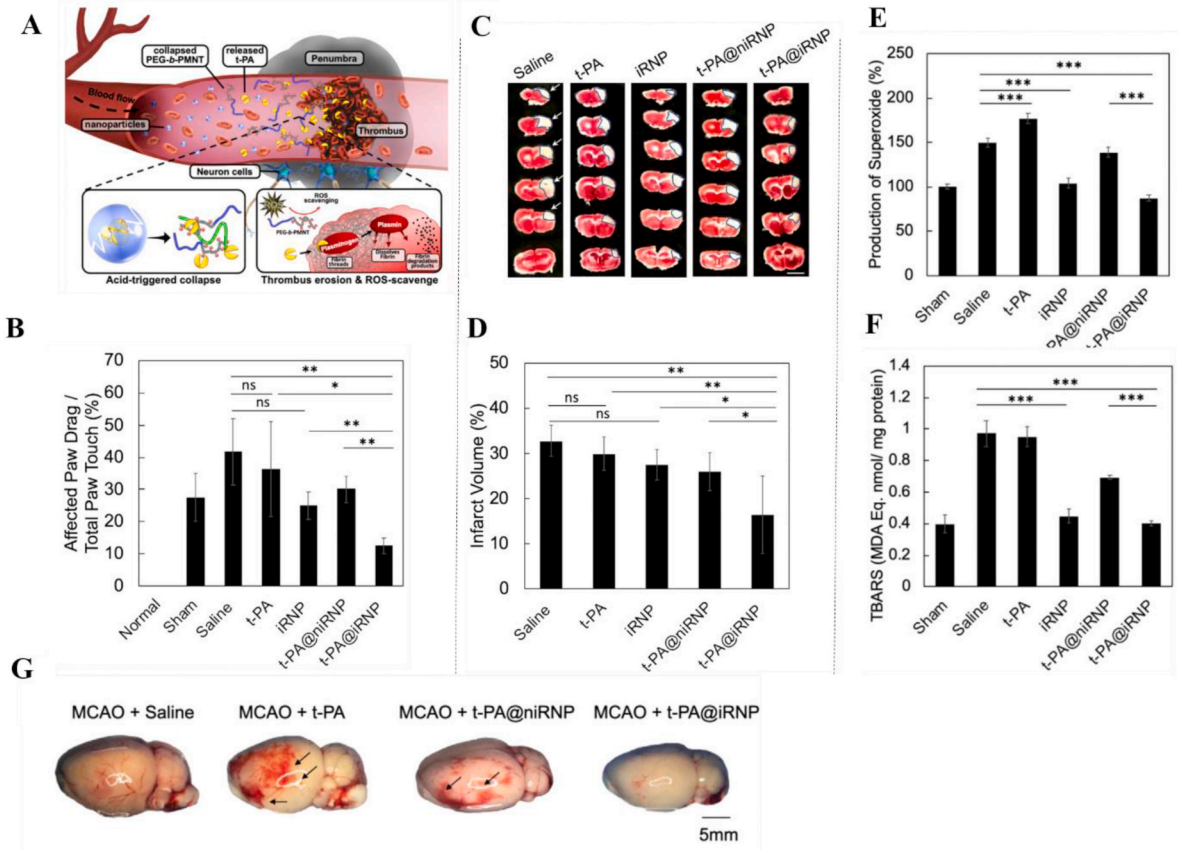

Fig. 7. A. Graphical illustration of the mode of action of t-PA-installed polyion complex possessing ROS-scavenging moieties (t-PA@iRNP) in the thrombus: t-PA@iRNP collapse within the acidic ischemic penumbra region, release t-PA, perform thrombosis and antioxidant activity. (B–G) The therapeutic effect of t-PA@iRNP *in vivo* after middle cerebral artery occlusion (MCAO). B. Analysis of paw-dragging behavior in the cylinder test reveals a reduction in the neurological deficit score for the t-PA@iRNP group. C. Representative images of TTC stained cerebral coronal of the mouse brain, white sections indicate the brain infarct zones (scale bar = 0.5 cm). D. Corresponding quantification of cerebral infarct volume (%). E. Treatment with t-PA@iRNP decreased cerebral superoxide levels, measured by dihydroethidium, at 24 h after injection. F. Treatment with iRNP and t-PA@iRNP reduced thiobarbituric acid-reactive substances (TBARS) level – index of lipid peroxidation in the brain – due to the antioxidant effect. G. Treatment with t-PA@iRNP suppressed t-PA induced cerebral subarachnoid hemorrhage (shown with arrows) with representative images at 24 h after treatment. Adapted with permission from Ref. [48]. Copyright 2019 Elsevier Ltd.

compared to free rtPA group (25 min at 0.13 mg/kg vs. 85 min at 10 mg/kg) and diminished the post-stroke infarct volume *in vivo*. Despite the absence of liver and kidney toxicity of the MRs, they aggregated *in vitro* and required sonication to remain homogeneously dispersed in the suspension.

The drawbacks of uncoated magnetite NPs is that they are prone to oxidation and rapidly aggregate due to strong magnetic dipole-dipole attraction between particles, leading to a loss of magnetization. After the synthesis, a surface coating by SiO_2 or biopolymers is required to improve NP environmental stability, stealth effects, and prolong the blood circulation time. It may additionally provide a variety of high-capacity surface functional groups for bioconjugation of the molecules of interest.

Kempe et al. produced octahedral silica-coated Fe_3O_4 NPs for ferromagnetic implant-assisted magnetic drug targeting of in-stent thrombosis [116]. Silica coating enlarged the hydrodynamic size of the NPs from 10 to 30 nm–~300 nm due to the tight aggregation of naked NPs. rtPA was immobilized onto NP surface via EDC/sulfo-NHS chemistry (71 μg rtPA/1 mg magnetite NPs). In a preliminary experiment on the porcine brachial artery, rtPA-NPs were effective for magnetically guided lysis of in-stent thrombosis at a low rtPA dose of 0.38 mg. In another study [117], silica-coated magnetic nanoparticle (SiO_2-MNP), prepared by the sol-gel method, covalently grafted rtPA with a glutaraldehyde (0.5 mg/mL rtPA/5 mg SiO_2-MNP). After nano-conjugation, the rtPA storage stability increased 9.5-fold in the PBS and 2.8-fold in whole blood. Time of thrombolysis of SiO_2-MNP-rtPA improved by 65% vs. free rtPA in the *ex vivo* intravascular model under magnetic guidance.

The high porosity of the silica coating promotes the encapsulation of the pharmaceutical drugs inside the pores. Wang et al. reported that silica-coated magnetic NPs, prepared by the surfactant templating, with an expanded 6 nm pore size permitted 30-fold more efficient uPA adsorption with sustainable drug release [118]. *In vitro* thrombolytic efficiency was 2-fold superior vs. free uPA and ~1.5-fold faster vs. uPA-loaded supermagnetic non-mesoporous silica NPs under 0.2 T magnet. Yet, silica clinical application needs to be carefully regulated because of the hemolytic effect it might induce as it acts as a hydrogen donor in interactions with cell membrane phospholipids and generates ROS [119,120]. Additionally, silica is shown to provoke an immune response by releasing pro-inflammatory cytokines [121].

Common in cancer therapy *in vivo*, hyperthermia was used as adjuvant therapy for thrombolysis by Voros et al. [75]. Multiple clustered iron oxide nanocubes (NCs), synthesized by a high-temperature thermal decomposition, were surface-coated with a mixture of rtPA and Bovine Serum Albumin (BSA) and produced a local overheating under alternating magnetic fields (295 kHz). rtPA release from NCs doubled at 42 °C from the one at 37 °C within 24 h.

The presence of functional amino and hydroxyl groups makes chitosan and its derivatives a suitable candidate for the magnetic NP surface coating. Chen et al. [122] prepared iron oxide MNP by the chemical co-precipitation and coated with chitosan as a dispersing agent. They immobilized rtPA by glutaraldehyde-mediated amide bond formation

with loading efficiency 95% (0.5 mg rtPA/5 mg chitosan-MNP), maintaining its enzymatic and thrombolytic activities *in vitro*. *In vivo* rat arterial embolic model further evidenced tissue perfusion after treatment of 6,000 G magnetically guided Cs-MNP-rtPA at a dosage of 0.2 mg/kg but not of saline. Alternatively [123], chitosan coating of Fe_3O_4 MNPs was achieved by crosslinking with sodium tripolyphosphate via ionic gelation in the presence of rtPA. On top of targeted magnetic delivery, rtPA-encapsulated NPs unveiled a triggered release: in serum at 37 °C, but not in PBS, which was on/off magnet-sensitive and could be retarded in the presence of a magnetic field. According to the *in vivo* study on the rat embolic model, rtPA-NPs restored blood flow at rtPA dose of 2 mg/kg under magnetic guidance in contrast to NP administration alone.

Dextran, complex branched glucose, is largely used in the coating of MNP. Magneto-fluorescent crosslinked dextran-coated iron oxide (CLIO) NPs targeted arterial and venous thrombi *in vivo* via an activated factor XIII (FXIIIa)-sensitive peptide (GNQEQVSPLTLLKC-NH2) [68]. These theranostic NPs generated optical imaging with NIR VivoTag 680 fluorophore and were covalently functionalized with rtPA via PEG. Thrombolytic efficiency was comparable to the one of free rtPA in the humanized mouse model of pulmonary embolism.

Cytocompatibility of dextran-coated superparamagnetic iron oxide NPs (SPIONs) on human umbilical vein endothelial cells (HUVECs) (~85% cell viability) without changes in mitochondrial membrane potential, a DNA degradation or cell cycle alteration was stated by Heid et al. [124]. When comparing an adsorptive or covalent (EDC/NHS) method to load an arginine-purified rtPA, >80% loading efficiency was achieved for both approaches. Yet, SPIONs with covalently bound rtPA were more efficient to be targeted by a 0.4 T magnet into fibrin clot and to perform a local *in vitro* thrombolysis.

Owing to its natural, biodegradable, and non-toxic character, agarose, a linear polysaccharide extracted from red seaweed, is applied in diverse biotechnological applications. Agarose gel-coated Fe_3O_4 NPs were covalently grafted with uPA via EDC/sulfo-NHS [125]. Urokinase-loaded NPs increased the thrombolytic rate by 50% in the *in vitro* blood clot assay vs. free uPA, as well as in microfluidics test under a static magnetic field of 624 A/m.

Prilepskii et al. [126] crosslinked MNPs with heparin, FDA-approved polysaccharide with anticoagulant activity, and adsorbed uPA with encapsulation of 99% (Fig. 8A). The size of the resulting nanocomposite was around 100 nm (Fig. 8B). Without the inhibitory effect of the heparin on uPA, the thrombolysis rate amplified in the presence of a permanent magnet *in vitro* (12 min vs. 7 min for 60% clot reduction) (Fig. 8C). In the $FeCl_3$ rat carotid artery and rabbit femoral artery models, the MNPs@uPA group speeded reperfusion time and increased blood flow rate ~4 times compared to that of native uPA (Fig. 8D and E).

The synthetic polymer coating is similarly explored for the preparation of magnetic field-responsive and biocompatible NPs. Huang et al. [127] stabilized MNPs with PAA by providing electrostatic and steric repulsion and loaded rtPA via EDC/NHS due to PAA abundant carboxyl groups. The clot lysis efficiency of MNP-rtPA was improved under the rotating magnetic field compared to free rtPA *in vitro*. Besides, MNP-rtPA diminished the brain infarct area in the distal cerebral occlusion *in vivo* model vs. free rtPA (8.65 ± 3.63 mm^3 vs. 4.40 ± 2.46 mm^3).

Another publication compared covalent vs. non-covalent methods of rtPA loading to polyacrylic acid-co-maleic acid (PAM)-coated SPIONs [128]. Better loading efficiency was reported with a covalent method vs. adsorption ($98.6 \pm 0.8\%$ vs. $47.7 \pm 5.4\%$). Amidolytic and fibrinolytic activities on the PAM-SPIONs with covalent loading were superior and better preserved after 40 days of storage. Hence, the covalent binding of the rtPA was advantageous for the application with SPIONs.

Hung-Wei Yang et al. [129] synthesized the magnetic nanocarriers (MNCs) with a water-soluble poly [aniline-co-N-(1-one-butyric acid) aniline] (SPAnH) shell that could load a high amount of rtPA via

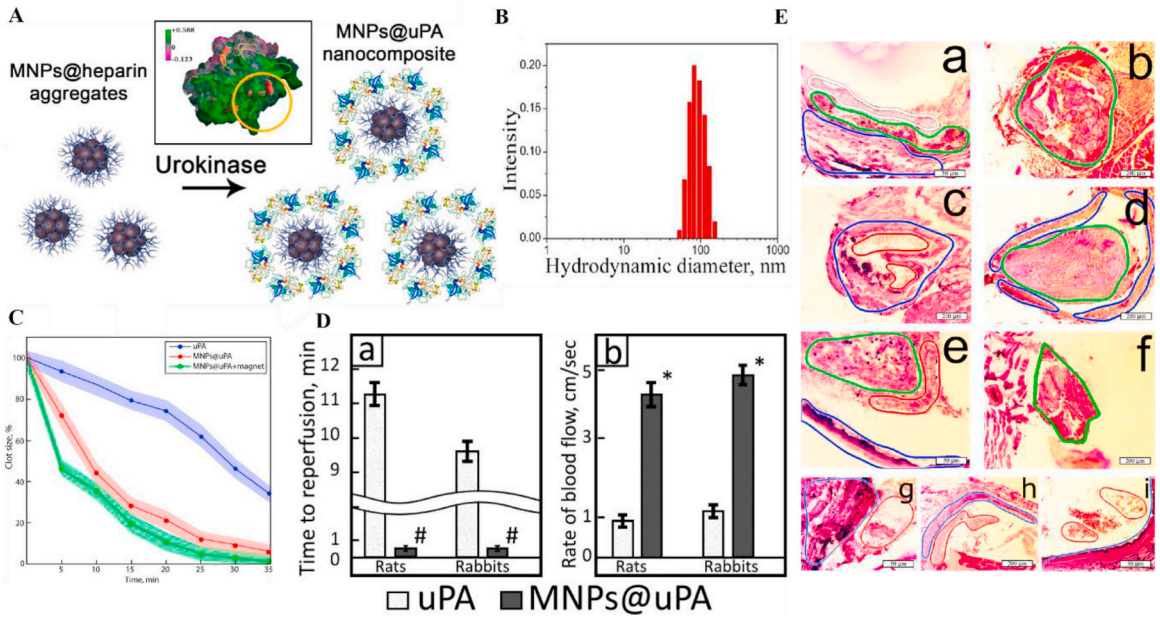

Fig. 8. A. Schematic of the adsorption of uPA to the heparin-coated MNPs to obtain MNPs@uPA. Inset: 3D structure of urokinase with colored electrostatic potentials. Kringle domains responsible for interaction with heparin are in orange. B. The hydrodynamic diameter of MNPs@uPA composite. C. *In vitro* clot lysis rate upon exposure to uPA and MNPs@uPA with or without a magnetic field. The difference in the thrombolysis for MNPs@uPA with and without magnet within the initial 25 min is statistically significant ($p < 0.05$). D. Restoration of blood flow *in vivo* of uPA and MNPs@uPA. (a) Time to vessel reperfusion. (b) Rate of blood flow 24 h post-injection. E. Sections of the rat carotid artery and (g–i) rabbit femoral artery 24 h post-clot formation. Colors: blue, vessel walls; red, erythrocyte aggregates; green, red clot; white, white clot. (a, b, g) Saline. The clot tightly adhered to the vessel wall observed in (a) (marked in green). The vessel fully occluded by the clot (encircled in green) presented in (b). (c, d, h) uPA. Note a clear vessel lumen space between the clot (green) and the vessel wall (blue) in (d). (e, f, i) MNPs@uPA. Note a bigger free space in the vessel lumen and reduced size of the clot in (f) and (i). (a, c, e, g–i): H&E staining. (b, d, f): Picro-Mallory staining. Adapted with permission from Ref. [126]. Copyright 2018 American Chemical Society. (For interpretation of the references to color in this figure legend, the reader is referred to the Web version of this article.)

1-ethyl-3-(3-dimethylaminopropyl)carbodiimide/N-hydroxysuccinimide (EDC/NHS) chemistry (276 μg rtPA per 1 mg MNC). Magnet-guided MNC-rtPA demonstrated significantly improved thrombolysis in rat iliac embolism model at 0.2 mg/kg rtPA dose.

5.2. Gold nanoparticles

Gold nanoparticles (AuNPs) benefit from diverse optical and photothermal properties. They are synthesized by the reduction of gold salts to gold metals in the presence of stabilizing agents to prevent the aggregation during NP formation, and their tunable size modulates their toxicity and biodistribution. Gold NPs can be applied in photothermal therapy in cancer [130] as well as in drug delivery. Moreover, AuNPs are characterized by their high X-ray absorption coefficient enhancing CT signal. The quantitative imaging method *in vivo* was established to monitor the thrombolysis with rtPA using fibrin-targeted glycol chitosan-coated gold NPs [131]. Direct discrimination of thrombi from the underlying tissue was obtained with gold NPs conjugated with a thrombin activatable fluorescent peptide that discharged a near-infrared signal (NIRF) when cleaved [132]. This dual NIRF/micro-CT imaging protocol was tested *in vivo* and suggested a high spatial resolution for a rapid and direct thrombi diagnosis. Indeed, gold NPs represent an interesting perspective to overcome the pitfalls of standard imaging protocols and might allow a better triaging of patients according to their thrombotic conditions.

Gold nanoparticles are similarly capable of delivering large biomolecules, like plasminogen activators. Tang et al. conjugated rtPA with AuNPs with a diameter of 37.8 nm via bio-affinity ligation that is based on the interactions between rtPA and 3-lysine ligand on the AuNPs surface through polyvinyl pyrrolidone (PVP) spacer [51]. Notably, obtained conjugate indicated protection from inhibition by PAI-1 *in vitro* by pre-incubation with the enzyme and prolonged circulation time *in vivo* (6.5 min vs. 20.5 min). Another intelligent nanoplatform for hyperthermia-induced thrombolysis was documented by Wang et al. [47]. Gold@mesoporous silica core-shell nanospheres immobilized uPA in the pores by a solid 1-tetradecanol (tet) (Fig. 9A). Owing to hyperthermia caused by Au absorption of NIR under NIR laser irradiation, tet transformation to liquid phase stimulated a temperature-sensitive controlled release of uPA, whereas only 10.5% of the drug was released at 37 °C vs. 89.5% at 39 °C (Fig. 9B and C). In the carrageenan-induced murine tail thrombus model, NIR-irradiated uPA-NPs group enhanced thrombolytic effect ~2-fold vs. free uPA (Fig. 9D).

In conclusion, several remarkable concepts of inorganic PA-bearing NPs for targeted thrombolysis were published in the last 10 years that have the potential to become theranostics. Despite most of MNP rely on magnet-assisted accumulation on the thrombus, this targeting approach seems to be tricky to accomplish in healthcare settings. An interesting application of inorganic NPs is hyperthermic exposure as adjuvant therapy to fibrinolytic therapy. Nevertheless, it must be remembered

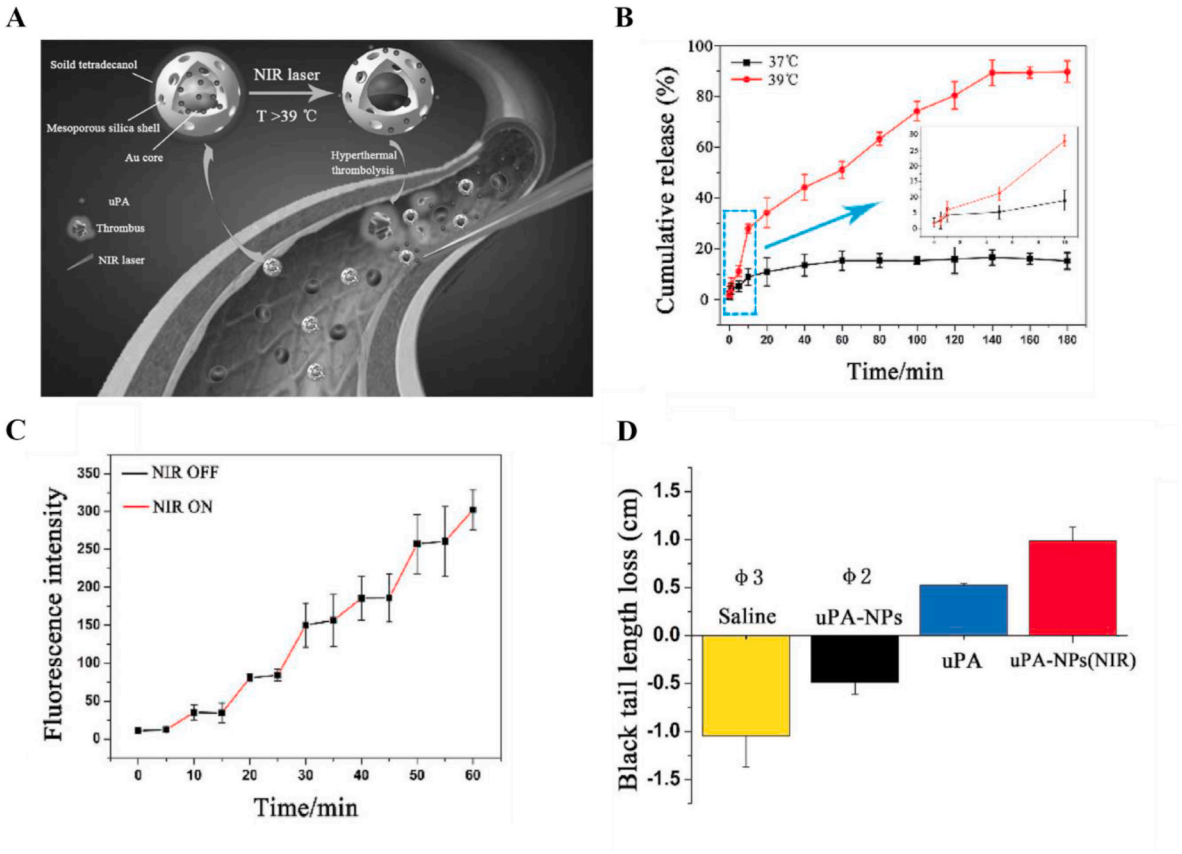

Fig. 9. A. Schematic illustration of the hyperthermia-induced enhanced thrombolysis with uPA-immobilized gold@mesoporous silica nanospheres. B. *In vitro* release profiles of fluorescent uPA from uPA-NPs at 37 °C and 39 °C, respectively. The enlarged release profile in 10 min is shown at the inset graph. C. NIR laser triggers pulsed uPA release profile *in vitro* of fluorescent uPA-NPs. D. *In vivo* thrombolysis in murine tail thrombus model via injecting carrageenan. The statistical black tail length loss (thrombolytic effect) of mice after treatment for 9 days, where ϕ represents the amputated tail, and the number represents the number of mice with the amputated tail. Adapted with permission from Ref. [47]. Copyright 2017 WILEY-VCH Verlag GmbH & Co. KGaA, Weinheim. (For interpretation of the references to color in this figure legend, the reader is referred to the Web version of this article.)

that NPs from inorganic materials are difficult to degrade *in vivo* and they persist for long periods (more details on safety and metabolism in Section 8.1).

6. Bio-inspired nanocarriers

Nature inspires the development of nanotechnological solutions in drug-delivery systems. Bio-inspiration and biomimicry technologies can not only simulate biological materials by their chemical structure but also by their biological functions [133].

Camouflage. An elegant strategy to reduce thrombolytic drug elimination and increase its plasma half-life is to camouflage it as endogenous proteins. This approach was demonstrated by Absar et al. [134] when the targeted/triggered release of rtPA was mediated by the presence of thrombin in the thrombus. rtPA was camouflaged by conjugating with human serum albumin (HSA) via a thrombin-cleavable peptide (tcP) and decorated with a homing-peptide targeting GPIIb/IIIa. This construct permitted to temporarily suppress the enzymatic and fibrinolytic activities of camouflaged rtPA, however, to spontaneously restore it upon incubation with thrombin by the cleavage of the peptide linker.

Red blood cell (RBC)-derived nanocarriers. Erythrocytes are recognized for their extended blood circulation as they manage to avoid clearance by the macrophages up to 3 months. A number of factors are believed to contribute to that, including their discoidal shape, deformability, and the expression of self-recognition biomarkers, such as CD47 and CD200 [133,135]. RBC seem to be a particularly promising carrier of thrombolytic drugs that exert their pharmacological activity within blood vessels.

Vankayala et al. [136] designed theranostic nanoconstructs for near-infrared (NIR) fluorescence imaging and thrombolytic activity. Specifically, after hypotonic treatment of RBCs, obtained erythrocyte ghosts were coupled with indocyanine green, FDA-approved NIR imaging agent, and conjugated with rtPA via amine-aldehyde chemistry. Their thrombolytic efficacy was comparable to the free rtPA *in vitro*. Erythrocytes have already reached clinical trials as nanocarriers for drug delivery (Clinicaltrials.gov Identifiers: NCT01255358, NCT01171807, NCT00484965) but not in thrombolytic therapy yet [133].

Platelet-like nanocarriers. Platelet membrane-camouflaged PLGA-core NPs, conjugated with rtPA, were recently proposed as a biomimetic technique by Xu et al. [76]. These so-called "nanoplatelets" behave like platelets in the blood circulation (Fig. 10A and B) and bind to the thrombus *in vitro* and *ex vivo*. rtPA-NPs treatment was beneficial in multiple *in vivo* models: improved the mouse survival time from 4-7 days to 14.5 days and ~4.5-fold reduced the thrombus area vs. free rtPA in the pulmonary embolism model (Fig. 10C and D); stimulated complete thrombus removal contrary to free rtPA in the $FeCl_3$-induced mesenteric arterial model. Notably, post-thrombolytic brain damage was weaker for the rtPA-NPs group as defined by a lower neurological deficit score and smaller ischemic area in the ischemic stroke mouse model, as depicted on Fig. 10E–G.

There has been a growing interest in exploring neuroprotective strategies following acute ischemic stroke to reduce brain injury [137]. Another version of the "nanoplatelets" was proposed as a combinational approach for the treatment of acute ischemic stroke based on thrombolysis and neuroprotection [138]. The NPs with a size of ~150 nm contained the core of acetal modified dextran & neuroprotective agent and were covered with a platelet membrane conjugated with thrombin-cleavable Tat-peptide (Tat-LTPRGWRLGGC) that coupled rtPA (Fig. 11A). In this nanodesign, rtPA could be released upon thrombin presence while exposing Tat-peptide on the NPs and

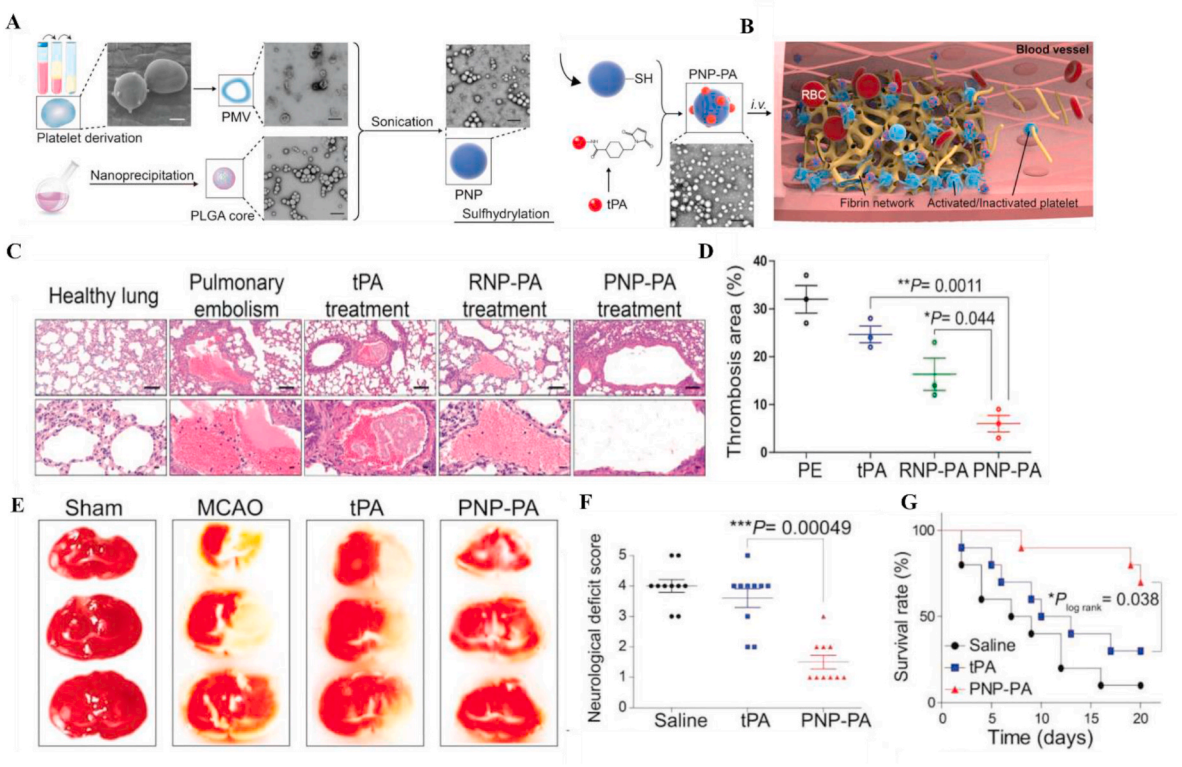

Fig. 10. A. Schematic illustration of the synthesis of PNP-PA NPs. Briefly, the membrane of platelets (scale bar = 1 μm), acquired from the whole blood of mice, were used to coat the PLGA cores (scale bar = 400 nm). t-PA was subsequently conjugated via –SH groups onto the surface of the platelet membrane to form PNP-PA. B. The proposed mechanism of action *in vivo*: mimicking platelets, PNP-PA are specifically targeted to the thrombus and dissolve the fibrin clot. C. Therapeutic potential of PNP-PA in a pulmonary embolism mouse model. Lung sections with H&E staining administered the indicated treatments (scale bar = 50 μm). D. Quantitative analysis of the thrombus area in panel C. E-G. Therapeutic effects of PNP-PA in the ischemic stroke mouse model. E. Representative TTC staining images of MCAO mouse brains treated with the indicated formulations. F. Neurological deficit scores in the treatment groups of MCAO mice. G. The survival rate of MCAO mice treated with the mentioned formulations. Adapted with permission from Ref. [76]. Copyright 2019 WILEY-VCH Verlag GmbH & Co. KGaA, Weinheim.

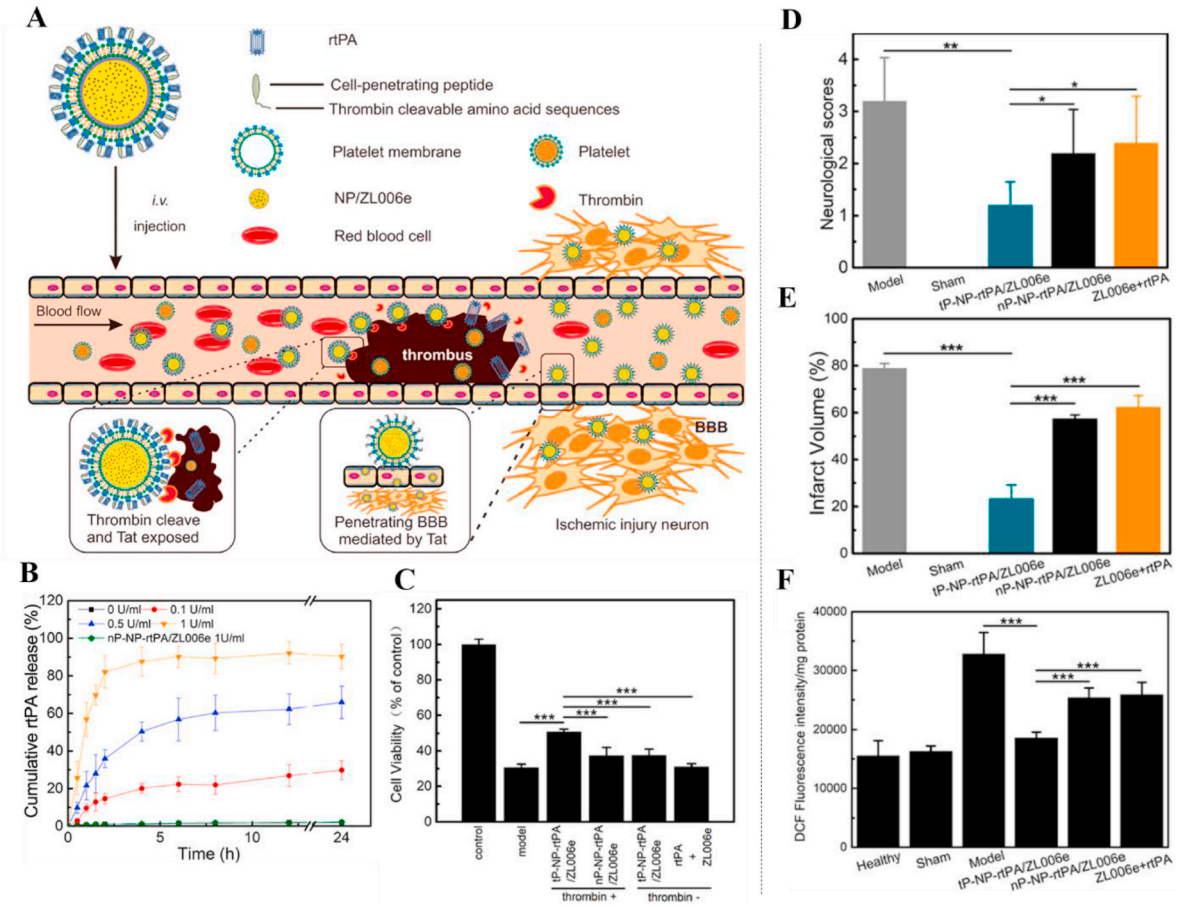

Fig. 11. A. Schematic design of tP-NP-rtPA/ZL006e and its components and mode of action. After intravenous injection, tP-NP-rtPA/ZL006e are targeted to the thrombus for thrombin-triggered release of rtPA and thrombolysis. Nanocarrier transport into the brain via Tat-mediated transcytosis for neuroprotective activity. B. Cumulative release of rtPA from tP-NP-rtPA/ZL006e with different thrombin concentrations. nP-NP-rtPA/ZL006e are the control particles in 1 U/mL thrombin. C. *In vitro* neuroprotective effect of tP-NP-rtPA/ZL006e and nP-NP-rtPA/ZL006e with or without thrombin and free ZL006e + rtPA via the coculture model of the BCEC monolayer and glutamate-stimulated PC-12 cells. D. Neurological scores of the MCAO rats after the treatment. E. Quantification of brain infarct volume/ischemic brain hemisphere at 24 h post-treatment MCAO rats. F. ROS level in the ischemic region. Adapted with permission from Ref. [138]. Copyright 2019 American Chemical Society.

penetrating BBB for neuroprotectant delivery in the brain (Fig. 11B and C). In the *in vivo* model of middle cerebral artery (MCA) occlusion, a treatment with this nanocomplex decreased infarct size by 63%, ameliorated neurological deficit, and diminished ROS level of the ischemic region by 52% compared to the free drug combination (Fig. 11D–F).

Leukocyte-derived microvesicles. Cell microvesicles that originate from the plasma membrane of most cell types, including blood cells, are essential effectors in the intercellular communication and may transport bioactive molecules [139]. Silva et al. reported an unconventional method when microvesicles (D = 673 ± 168 nm), secreted from macrophages upon serum depletion cellular stress, were capable of enclosing both iron oxide NPs and rtPA [140]. The work exemplified a biogenic strategy of theranostic application of hybrid microvesicles for MRI imaging and spatially-controlled rtPA delivery via magnetic field gradient targeting.

Bacterial spores. In another bio-inspired approach, the spores of bacterium *Bacillus amyloliquefaciens* with peptidoglycans on their surface were prior inactivated with a high-pressure steam sterilizer and used as nanocarriers with uPA and RGDS peptide [141]. The solid monodisperse oval spheres ([0.67 ± 0.20 μm] × [1.27 ± 0.20 μm]) were non-biotoxic following histological evaluation of the heart, kidneys, and liver. With a higher thrombolysis rate *in vitro*, *in vivo* tail bleeding times of the uPA-NPs group were shorter than that of free uPA (601 s vs. 1145 s), suggesting a lower risk of hemorrhages.

Viral nanoparticles. Based on bacteriophages and plant viruses, viral nanoparticles (VNPs) are biocompatible, biodegradable, and nonpathogenic nanocarriers in humans. Because of the remarkable proliferation of viruses, they could be easily manufactured up to an industrial scale. In the NPs based on the tobacco mosaic virus, the nucleic acids are tightly enclosed in a stiff hollow tubular capsid comprising coat proteins [142]. To develop a nanocarrier with optimal flow properties for thrombolytic therapy, Pitek et al. conjugated rtPA to tobacco mosaic virus mutant soft elongated nanorods containing lysine side chain (TMV-Lys) via PEG linkers, obtaining the NPs with dimensions of 300 × 18 nm [143]. TMV-rtPA could passively accumulate at the thrombus at a higher rate than TMV-PEG *in vivo*. Both rtPA and TMV-rtPA resumed the circulation in the mouse thrombosis model, but TMV-rtPA reduced bleeding time ~2-fold vs. free rtPA. Despite an absence of pathogenicity, the potential immunogenicity of nanodelivery systems based on pathogens such as bacteria and viruses should be not be neglected.

To conclude, biomimetic delivery systems have the countless potential for the advancement of drug delivery technologies. The reproduction of the biological complexity on nanocarriers' surface imitates biological features, like biocompatibility, targeting to the thrombus tissue, efficient circulation profiles, etc. To be suitable for clinical translation, both toxicological (e.g., safety, immunogenicity) and pharmaceutical (e.g., reproducibility, scale-up, standardization of chemical composition) concerns have to be examined [144].

7. Ultrasound-responsive carriers & sonothrombolysis

Microbubbles (MBs) are defined as spheroid objects stabilized by a coating material [145], such as lipids, polymers [146], or denatured proteins, and filled with a gas or a combination of gases (air or perfluorocarbons). Their average size should not exceed red blood cell size (6–8 μm) to avoid embolization [147].

The application of these novel therapeutic agents originated from US imaging, since local US insonation induces acoustic steaming of the surrounding tissues [148] that may help drugs to penetrate deeper into the clot by local mechanical stress induction. Sawaguchi et al. illustrated this hypothesis with an *in vitro* blood clot lysis experiment and demonstrated that the US itself can accelerate thrombolysis [149]. Using 500 kHz US insonation, the authors pointed out that the thrombolysis acceleration ratio was about 2.5 times greater with rtPA combined with the US than rtPA treatment alone. Thrombolytic therapy combined with the US could reduce the dose of rtPA by 60% owing to the synergistic effect.

In the cardiovascular field, microbubbles are mostly designed as contrast agents for ultrasound molecular imaging due to their ability of radiation oscillation, upraising the contrast of tissues. Every bubble is subjected to stable cavitation in low range frequencies and can undergo inertial cavitation (burst) under higher frequencies [150]. Cavitation is the process of induced bubble growth and collapse and can be achieved by different mechanisms [151], including ultrasonic waves [152]. Association of ultrasound insonation and microbubble stimulation is called sonothrombolysis (Fig. 12) and is promising to enhance thrombolysis.

The focus on MBs for thrombolytic therapy was initially published by Tachibana et al. [153] and Porter et al. in 1996 [60] with an *in vitro* model of enhanced thrombolysis using dextrose albumin MBs and a low-frequency transducer. Nowadays, most of the lab-made microbubbles are phospholipid-based and obtained from a sonication-lyophilization-rehydration process [154–157], microfluidics [158], or coaxial electrohydrodynamic atomization process [159], and called echogenic liposomes (ELIP) [160]. Laing et al. took benefit from the rehydration step to incorporate rtPA and obtain thrombolytic-loaded ELIP. With natural rtPA affinity to fibrin [156], the authors highlighted the significant contribution of a high mechanical index (0.4) on the recanalization rate of the obstructed artery in the rabbit model. Mechanical Index (MI) is a unitless ratio between the peak of negative pressure and the square root of the frequency in MHz. It is applied to predict the bioeffect of ultrasound; when MI is > 0.3, microbubbles are easily destructed [161] but may have harmful bioeffects above 1.9 value [162]. One of the limitations of this study was the lack of stable cavitation of these air-filled MBs. To remediate this issue, other gas fillers were explored, like Shekhar's [155] octafluoropropane targeting ELIP that allowed more robust stable cavitation, significantly enhancing thrombolysis *in vitro*.

Literature accordingly claims that US insonation of microbubbles on the thrombus site triggers sonothrombolysis due to the cavitation process [157]. The average lytic rate obtained with rtPA loaded ELIP and the US was recorded to be over 2-fold higher than free rtPA with an *in vitro* flow model [155]. Zhu et al. [163] published similar results with their uPA loaded targeted microbubbles from Targerson Inc. and the US.

Microbubble targeting agents are similar to other functionalized NPs: mostly RGDS peptide targeting GPIIb/IIIa on activated platelets [163–166], heat denaturated collagen that binds vWF [167], or scFv targeting GPIIb/IIIa grafted on Nonlinear Ultrasound Contrast Agent by Visual Sonics® via biotin/streptavidin coupling [168]. Hua et al. [164] published the *in vivo* study presenting the theranostic potential of their rtPA-loaded MBs with RGD peptide and 2 MHz ultrasound. A high recanalization rate was obtained with a 15 times lower dose of rtPA.

The magnetic field was also observed as a targeting strategy [169] by using ferrofluid in the composition of the MBs. As expected, significant enhancement of the cavitation energy was observed when a magnet was placed on the thrombi location, limiting the prolonged exposure of ultrasonic waves. Potentially, this magnetic element in the MBs may allow MRI imaging [167].

A complete overview of small animal sonothrombolysis stroke models has been published by Auboire et al. [170] in 2018. The overall perspective for further treatment model is suggested to be on the range of sub-Mhz frequencies and intensities that favor stable cavitation of the MBs. It described sonothrombolysis as a potential treatment for small vessel impairment or larger arteries occlusion.

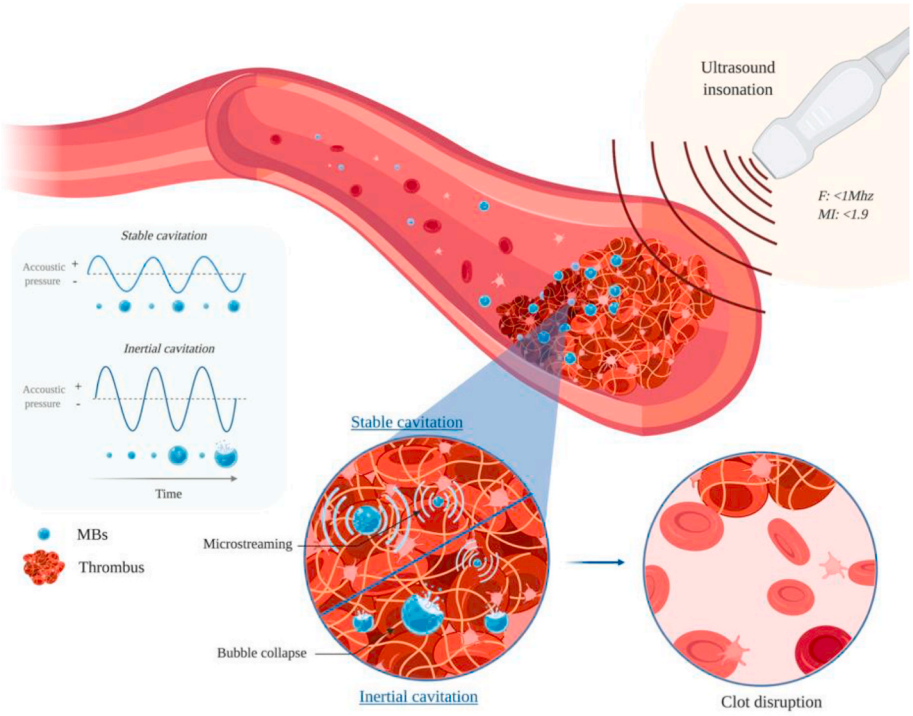

Fig. 12. Sonothrombolysis precept for enhanced thrombolysis. Sonothrombolysis is performed by the ultrasound insonation of MBs on the thrombus site. Microbubble radial oscillation properties are sensitive to acoustic pressure. The bubbles can undergo stable cavitation inducing microstreaming of the surrounding environment or inertial cavitation leading to the collapse of the bubble. While MBs alone are proven to destabilize a clot with US insonation, sonothrombolysis efficacy is enhanced with the thrombus specific targeting and loaded thrombolytic agent on the MBs. Abbreviations: *F*, frequency; *MI*, mechanical index; *MBs*, microbubbles.

Preclinical trial on big animals was performed on a porcine model at the VU University Medical center in the Netherlands [166] with RGDS targeted SonoVue® microbubbles loaded with uPA. Pigs received the premedication to prevent the potential allergic reactions to the lipid shells of the MBs. MBs were injected intraluminally to simulate a clinical setting, and 1.1 MI was applied. Three out of 5 pigs of the uPA targeted MBs group showed an increase in the arterial flow and recanalization rate, whereas only 1 out of 4 in the uPA group showed a slight improvement. A major limitation of this study was a lack of information about the exact concentration of the encapsulated drug.

Because of their echogenic properties, some microbubbles are already clinically used as a diagnostic tool [171], such as DEFINITY® (Lantheus Medical Imaging) or SonoVue® (Bracco Diagnostics), in order to enhance ventricular opacification and US imaging of tumor angiogenesis. Those approved microbubbles are composed of a phospholipid shell but not yet loaded with therapeutic agents. Yet, preclinical studies on acute cerebral ischemia on rats demonstrated that focused weak energy US associated with SonoVue® injection was as efficient as fibrinolysis with rtPA [172]. Recanalization in an occluded vein model was efficient with microbubble cavitation only under US insonation directly on the vein within 10 min [173], which may be advantageous to limit hemorrhage risks induced by PA.

Sonothrombolysis treatment has already stepped up to clinical trials with the following ones: MUST (Microbubbles and Ultrasound in Stroke Trial, Clinicaltrials.gov Identifiers: NCT00132691) performed at the University of Toulouse in France and CLOTBUST Hands-Free (Combined Lysis of Thrombus in Brain Ischemia With Transcranial Ultrasound and Systemic T-PA-Hands-Free, ClinicalTrials.gov Identifier: NCT01240356) at The University of Texas Health Science Center, Houston. While MUST trial was aborted after incidences of intracerebral hemorrhages [171], CLOTBUST Hands-Free showed great recanalization rates in combination with systemic rtPA on ischemic stroke patients [174]. Finally, an ongoing clinical trial is evaluating the efficacy of SonoVue® MBs associated with rtPA and US insonation compared to classic rtPA injection on acute ischemic stroke patients in the 4.5 h window treatment. This study takes place in Barcelona, Spain on 24 participants and results have not been reported yet (ClinicalTrials.gov Identifier: NCT01678495).

Recent work focused on nanobubbles (NBs) coupled with cRGD peptide [71], instead of their microscale peers, to facilitate deeper blood clot penetration. Jiang et al. used the high-frequency US to burst these NBs to decrease the risk of clinical bleeding due to the enhancement of permeability of low frequencies. Comparing SonoVue® MBs to the NBs, both in combination with uPA and submitted to the US, it was observed a difference in the clot degradation: a peripheral relaxation in the MBs group vs. a fissure like a collapse in the NBs one. The nanometric scale of these particles seemed to deconstruct the clot from the inside.

Ultrasound is mainly applied in diagnostics in the clinic because it is safe, easy and quick to utilize at an affordable cost. The therapeutic potential of US-responsive carriers and sonothrombolysis is promising in fibrinolytic therapy. The main goal is to improve the efficiency of thrombolytic therapy on highly retracted thrombi where the medications struggle to penetrate [175], but where the mechanical properties of the MBs and NBs could be a significant gain.

8. Nanoparticle optimal design for thrombolytic therapy

8.1. Pharmacokinetics, biodistribution, and safety

After the intravenous administration, nanocarriers for fibrinolytic therapy are subjected to biological barriers and might pose particular safety concerns that would limit a desirable therapeutic outcome. What would be an optimal nanoparticle design to incorporate in order to load plasminogen activator and perform a safe and efficient local thrombolysis?

Primarily, favorable *in vivo* biodistribution and pharmacokinetics of the injectable inorganic, lipid, and polymeric micelle/nanoparticle must be ensured. Particle *in vivo* fate is varied and dictated by the interaction between multiple parameters: nanoparticle size, surface characteristics, stability, etc. For site-specific accumulation of the thrombolytic agent, NPs need to have sufficient circulation time *in vivo*. Ultra-small NPs with diameters <5.5 nm are rapidly filtered out by renal clearance upon intravenous administration [176]. The elimination of the larger engineered NPs by the MPS represents a substantial obstacle. Plasma proteins, including serum albumin, apolipoproteins, complement components, and immunoglobulins, bind onto the surface of circulating NPs and form the protein corona in a process called particle opsonization [177]. Subsequently, phagocytic cells of MPS – mainly resident macrophages in the spleen, lymph nodes, and liver – sequesters the NPs. There is an evident direct correlation between particle size and serum protein absorption, also meaning faster elimination [178]. Typically, rigid spherical NPs with a size of 100–200 nm are long-circulating, being large enough to avoid uptake in the liver but small enough to avoid filtration in the spleen [135]. Particles in the micrometer range (2–5 μm) accumulate within capillaries of the lungs, as well as in spleen and liver [33]. The shape of the particles has a dramatic effect on their *in vivo* destiny, as demonstrated in the filamentous polymer micelles that persisted in the circulation for up to one week after the intravenous injection – 10 times longer than the spherical ones [179]. In addition, softer, prone to deformability, NPs have prolonged circulation profiles than solid ones with reduced splenic filtration, as investigated in the nanogels with different levels of crosslinking [180]. Irrespective of the size and shape, softer nanoconstructs evaded up to 5 times more efficiently macrophage internalization as compared to rigid nanoconstructs [181].

The biodistribution of nanomaterials is influenced by their surface characteristics. NPs with a neutral and negative surface charge, in contrast to cationic formulations, experience reduced protein adsorption that results in more extended circulation half-lives [33]. Other concerns of the cationic NPs are the stimulation of inflammatory responses of human neutrophils and increased ROS production that was demonstrated on the cationic liposomes [182] and solid lipid NPs [183]. Cytotoxicity was induced by both cationic polymeric and lipid NPs [184]. In addition, positively charged NPs have a high rate of cellular uptake, as revealed that polymeric microparticles with a primary amine at the surface underwent more phagocytosis as compared to the ones having sulfate, hydroxyl, or carboxyl groups [178]. This makes cationic NPs a suitable vehicle for gene delivery; however, it would probably be preferred to design anionic nanoformulation for thrombolysis.

To avert the opsonization of the naked circulating NPs, their surface can be functionalized with PEG to create a hydrating layer that hinders the formation of a protein corona [33]. In addition to prevalent PEG, that is non-biodegradable and may cause complement activation, alternative hydrophilic polymers, such as polaxamer, polyvinyl alcohol, poly(amino acid)s, and polysaccharides [185] as well as "self" peptide CD47 [186] are researched. As a biomimetic surface, the coating of NPs with cell membranes extracted from autologous leukocytes and erythrocytes similarly extends their *in vivo* circulation [133].

Collectively, these findings demonstrate the importance of tunable particle size and surface composition & functionality for the development of long-circulating NPs for thrombolysis.

While the full analysis of the toxicology of NPs is beyond the scope of this paper, it is necessary to comment on certain safety issues of the nanomaterials used for a thrombolytic application.

NPs can perturbate vascular hemostasis and blood platelet function. Saikia et al. reported that silica NPs induced the overexpression of platelet endothelial cell adhesion molecule-1 on the endothelium that augmented the platelet-endothelial interaction [187]. Moreover, silica NPs triggered inflammation-coagulation response and thrombotic effects *in vivo* via JAK1/TF signaling pathway [188]. Amorphous silica NPs penetrated the platelet plasma membrane and stimulated an unfavorably low nitric oxide to peroxynitrite [NO]/[$ONOO^-$] ration that is crucial for cardiovascular homeostasis; they also induced platelet activation and aggregation via the MMP2 and ADP pathways [189].

Increasing concentrations of gold NPs led to a reduction in mouse body weight, red blood cell count, and hematocrit [190].

Multiple publications reported nanoparticle size-dependent toxicity. For instance, smaller gold, SiO_2, or polymer NPs were more hemolytic and provoked a higher level of ROS production than larger particles [191]. Cytotoxicity in four different cell lines was observed with the triphenylphosphine-stabilized gold NPs of 1–2 nm diameter, while 15-nm particles were non-toxic even at 100-fold higher concentration [192]. In a size-dependent manner, PEGylated AuNPs affected the normal function of human erythrocytes, such as deformability and oxygen-delivering ability [193]. Alterations of renal, hepatic, and splenic functions were dependent on the particle size and surface chemistry in ultrasmall SPION [194].

Distribution of the NPs in the non-target cells and organs is one of the challenges. The report of Lasagna-Reeves et al. suggested that gold NPs were able to cross the blood-brain barrier (BBB) and accumulated in the neural tissue [195]. Poly(alkyl cyanoacrylate) NPs could enter into the brain both in healthy animals and models of central nervous system diseases [196]. Siddiqi et al. concluded that AuNPs generated oxidative stress and an impairment of the antioxidant enzyme glutathione peroxidase in rat brain as well as significantly decreased the levels of dopamine and serotonin neurotransmitters [197]. Given that the BBB integrity is disrupted during ischemic stroke [198], and nano-formulation is assumed to limit the accumulation of nanoparticle-associated rtPA within the brain parenchyma to reduce the risk of cerebral hemorrhages and rtPA-mediated neurotoxicity [199], it would be vital to ensure that the nanotherapeutics are retained within the vascular compartment and do not cross the BBB.

The nanomaterials accumulate substantially in the liver upon intravenous injection. Bartneck et al. found that peptide-functionalized gold nanorods induced the prepolarization of hepatic macrophages, which aggravated a liver injury in a model of acute hepatitis [200]. High doses of silica nanorattle particles could induce liver damages, presumably due to decreased activity of superoxide dismutase [201]. Treatment with silica NPs revealed the hepatic microgranulation and splenic megakaryocyte accumulation by histological analysis [202]. Iron oxide NPs accumulated in liver phagocytes and elicited hepatic lipid peroxidation [203].

It is likely that organic biodegradable engineered NPs are of lesser concern to toxicity, as they will degrade by metabolic pathways. While the *in vitro* tests indicated that amphiphilic polymeric micelles induced an inflammatory response, no pathological changes were observed in the target organs *in vivo* [204]. Both PLGA and Cs NPs at concentrations relevant for drug-delivery application (<10 μg/mL) were platelet-compatible [205].

In contrast, inorganic non-biodegradable NPs, including multifunctional magnetic NPs, may persist for considerable periods, sometimes up to several years [206], and result in prolonged exposure with still-to-be-determined consequences. Apart from that, the growing presence of non-degradable nanotechnology products and the environmental risks need to be seriously assessed [207]. NPs composed of inorganic materials are difficult to break down by lysosomal enzymes. As an example, AuNPs accumulation in Kupffer cells in the liver and lysosome/endosome-like vesicles was present after six months post-injection in mice [208]. Moreover, Feng et al. found that dextran-coated and uncoated SPION administration affected several metabolism pathways, including energy, lipid, glucose, and amino acid metabolism in rodents [209]. PAA-coated iron oxide NPs triggered an inflammatory process *in vivo*, evidenced by abnormal differential blood count of neutrophils and large lymphocytes [203]. Fe_3O_4-MNPs significantly augmented ROS production *in vivo*. A sharp decline in RBC counts and hemoglobin concentration indicated an excessive degradation of erythrocytes, suggesting an associated anemia risk [210].

Generally, higher metabolic and functional injuries are prompted by uncoated NPs compared to coated ones with potential aggregation in the biological fluids. Surface modification with polymeric chains ameliorates the nanoparticle stability, masks the existing toxicity of the NPs, and extends their circulation half-life [121,211]. It is worth admitting that the NPs do not exhibit any toxicity until a certain threshold dose [121]. During the preclinical thrombolytic evaluation, it is also important to verify that the required dose of the NPs is based on estimates of potential future human exposure to avoid unrealistically high nanoparticle doses with no relevance to the clinics. Overall, this is critical to evaluate each newly engineered NPs as an individual case, since even slight changes in physicochemical properties to an existing and well-studied particle can result in a completely different toxicological profile.

8.2. Strategies for the nanoencapsulation of PA

PA are hydrophilic macromolecules (40–70 kDa) that require special nanoparticle design and drug complexation methods. While PA can be incorporated into the aqueous phase during nanoparticle fabrication for lipid or polymeric particles, harsh synthesis conditions – high energy processes (ultrasound, ultraturrax), elevated temperatures, the use of organic solvents – are not suitable for fragile molecules such as proteins [212]. Otherwise, the fibrinolytic agent may be attached to the surface through covalent or non-covalent protocols. The covalent methods provide more stable conjugation (avoiding “burst release”), however, they sometimes require chemical modification of the drug and might affect changes in the protein structure that might result in its partial denaturation and loss of enzymatic activity [213]. Physical adsorption is a mild drug encapsulation method that results in high loading efficacy for the nanocarriers with hydrophilic surfaces. As PA are predominantly positively charged at physiological pH with an isoelectric point (IP) > 7 (except for SK, IP $= 5.12$), they can form a complexation with anionic NPs due to electrostatic interactions. The existence of a positive charge on the polymer, as, for instance, chitosan, limits the encapsulation of cationic drugs because of repulsive interactions between a drug and polymer [212]. Comparing covalent vs. non-covalent methods, adsorptive bound PA liberates faster from the particles and diffused more readily into the fibrin matrix of the clot than covalently bound PA [128] and does not impair the biological activity of the drug [214] that may be beneficial in targeted thrombolysis. In addition, effective entrapment of hydrophilic drugs may occur in the crosslinked polymeric network of hydrogel nanoparticles that imbibe large quantities of water [215].

To sum up, depending on the type and composition of the nanocarrier, different encapsulation techniques may be applied. Extensive *in vitro* tests demonstrating high loading efficiency, sustainable release, preservation of the amidolytic and fibrinolytic activates of the PA after conjugation must be verified.

9. Discussion & conclusion

The rapid recanalization of the vascular occlusion is of the utmost importance for the patients suffering from acute thrombotic diseases. The innovative nanomedical approaches have been intensively proposed for targeted thrombolytic therapy to address the challenges of systemic drug administration.

The accomplishments of nanomedicine in thrombotic diseases include the protection of thrombolytics from inactivation by PAI-1, improvement in the blood half-life, enhanced thrombolytic effect at a lower dose, reduction in systemic bleeding, and post-ischemic infarct zone, etc. Recent studies have demonstrated that nanocarriers, such as liposomes, polymeric or inorganic NPs, bio-inspired nanocarriers, and microbubbles, provide benefits for thrombolytic therapy either alone or in combination with ultrasound or magnetic force (Table 2). Current nano-approaches in targeted thrombolysis are summarized schematically in Fig. 13. Among the numerous thrombolytic-bearing nanocarriers that are tested in preclinical models, sonothrombolysis with lipid-based microbubbles and intravenous rtPA is already being validated in clinical trials with thrombolysis improvement. However, lipid microbubbles

Table 2
Different nanocarriers for thrombolytic therapy.

Nanocarriers	Advantages	Disadvantages	Therapeutic effects
Liposomes	• Biodegradable, biocompatible, non-toxic • Clinically approved	• Low PA encapsulation rate • Low stability • Phospholipids may undergo oxidation and hydrolysis	• Improved thrombolysis rate • Lower risks of hemorrhages
Polymeric	• Biocompatible and often biodegradable • Easy surface functionalization	• High PA encapsulation rate • Improved stability	• Superior thrombolytic efficacy • Accelerated thrombolysis • Protection BBB permeability damage • Increased survival *in vivo* • Improved neurological deficit • Reduction in cerebral ROS • Reduction in subarachnoid hemorrhage
Inorganic Fe_3O_4 NPs AuNPs	• Biocompatible • Superparamagnetic properties • Magnet-guided thrombolysis • Optical and photothermal properties • Multifunctional theranostic systems	• May enter BBB and generate ROS • Accumulation in the body • May induce immunogenic response or inflammation	• Faster vessel recanalization • Mechanical clot dissolution with an external magnet • Hyperthermia as adjuvant therapy • Increased blood flow rate • Reduction in infarct volume
Bio-inspired	• Prolonged *in vivo* circulation • Natural thrombus targeting	• Low reproducibility • Lack of standardization • Source availability • Immunogenicity • Scale-up	• Improved survival rate • Superior thrombolytic efficacy • Lower neurological deficit score • Smaller ischemic zone • Better neurological outcome • Diminished ROS level in the brain • Lower risk of hemorrhages
US-responsive	• Enhanced thrombolysis with US insonation • Biocompatibility • US imaging	• Low stability • Merging into big MBs • Vessel occlusion	• US stable cavitation - higher penetration of drugs or MBs into the clot • US inertial cavitation: sonothrombolysis

Abbreviations: *PA*, plasminogen activator; *BBB*, blood-brain barrier; *NPs*, nanoparticles; *ROS*, reactive oxygen species; *US*, ultrasound; *MBs*, microbubbles.

may coalesce and form resonant bubbles with a size of over 20 μm [158], inducing the risk of pulmonary embolism [155]. Alternatively, polymeric microbubbles have enhanced stability *in vivo* over the soft shell ones [216], and the recent work [217] described echogenic polymeric fucoidan-functionalized microbubbles, able to target thrombosis via P-selectin interactions.

Active drug targeting of the nanocarriers allows drug accumulation at the thrombus site and has the potential to enhance thrombolytic penetration into deeply localized thrombi. This is currently realized by directing NPs mostly towards fibrin and platelets, though, identification of the new target molecules and development of the inexpensive and specific targeting moieties will be useful. Fucoidan, which is at present under clinical investigation as a diagnostic agent for the imaging of thrombosis [218,219], may become an affordable and high-quality alternative to antibodies and peptides. Another thrombus targeting strategy relies on the use of magnetic NPs under external magnetic force irradiation. Yet, despite an abundance of preclinical works dealing with magnetic field-assisted guiding, there is no clinically approved medical device to impose a high magnetic force on NPs in deep blood vessels. Therefore, it is probably preferable to design NPs capable of targeting thrombosis without external triggers.

A growing number of reports demonstrate a controlled release of the thrombolytics. On top of the ultrasound that can control the drug release from the echogenic liposomes, microbubbles, and some polymer (gelatin and chitosan) NPs, other strategies, such as enzyme exposure ($sPLA_2$ or thrombin), pH, temperature, shear stress, magnet, are employed (Fig. 13).

Apart from the necessity of the rapid restoration of blood flow after thrombotic occlusions, combating the ischemia-reperfusion injury such as inflammation and oxidative damage is vital for a good prognosis. Hence, complementing fibrinolytic therapy with nanodelivery of a potent antioxidant would be a sensible approach. For instance, poly (isobutyl cyanoacrylate)-polysaccharide NPs bearing microRNA-155–5p were proposed as a cardio-protective therapy for MI due to their antioxidant and cytoprotective properties [220]. Besides, rtPA might be accompanied by neuroprotection to prevent brain injury and neuronal damage during or after exposure to ischemia following acute ischemic stroke [221]. Discovery of next-generation thrombolytic drugs is further required to improve the safety and efficacy of nanomedicine-based thrombolysis. Goulay et al. engineered a non-neurotoxic rtPA variant with an equal fibrinolytic potential but without stimulating NMDA-dependent neurotoxicity [222].

The design of theranostic nanosystems with both thrombolytics and imaging agents (e.g., NIR fluorescent probes, gold, iron oxides, or perfluorocarbon) integrates diagnostic and therapeutic modalities. This strategy may not only provide visualization of drug delivery in real-time but also evaluate the effectiveness of treatment by MRI, CT, or US.

It is critical to face the challenges of nanomedicine, particularly in an attempt for clinical translation. To ensure clinical safety, the potential toxicity of NPs needs to be considered with a careful examination of their physical and chemical characteristics and accumulation in the non-target organs and tissues [223]. Indeed, some NPs may cause oxidative stress generation, immunological response, protein misfolding, immune response, and DNA damage [121]. Selecting biocompatible and fully biodegradable materials with FDA-approval, as well as a scalable production of the nanoformulations according to Good Manufacturing Practice (GMP), is essential [224]. Incorporation of sophisticated nanodesigns (e.g., cell-derived biomimetic surfaces) should accord with a risk analysis of reproducibility, quality control, and toxicity that might complicate regulatory approvals [33].

There is an evident gap between scientific discovery and clinical practice in nanomedicine-guided thrombolytic therapy. An astonishing ~10-fold increase from 2010 to 2020 in the number of publications in the field with beneficial therapeutic effects demonstrates a solid argument towards an imminent clinical translation. At the development stage, the tendency is to design complex targeted biomimetic multifunctional nanocarriers, sometimes bearing several active molecules. By examining nanoparticle delivery systems that are currently approved or under clinical investigation [35,36], we speculate that the first nanoparticulate candidate for site-specific delivery of PA tested in humans will probably be built on long-established technologies – primarily PEGylated liposomes, but also albumin-coated PA or nanocarriers from FDA-approved polymers. More sophisticated systems with targeting moieties, stimuli-responsive control of drug release will follow.

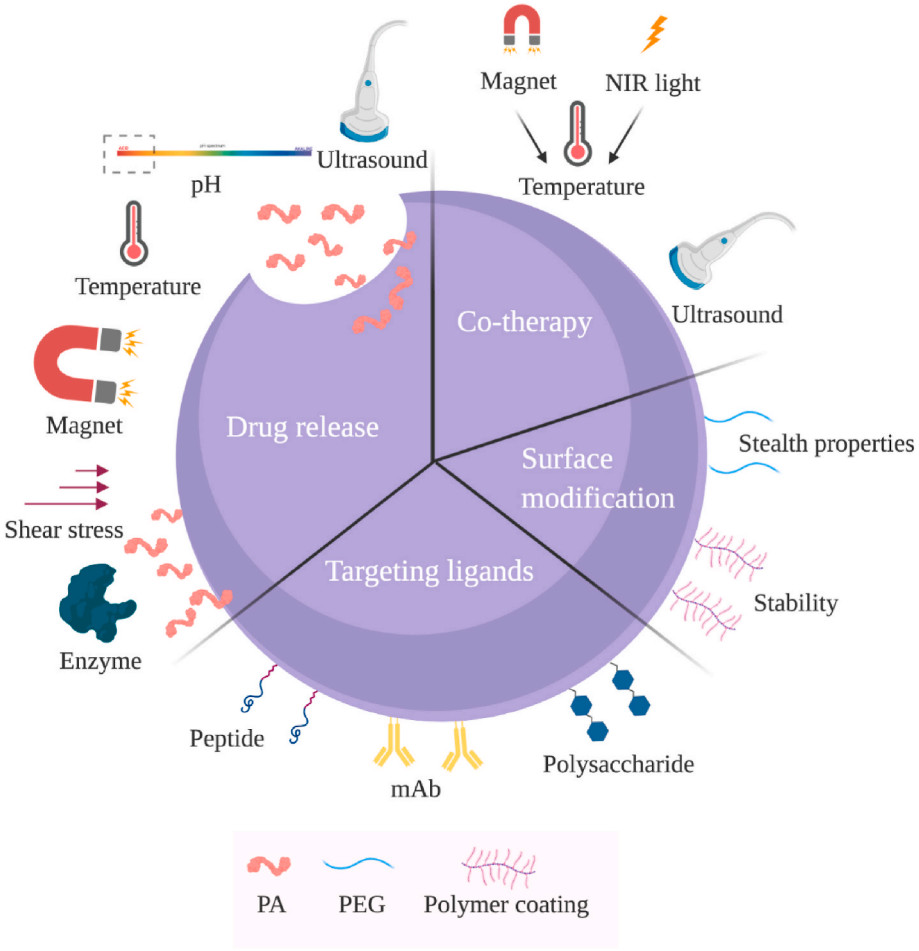

Fig. 13. Schematic illustration of the main strategies in the development of thrombolytic drug delivery nanocarriers. Surface modification with PEG or other hydrophilic polymeric chains is effectuated to ameliorate the nanoparticle stability, prevent the opsonization, and extend the nanoparticle blood circulation time. Nanoparticles may be decorated with targeting moieties against thrombus biomarkers with monoclonal antibodies, peptides, or sulfated polysaccharide fucoidan to attain site-specific thrombolysis. Several endogenous (enzymes in the thrombi, high shear stress in stenotic vessels, or low pH in the ischemic area) and exogenous (magnetic field, elevated temperature, ultrasound) principles are researched for the spatial & temporal control of PA release, prior incorporated either in the core of the nanoparticles or onto their surface. As an adjuvant therapy, ultrasound irradiation or elevated temperature by magnet and NIR light enhances nanomedicine-assisted thrombolytic efficacy. Abbreviations: *PA*, plasminogen activator; *mAb*, monoclonal antibody; *PEG*, Polyethylene glycol; *NIR*, near-infrared.

Meanwhile, public initiatives contribute to nanomedicine development. Recently, the European Union project NanoAthero (http://www.nanoathero.eu/) was completed. It intended to use nanomedicine for molecular imaging and targeted treatment of atherothrombosis with research activities ranging from nanosystems design to clinical validation and industrial production [225]. Several Phase I clinical trials demonstrated its feasibility for patients [219,226–228]. This consortium of 16 partners lasted 5.5 years (February 2013–July 2018) with the European Commission contribution of 10 million euros.

To conclude, the development of novel nanoparticulate strategies with plasminogen activators for the treatment of thrombotic disease will continue to flourish as they represent a potent evolution to free drug administration. The encouraging results in preclinical research predict future clinical translation of some of the formulations and progress in the nanomedicine-based precise therapy of thrombotic pathologies.

Author contributions

Alina Zenych: Conceptualization, Writing - original draft, Visualization; Louise Fournier: Writing - original draft (Section: 7 Ultrasound-Responsive Carriers & Sonothrombolysis), Visualization; Cédric Chauvierre: Writing - review & editing, Supervision, Funding acquisition.

Declaration of competing interest

The authors declare that they have no known competing financial interests or personal relationships that could have appeared to influence the work reported in this paper.

Acknowledgment

Authors thank INSERM, Université de Paris, and Université Sorbonne Paris Nord for the financial support. This work also received funding from the EU project FP7-NMP-2012-LARGE-6-309820 “NanoAthero”. Alina Zenych is grateful for the Ph.D. fellowship from the INSPIRE program of the European Union’s Horizon 2020 research and innovation program (Marie Sklodowska-Curie grant # 665850). The illustrations were designed with BioRender software (biorender.com).

References

[1] World Health Organisation (WHO), [Internet] World Health Organization, Media Centre: Cardiovascular disease, 2020. https://www.who.int/health-topics/cardiovascular-diseases/#tab=tab_1.

[2] E.J. Benjamin, P. Muntner, A. Alonso, M.S. Bittencourt, C.W. Callaway, A. P. Carson, A.M. Chamberlain, A.R. Chang, S. Cheng, S.R. Das, F.N. Delling, L. Djousse, M.S.V. Elkind, J.F. Ferguson, M. Fornage, L.C. Jordan, S.S. Khan, B. M. Kissela, K.L. Knutson, T.W. Kwan, D.T. Lackland, T.T. Lewis, J.H. Lichtman, C. T. Longenecker, M.S. Loop, P.L. Lutsey, S.S. Martin, K. Matsushita, A.E. Moran, M.E. Mussolino, M. O'Flaherty, A. Pandey, A.M. Perak, W.D. Rosamond, G. A. Roth, U.K.A. Sampson, G.M. Satou, E.B. Schroeder, S.H. Shah, N.L. Spartano, A. Stokes, D.L. Tirschwell, C.W. Tsao, M.P. Turakhia, L.B. VanWagner, J. T. Wilkins, S.S. Wong, S.S. Virani, Heart disease and stroke statistics—2019 update: a report from the American heart association, Circulation (2019), https://doi.org/10.1161/CIR.0000000000000659.

[3] H. Thomas, J. Diamond, A. Vieco, S. Chaudhuri, E. Shinnar, S. Cromer, P. Perel, G.A. Mensah, J. Narula, C.O. Johnson, G.A. Roth, A.E. Moran, Global atlas of cardiovascular disease 2000-2016: the path to prevention and control, Glob. Heart. 13 (2018) 143–163, https://doi.org/10.1016/j.gheart.2018.09.511.

[4] J. Leal, R. Luengo-Fernández, A. Gray, S. Petersen, M. Rayner, Economic burden of cardiovascular diseases in the enlarged European Union, Eur. Heart J. 27 (2006) 1610–1619, https://doi.org/10.1093/eurheartj/ehi733.

[5] D.N. Granger, P.R. Kvietys, Reperfusion injury and reactive oxygen species: the evolution of a concept, Redox Biol 6 (2015) 524–551, https://doi.org/10.1016/j.redox.2015.08.020.

[6] C.K. Glass, J.L. Witztum, Atherosclerosis: the road ahead, Cell 104 (2001) 503–516, https://doi.org/10.5005/jp/books/12883_4.

[7] E. Falk, Pathogenesis of atherosclerosis, J. Am. Coll. Cardiol. 47 (2006) C7–C12, https://doi.org/10.1016/j.jacc.2005.09.068.

[8] Y.S. Chatzizisis, A.U. Coskun, M. Jonas, E.R. Edelman, C.L. Feldman, P.H. Stone, Role of endothelial shear stress in the natural history of coronary atherosclerosis and vascular remodeling. Molecular, cellular, and vascular behavior, J. Am. Coll. Cardiol. 49 (2007) 2379–2393, https://doi.org/10.1016/j.jacc.2007.02.059.

[9] G.G. Caro, Discovery of the role of wall shear in atherosclerosis, Arterioscler. Thromb. Vasc. Biol. 29 (2009) 158–161, https://doi.org/10.1161/ATVBAHA.108.166736.

[10] J. Jongstra-Bilen, M. Haidari, S.N. Zhu, M. Chen, D. Guha, M.I. Cybulsky, Low-grade chronic inflammation in regions of the normal mouse arterial intima predisposed to atherosclerosis, J. Exp. Med. 203 (2006) 2073–2083, https://doi.org/10.1084/jem.20060245.

[11] P. Libby, Inflammation in atherosclerosis, Nature 420 (2002) 868–874, https://doi.org/10.1038/nature01323.

[12] Z.S. Galis, G.K. Sukhova, R. Kranzhöfer, S. Clark, P. Libby, Macrophage foam cells from experimental atheroma constitutively produce matrix-degrading proteinases, Proc. Natl. Acad. Sci. U.S.A. 92 (1995) 402–406, https://doi.org/10.1073/pnas.92.2.402.

[13] M.R. Dweck, E. Aikawa, D.E. Newby, J.M. Tarkin, J.H.F. Rudd, J. Narula, Z. A. Fayad, Noninvasive molecular imaging of disease activity in atherosclerosis, Circ. Res. 119 (2016) 330–340, https://doi.org/10.1161/CIRCRESAHA.116.307971.

[14] A. Shioi, Y. Ikari, Plaque calcification during atherosclerosis progression and regression, J. Atherosclerosis Thromb. 25 (2018) 294–303, https://doi.org/10.5551/jat.RV17020.

[15] G. Lippi, M. Franchini, G. Targher, Arterial thrombus formation in cardiovascular disease, Nat. Rev. Cardiol. 8 (2011) 502–512, https://doi.org/10.1038/nrcardio.2011.91.

[16] N. Mackman, Triggers, targets and treatments for thrombosis, Nature 451 (2008) 914–918, https://doi.org/10.1038/nature06797.

[17] I. Martinelli, P. Bucciarelli, P.M. Mannucci, Thrombotic risk factors: basic pathophysiology, Crit. Care Med. 38 (2010), https://doi.org/10.1097/CCM.0b013e3181c9cbd9.

[18] C.T. Esmon, Basic mechanisms and pathogenesis of venous thrombosis, Blood Rev. 23 (2009) 225–229, https://doi.org/10.1016/j.blre.2009.07.002.

[19] J.A. López, J. Chen, Pathophysiology of venous thrombosis, Thromb. Res. 123 (2009) 30–34, https://doi.org/10.1016/S0049-3848(09)70140-9.

[20] A. Bivard, L. Lin, M.W. Parsonsb, Review of stroke thrombolytics, J. Stroke. 15 (2013) 90, https://doi.org/10.5853/jos.2013.15.2.90.

[21] C. Kluft, J.J. Sidelmann, J.B. Gram, Assessing safety of thrombolytic therapy, Semin. Thromb. Hemost. 43 (2017) 300–310, https://doi.org/10.1055/s-0036-1584130.

[22] R.S. Marshall, Progress in intravenous thrombolytic therapy for acute stroke, JAMA Neurol 72 (2015) 928–934, https://doi.org/10.1001/jamaneurol.2015.0835.

[23] V.J. Marder, Thrombolytic therapy. Consult. Hemost. Thromb., Elsevier, 2013, pp. 526–537, https://doi.org/10.1016/B978-1-4557-2296-9.00028-2.

[24] J. Schaller, S.S. Gerber, The plasmin-antiplasmin system: structural and functional aspects, Cell, Mol. Life Sci. 68 (2011) 785–801, https://doi.org/10.1007/s00018-010-0566-5.

[25] A. Pal Khasa, Y. Pal Khasa, The evolution of recombinant thrombolytics: current status and future directions, Bioengineered 8 (2017) 331–358, https://doi.org/10.1080/21655979.2016.1229718.

[26] G.N. Levine, E.R. Bates, J.C. Blankenship, S.R. Bailey, J.A. Bittl, B. Cercek, C. E. Chambers, S.G. Ellis, R.A. Guyton, S.M. Hollenberg, U.N. Khot, R.A. Lange, L. Mauri, R. Mehran, I.D. Moussa, D. Mukherjee, H.H. Ting, P.T. O'Gara, F. G. Kushner, D.D. Ascheim, R.G. Brindis, D.E. Casey, M.K. Chung, J.A. De Lemos, D.B. Diercks, J.C. Fang, B.A. Franklin, C.B. Granger, H.M. Krumholz, J. A. Linderbaum, D.A. Morrow, L.K. Newby, J.P. Ornato, N. Ou, M.J. Radford, J. E. Tamis-Holland, C.L. Tommaso, C.M. Tracy, Y.J. Woo, D.X. Zhao, 2015 ACC/AHA/SCAI focused update on primary percutaneous coronary intervention for patients with ST-elevation myocardial infarction an update of the 2011 ACCF/AHA/SCAI guideline for percutaneous coronary intervention and the 2013 ACCF/AHA guideline for th, J. Am. Coll. Cardiol. 67 (2016) 1235–1250, https://doi.org/10.1016/j.jacc.2015.10.005.

[27] B. Ibanez, S. James, S. Agewall, M.J. Antunes, C. Bucciarelli-Ducci, H. Bueno, A.L. P. Caforio, F. Crea, J.A. Goudevenos, S. Halvorsen, G. Hindricks, A. Kastrati, M. J. Lenzen, E. Prescott, M. Roffi, M. Valgimigli, C. Varenhorst, P. Vranckx, P. Widimský, A. Baumbach, R. Bugiardini, I.M. Coman, V. Delgado, D. Fitzsimons, O. Gaemperli, A.H. Gershlick, S. Gielen, V.P. Harjola, H.A. Katus, J. Knuuti, P. Kolh, C. Leclercq, G.Y.H. Lip, J. Morais, A.N. Neskovic, F.J. Neumann, A. Niessner, M.F. Piepoli, D.J. Richter, E. Shlyakhto, I.A. Simpson, P.G. Steg, C. J. Terkelsen, K. Thygesen, S. Windecker, J.L. Zamorano, U. Zeymer, M. Chettibi, H.G. Hayrapetyan, B. Metzler, F. Ibrahimov, V. Sujayeva, C. Beauloye, L. Dizdarevic-Hudic, K. Karamfiloff, B. Skoric, L. Antoniades, P. Tousek, C. J. Terkelsen, S.M. Shaheen, T. Marandi, M. Niemelᵭa, S. Kedev, M. Gilard, A. Aladashvili, A. Elsaesser, I.G. Kanakakis, B. Merkely, T. Gudnason, Z. Iakobishvili, L. Bolognese, S. Berkinbayev, G. Bajraktari, M. Beishenkulov, I. Zake, H. Ben Lamin, O. Gustiene, B. Pereira, R.G. Xuereb, S. Ztot, V. Juliebø, J. Legutko, A.T. Timoteo, G. Tatu-Chitoiu, A. Yakovlev, L. Bertelli, M. Nedeljkovic, M. Studencan, M. Bunc, A.M.G. de Castro, P. Petursson, R. Jeger, M.S. Mourali, A. Yildirir, A. Parkhomenko, C.P. Gale, 2017 ESC Guidelines for the management of acute myocardial infarction in patients presenting with ST-segment elevation, Eur. Heart J. 39 (2018) 119–177, https://doi.org/10.1093/eurheartj/ehx393.

[28] G. Turc, P. Bhogal, U. Fischer, P. Khatri, K. Lobotesis, M. Mazighi, P. D. Schellinger, D. Toni, J. de Vries, P. White, J. Fiehler, European stroke organisation (ESO) – European society for minimally invasive neurological therapy (ESMINT) guidelines on mechanical thrombectomy in acute ischaemic StrokeEndorsed by stroke alliance for europe (SAFE), Eur. Stroke J. 4 (2019) 6–12, https://doi.org/10.1177/2396987319832140.

[29] W.J. Powers, A.A. Rabinstein, T. Ackerson, O.M. Adeoye, N.C. Bambakidis, K. Becker, J. Biller, M. Brown, B.M. Demaerschalk, B. Hoh, E.C. Jauch, C. S. Kidwell, T.M. Leslie-Mazwi, B. Ovbiagele, P.A. Scott, K.N. Sheth, A. M. Southerland, D.V. Summers, D.L. Tirschwell, Guidelines for the early management of patients with acute ischemic stroke: 2019 update to the 2018 guidelines for the early management of acute ischemic stroke: a guideline for healthcare professionals from the American heart association/American stroke, Stroke 50 (2019) e344–e418, https://doi.org/10.1161/STR.0000000000000211.

[30] L. Derex, T.H. Cho, Mechanical thrombectomy in acute ischemic stroke, Rev. Neurol. (Paris) 173 (2017) 106–113, https://doi.org/10.1016/j.neurol.2016.06.008.

[31] S.A. Munich, K. Vakharia, E.I. Levy, Overview of mechanical thrombectomy techniques, Clin. Neurosurg. 85 (2019) S60–S67, https://doi.org/10.1093/neuros/nyz071.

[32] G. Forestier, B. Kerleroux, K. Janot, F. Zhu, V. Dumas, J.-F. Hak, E. Shotar, W. BenHassen, R. Bourcier, S. Soize, J. Berge, O. Naggara, H. Desal, G. Boulouis, A. Rouchaud, Mechanical thrombectomy practices in France: exhaustive survey of centers and individual operators, J. Neuroradiol. (2020) 1–14, https://doi.org/10.1016/j.neurad.2020.05.001.

[33] E. Blanco, H. Shen, M. Ferrari, Principles of nanoparticle design for overcoming biological barriers to drug delivery, Nat. Biotechnol. 33 (2015) 941–951, https://doi.org/10.1038/nbt.3330.

[34] Y. Barenholz, Doxil® - the first FDA-approved nano-drug: lessons learned, J. Contr. Release 160 (2012) 117–134, https://doi.org/10.1016/j.jconrel.2012.03.020.

[35] A.C. Anselmo, S. Mitragotri, Nanoparticles in the clinic, Bioeng. Transl. Med. 1 (2016) 10–29, https://doi.org/10.1002/btm2.10003.

[36] A.C. Anselmo, S. Mitragotri, Nanoparticles in the clinic: an update, Bioeng. Transl. Med. 4 (2019) 1–16, https://doi.org/10.1002/btm2.10143.

[37] T. Matoba, J.-I. Koga, K. Nakano, K. Egashira, H. Tsutsui, Nanoparticle-mediated drug delivery system for atherosclerotic cardiovascular disease, J. Cardiol. 70 (2017) 206–211, https://doi.org/10.1016/j.jjcc.2017.03.005.

[38] T. Alam, S. Khan, B. Gaba, M.F. Haider, S. Baboota, J. Ali, Nanocarriers as treatment modalities for hypertension, Drug Deliv. 24 (2017) 358–369, https://doi.org/10.1080/10717544.2016.1255999.

[39] C.K.W. Chan, L. Zhang, C.K. Cheng, H. Yang, Y. Huang, X.Y. Tian, C.H.J. Choi, Recent advances in managing atherosclerosis via nanomedicine, Small 14 (2018) 1–16, https://doi.org/10.1002/smll.201702793.

[40] T. Cyrus, S.A. Wickline, G.M. Lanza, Nanotechnology in interventional cardiology, Wiley Interdiscip. Rev. Nanomedicine Nanobiotechnology. 4 (2012) 82–95, https://doi.org/10.1002/wnan.154.

[41] L. Yu, B.J. Scherlag, K. Dormer, K.T. Nguyen, C. Pope, K.M. Fung, S.S. Po, Autonomic denervation with magnetic nanoparticles, Circulation 122 (2010) 2653–2659, https://doi.org/10.1161/CIRCULATIONAHA.110.940288.

[42] T. Simon-Yarza, I. Bataille, D. Letourneur, Cardiovascular bio-engineering: current state of the art, J. Cardiovasc. Transl. Res. 10 (2017) 180–193, https://doi.org/10.1007/s12265-017-9740-6.

[43] D.R. Esfahani, V. Viswanathan, A. Alaraj, Nanoparticles and stem cells–has targeted therapy for aneurysms finally arrived? Neurol. Res. 37 (2015) 269–277, https://doi.org/10.1179/1743132814Y.0000000435.

[44] C. Psarros, R. Lee, M. Margaritis, C. Antoniades, Nanomedicine for the prevention, treatment and imaging of atherosclerosis, Nanomed. Nanotechnol. Biol. Med. 8 (2012) S59–S68, https://doi.org/10.1016/j.nano.2012.05.006.

[45] B. Singh, T. Garg, A.K. Goyal, G. Rath, Recent advancements in the cardiovascular drug carriers, Artif. Cells, Nanomedicine Biotechnol 44 (2016) 216–225, https://doi.org/10.3109/21691401.2014.937868.

[46] C.H. Liu, H.L. Hsu, J.P. Chen, T. Wu, Y.H. Ma, Thrombolysis induced by intravenous administration of plasminogen activator in magnetoliposomes: dual targeting by magnetic and thermal manipulation, Nanomed. Nanotechnol. Biol. Med. 20 (2019) 1–12, https://doi.org/10.1016/j.nano.2019.03.014.

[47] X. Wang, C. Wei, M. Liu, T. Yang, W. Zhou, Y. Liu, K. Hong, S. Wang, H. Xin, X. Ding, Near-infrared triggered release of uPA from nanospheres for localized hyperthermia-enhanced thrombolysis, Adv. Funct. Mater. 27 (2017) 1–8, https://doi.org/10.1002/adfm.201701824.

[48] T. Mei, A. Kim, L.B. Vong, A. Marushima, S. Puentes, Y. Matsumaru, A. Matsumura, Y. Nagasaki, Encapsulation of tissue plasminogen activator in pH-sensitive self-assembled antioxidant nanoparticles for ischemic stroke treatment-Synergistic effect of thrombolysis and antioxidant, Biomaterials 215 (2019) 1–12, https://doi.org/10.1016/j.biomaterials.2019.05.020.

[49] Q.L. Zhou, Z.Y. Chen, Y.X. Wang, F. Yang, Y. Lin, Y.Y. Liao, Ultrasound-mediated local drug and gene delivery using nanocarriers, BioMed Res. Int. 2014 (2014), https://doi.org/10.1155/2014/963891.

[50] V. Karagkiozaki, S. Logothetidis, A.M. Pappa, Nanomedicine for atherosclerosis: molecular imaging and treatment, J. Biomed. Nanotechnol. 11 (2015) 191–210, https://doi.org/10.1166/jbn.2015.1943.

[51] Z. Tang, D. Li, X. Wang, H. Gong, Y. Luan, Z. Liu, J.L. Brash, H. Chen, A t-PA/nanoparticle conjugate with fully retained enzymatic activity and prolonged circulation time, J. Mater. Chem. B. 3 (2015) 977–982, https://doi.org/10.1039/c4tb01625d.
[52] S. Absar, K. Nahar, Y.M. Kwon, F. Ahsan, Thrombus-targeted nanocarrier attenuates bleeding complications associated with conventional thrombolytic therapy, Pharm. Res. (N. Y.) 30 (2013) 1663–1676, https://doi.org/10.1007/s11095-013-1011-x.
[53] H. Jin, H. Tan, L. Zhao, W. Sun, L. Zhu, Y. Sun, H. Hao, H. Xing, L. Liu, X. Qu, Y. Huang, Z. Yang, Ultrasound-triggered thrombolysis using urokinase-loaded nanogels, Int. J. Pharm. 434 (2012) 384–390, https://doi.org/10.1016/j.ijpharm.2012.06.001.
[54] H. Kawata, Y. Uesugi, T. Soeda, Y. Takemoto, J.H. Sung, K. Umaki, K. Kato, K. Ogiwara, K. Nogami, K. Ishigami, M. Horii, S. Uemura, M. Shima, Y. Tabata, Y. Saito, A new drug delivery system for intravenous coronary thrombolysis with thrombus targeting and stealth activity recoverable by ultrasound, J. Am. Coll. Cardiol. 60 (2012) 2550–2557, https://doi.org/10.1016/j.jacc.2012.08.1008.
[55] J. Hu, S. Huang, L. Zhu, W. Huang, Y. Zhao, K. Jin, Q. Zhuge, Tissue plasminogen activator-porous magnetic microrods for targeted thrombolytic therapy after ischemic stroke, ACS Appl. Mater. Interfaces 10 (2018) 32988–32997, https://doi.org/10.1021/acsami.8b09423.
[56] N. Zhang, C. Li, D. Zhou, C. Ding, Y. Jin, Q. Tian, X. Meng, K. Pu, Y. Zhu, Cyclic RGD functionalized liposomes encapsulating urokinase for thrombolysis, Acta Biomater. 70 (2018) 227–236, https://doi.org/10.1016/j.actbio.2018.01.038.
[57] C.L. Pawlowski, W. Li, M. Sun, K. Ravichandran, D. Hickman, C. Kos, G. Kaur, A. Sen Gupta, Platelet microparticle-inspired clot-responsive nanomedicine for targeted fibrinolysis, Biomaterials 128 (2017) 94–108, https://doi.org/10.1016/j.biomaterials.2017.03.012.
[58] V. Torchilin, M. Papisov, N. Orekhova, A. Belyaev, A. Petrov, S. Ragimov, Magnetically driven thrombolytic preparation containing immobilized streptokinase-targeted transport and action, Haemostasis 18 (1988) 113-116, https://doi.org/10.1159/000215791.
[59] P.D. Nguyen, E.A. O'Rear, A.E. Johnson, E. Patterson, T.L. Whitsett, R. Bhakta, Accelerated thrombolysis and reperfusion in a canine model of myocardial infarction by liposomal encapsulation of streptokinase, Circ. Res. 66 (1990) 875–878, https://doi.org/10.1161/01.RES.66.3.875.
[60] T.R. Porter, R.F. LeVeen, R. Fox, A. Kricsfeld, F. Xie, Thrombolytic enhancement with perfluorocarbon-exposed sonicated dextrose albumin microbubbles, Am. Heart J. 132 (1996) 964–968, https://doi.org/10.1016/S0002-8703(96)90006-X.
[61] J.K. Leach, E. Patterson, E.A. O'Rear, Encapsulation of a plasminogen activator speeds reperfusion, lessens infarct and reduces blood loss in a canine model of coronary artery thrombosis, Thromb, Haemostasis 91 (2004) 1213–1218, https://doi.org/10.1160/th03-11-0704.
[62] J.-C. Murciano, S. Medinilla, D. Eslin, E. Atochina, D.B. Cines, V.R. Muzykantov, Prophylactic fibrinolysis through selective dissolution of nascent clots by tPA-carrying erythrocytes, Nat. Biotechnol. 21 (2003) 891–896, https://doi.org/10.1038/nbt846.
[63] M. Faria, M. Björnmalm, K.J. Thurecht, S.J. Kent, R.G. Parton, M. Kavallaris, A.P. R. Johnston, J.J. Gooding, S.R. Corrie, B.J. Boyd, P. Thordarson, A.K. Whittaker, M.M. Stevens, C.A. Prestidge, C.J.H. Porter, W.J. Parak, T.P. Davis, E.J. Crampin, F. Caruso, Minimum information reporting in bio–nano experimental literature, Nat. Nanotechnol. 13 (2018) 777–785, https://doi.org/10.1038/s41565-018-0246-4.
[64] T.W. Chung, S.S. Wang, W.J. Tsai, Accelerating thrombolysis with chitosan-coated plasminogen activators encapsulated in poly-(lactide-co-glycolide) (PLGA) nanoparticles, Biomaterials 29 (2008) 228–237, https://doi.org/10.1016/j.biomaterials.2007.09.027.
[65] F. Bi, J. Zhang, Y. Su, Y.C. Tang, J.N. Liu, Chemical conjugation of urokinase to magnetic nanoparticles for targeted thrombolysis, Biomaterials 30 (2009) 5125–5130, https://doi.org/10.1016/j.biomaterials.2009.06.006.
[66] Y.-H. Ma, S.-Y. Wu, T. Wu, Y.-J. Chang, M.-Y. Hua, J.-P. Chen, Magnetically targeted thrombolysis with recombinant tissue plasminogen activator bound to polyacrylic acid-coated nanoparticles, Biomaterials 30 (2009) 3343–3351, https://doi.org/10.1016/j.biomaterials.2009.02.034.
[67] M. Juenet, R. Aid-Launais, B. Li, A. Berger, J. Aerts, V. Ollivier, A. Nicoletti, D. Letourneur, C. Chauvierre, Thrombolytic therapy based on fucoidan-functionalized polymer nanoparticles targeting P-selectin, Biomaterials 156 (2018) 204–216, https://doi.org/10.1016/j.biomaterials.2017.11.047.
[68] J.R. McCarthy, I.Y. Sazonova, S.S. Erdem, T. Hara, B.D. Thompson, P. Patel, I. Botnaru, C.P. Lin, G.L. Reed, R. Weissleder, F.A. Jaffer, Multifunctional nanoagent for thrombus-targeted fibrinolytic therapy, Nanomedicine 7 (2012) 1017–1028, https://doi.org/10.2217/nnm.11.179.
[69] J. Zhou, D. Guo, Y. Zhang, W. Wu, H. Ran, Z. Wang, Construction and evaluation of Fe3O4-based PLGA nanoparticles carrying rtPA used in the detection of thrombosis and in targeted thrombolysis, ACS Appl. Mater. Interfaces 6 (2014) 5566–5576, https://doi.org/10.1021/am406008k.
[70] S.D. Tiukinhoy-Laing, S. Huang, M. Klegerman, C.K. Holland, D.D. McPherson, Ultrasound-facilitated thrombolysis using tissue-plasminogen activator-loaded echogenic liposomes, Thromb. Res. 119 (2007) 777–784, https://doi.org/10.1016/j.thromres.2006.06.009.
[71] L. Ma, Y. Wang, S. Zhang, X. Qian, N. Xue, Z. Jiang, O. Akakuru, J. Li, Y. Xu, A. Wu, Deep penetration of targeted nanobubbles enhanced cavitation effect on thrombolytic capacity, Bioconjugate Chem. 31 (2020) 369–374, https://doi.org/10.1021/acs.bioconjchem.9b00653.
[72] N. Korin, M. Kanapathipillai, B.D. Matthews, M. Crescente, A. Brill, T. Mammoto, K. Ghosh, S. Jurek, S.A. Bencherif, D. Bhatta, A.U. Coskun, C.L. Feldman, D. D. Wagner, D.E. Ingber, Shear-activated nanotherapeutics for drug targeting to obstructed blood vessels, Science 337 (2012) 738–742, https://doi.org/10.1126/science.1217815.
[73] Y. Uesugi, H. Kawata, Y. Saito, Y. Tabata, Ultrasound-responsive thrombus treatment with zinc-stabilized gelatin nano-complexes of tissue-type plasminogen activator, J. Drug Target. 20 (2012) 224–234, https://doi.org/10.3109/1061186X.2011.633259.
[74] S.T. Gunawan, K. Kempe, T. Bonnard, J. Cui, K. Alt, L.S. Law, X. Wang, E. Westein, G.K. Such, K. Peter, C.E. Hagemeyer, F. Caruso, Multifunctional thrombin-activatable polymer capsules for specific targeting to activated platelets, Adv. Mater. 27 (2015) 5153–5157, https://doi.org/10.1002/adma.201502243.
[75] E. Voros, M. Cho, M. Ramirez, A.L. Palange, E. De Rosa, J. Key, Z. Garami, A. B. Lumsden, P. Decuzzi, TPA immobilization on iron oxide nanocubes and localized magnetic hyperthermia accelerate blood clot lysis, Adv. Funct. Mater. 25 (2015) 1709–1718, https://doi.org/10.1002/adfm.201404354.
[76] J. Xu, Y. Zhang, J. Xu, G. Liu, C. Di, X. Zhao, X. Li, Y. Li, N. Pang, C. Yang, Y. Li, B. Li, Z. Lu, M. Wang, K. Dai, R. Yan, S. Li, G. Nie, Engineered nanoplatelets for targeted delivery of plasminogen activators to reverse thrombus in multiple mouse thrombosis models, Adv. Mater. 1905145 (2019) 1–14, https://doi.org/10.1002/adma.201905145.
[77] U. Bulbake, S. Doppalapudi, N. Kommineni, W. Khan, Liposomal formulations in clinical use: an updated review, Pharmaceutics 9 (2017) 1–33, https://doi.org/10.3390/pharmaceutics9020012.
[78] S. Mallick, J.S. Choi, Liposomes: versatile and biocompatible nanovesicles for efficient biomolecules delivery, J. Nanosci. Nanotechnol. 14 (2014) 755–765, https://doi.org/10.1166/jnn.2014.9080.
[79] K. Bowey, J.F. Tanguay, M. Tabrizian, Liposome technology for cardiovascular disease treatment and diagnosis, Expet Opin. Drug Deliv. 9 (2012) 249–265, https://doi.org/10.1517/17425247.2012.647908.
[80] J. Jamasbi, K. Ayabe, S. Goto, B. Nieswandt, K. Peter, W. Siess, Platelet receptors as therapeutic targets: past, present and future, Thromb. Haemostasis 117 (2017) 1249–1257, https://doi.org/10.1160/TH16-12-0911.
[81] S. Koudelka, R. Mikulik, J. Mašek, M. Raška, P. Turánek Knotigová, A.D. Miller, J. Turánek, Liposomal nanocarriers for plasminogen activators, J. Contr. Release 227 (2016) 45–57, https://doi.org/10.1016/j.jconrel.2016.02.019.
[82] B. Vaidya, G.P. Agrawal, S.P. Vyas, Platelets directed liposomes for the delivery of streptokinase: development and characterization, Eur. J. Pharmaceut. Sci. 44 (2011) 589–594, https://doi.org/10.1016/j.ejps.2011.10.004.
[83] Y. Huang, L. Yu, J. Ren, B. Gu, C. Longstaff, A.D. Hughes, S.A. Thom, X.Y. Xu, R. Chen, An activated-platelet-sensitive nanocarrier enables targeted delivery of tissue plasminogen activator for effective thrombolytic therapy, J. Contr. Release 300 (2019) 1–12, https://doi.org/10.1016/j.jconrel.2019.02.033.
[84] D. Varon, E. Shai, Platelets and their microparticles as key players in pathophysiological responses, J. Thromb. Haemostasis 13 (2015) S40–S46, https://doi.org/10.1111/jth.12976.
[85] H.-L. Hsu, J.-P. Chen, Preparation of thermosensitive magnetic liposome encapsulated recombinant tissue plasminogen activator for targeted thrombolysis, J. Magn. Magn Mater. 427 (2017) 188–194, https://doi.org/10.1016/j.jmmm.2016.10.122.
[86] P. Ghasemiyeh, S. Mohammadi-Samani, Solid lipid nanoparticles and nanostructured lipid carriers as novel drug delivery systems: applications, advantages and disadvantages, Res. Pharm. Sci. 13 (2018) 288–303, https://doi.org/10.4103/1735-5362.235156.
[87] J.N. Marsh, G. Hu, M.J. Scott, H. Zhang, M.J. Goette, J. Patrick, S.D. Caruthers, S. A. Wickline, D. Abendschein, M. Gregory, A fibrin-specific thrombolytic nanomedicine approach to acute ischemic stroke, Nanomedicine 6 (2011) 605–615, https://doi.org/10.2217/nnm.11.21.A.
[88] A. Bolhassani, S. Javanzad, T. Saleh, M. Hashemi, M.R. Aghasadeghi, Polymeric nanoparticles. Potent vectors for vaccine delivery targeting cancer and infectious diseases, Hum. Vaccines Immunother. 10 (2014) 321–332, https://doi.org/10.4161/hv.26796.
[89] Y. Zhang, T. Sun, C. Jiang, Biomacromolecules as carriers in drug delivery and tissue engineering, Acta Pharm. Sin. B. 8 (2018) 34–50, https://doi.org/10.1016/j.apsb.2017.11.005.
[90] K.S. Soppimath, T.M. Aminabhavi, A.R. Kulkarni, W.E. Rudzinski, Biodegradable polymeric nanoparticles as drug delivery devices, J. Contr. Release 70 (2001) 1–20, https://doi.org/10.1016/S0168-3659(00)00339-4.
[91] J. Zhang, W. Xia, P. Liu, Q. Cheng, T. Tahirou, W. Gu, B. Li, Chitosan modification and pharmaceutical/biomedical applications, Mar. Drugs 8 (2010) 1962–1987, https://doi.org/10.3390/md8071962.
[92] H.J. Jin, H. Zhang, M.L. Sun, B.G. Zhang, J.W. Zhang, Urokinase-coated chitosan nanoparticles for thrombolytic therapy: preparation and pharmacodynamics in vivo, J. Thromb. Thrombolysis 36 (2013) 458–468, https://doi.org/10.1007/s11239-013-0951-7.
[93] H. Baharifar, G. Tavoosidana, R. Karimi, S.A. Bidgoli, H. Ghanbari, M. A. Faramarzi, A. Amani, Optimization of self-assembled chitosan/streptokinase nanoparticles and evaluation of their cytotoxicity and thrombolytic activity, J. Nanosci. Nanotechnol. 15 (2015) 10127–10133, https://doi.org/10.1166/jnn.2015.11696.
[94] M. Shamsi, P. Zahedi, On-chip preparation of streptokinase entrapped in chitosan nanoparticles used in thrombolytic therapy potentially, J. Pharmacol. Sci. 106 (2017) 3623–3630, https://doi.org/10.1016/j.xphs.2017.08.001.
[95] J. Liao, X. Ren, B. Yang, H. Li, Y. Zhang, Z. Yin, Targeted thrombolysis by using c-RGD-modified N,N,N-Trimethyl Chitosan nanoparticles loaded with

lumbrokinase, Drug Dev. Ind. Pharm. 45 (2019) 88–95, https://doi.org/10.1080/03639045.2018.1522324.
[96] Y. Teng, H. Jin, D. Nan, M. Li, C. Fan, Y. Liu, P. Lv, W. Cui, Y. Sun, H. Hao, X. Qu, Z. Yang, Y. Huang, In vivo evaluation of urokinase-loaded hollow nanogels for sonothrombolysis on suture embolization-induced acute ischemic stroke rat model, Bioact. Mater. 3 (2018) 102–109, https://doi.org/10.1016/j.bioactmat.2017.08.001.
[97] R. Yasmin, M. Shah, S.A. Khan, R. Ali, Gelatin nanoparticles: a potential candidate for medical applications, Nanotechnol. Rev. 6 (2017) 191–207, https://doi.org/10.1515/ntrev-2016-0009.
[98] Y. Uesugi, H. Kawata, J.I. Jo, Y. Saito, Y. Tabata, An ultrasound-responsive nano delivery system of tissue-type plasminogen activator for thrombolytic therapy, J. Contr. Release 147 (2010) 269–277, https://doi.org/10.1016/j.jconrel.2010.07.127.
[99] C. Englert, J.C. Brendel, T.C. Majdanski, T. Yildirim, S. Schubert, M. Gottschaldt, N. Windhab, U.S. Schubert, Pharmapolymers in the 21st century: synthetic polymers in drug delivery applications, Prog. Polym. Sci. 87 (2018) 107–164, https://doi.org/10.1016/j.progpolymsci.2018.07.005.
[100] B. Sivaraman, A. Sylvester, A. Ramamurthi, Fibrinolytic PLGA nanoparticles for slow clot lysis within abdominal aortic aneurysms attenuate proteolytic loss of vascular elastic matrix, Mater. Sci. Eng. C-Materials Biol. Appl. 59 (2016) 145–156, https://doi.org/10.1016/j.msec.2015.09.056.
[101] M. Colasuonno, A.L. Palange, R. Aid, M. Ferreira, H. Mollica, R. Palomba, M. Emdin, M. Del Sette, C. Chauvierre, D. Letourneur, P. Decuzzi, Erythrocyte-inspired discoidal polymeric nanoconstructs carrying tissue plasminogen activator for the enhanced lysis of blood clots, ACS Nano 12 (2018) 12224–12237, https://doi.org/10.1021/acsnano.8b06021.
[102] C. Vauthier, C. Dubernet, E. Fattal, H. Pinto-Alphandary, P. Couvreur, Poly (alkylcyanoacrylates) as biodegradable materials for biomedical applications, Adv. Drug Deliv. Rev. 55 (2003) 519–548, https://doi.org/10.1016/S0169-409X(03)00041-3.
[103] L. Chollet, P. Saboural, C. Chauvierre, J.-N. Villemin, D. Letourneur, F. Chaubet, Fucoidans in Nanomedicine, Mar. Drugs. 14 (2016) 1–24, https://doi.org/10.3390/md14080145.
[104] T. Bonnard, J.-M. Serfaty, C. Journé, B. Ho Tin Noe, D. Arnaud, L. Louedec, M. Derkaoui, D. Letourneur, C. Chauvierre, C. Le Visage, Leukocyte mimetic polysaccharide microparticles tracked in vivo on activated endothelium and in abdominal aortic aneurysm, Acta Biomater. 10 (2014) 3535–3545, https://doi.org/10.1016/j.actbio.2014.04.015.
[105] B. Li, M. Juenet, R. Aid-Launais, M. Maire, V. Ollivier, D. Letourneur, C. Chauvierre, Development of polymer microcapsules functionalized with fucoidan to target P-selectin overexpressed in cardiovascular diseases, Adv. Healthc. Mater. 6 (2017) 1–11, https://doi.org/10.1002/adhm.201601200.
[106] H.R. Lijnen, B. Van Hoef, V. Beelen, D. Collen, Characterization of the murine plasma fibrinolytic system, Eur. J. Biochem. 224 (1994) 863–871, https://doi.org/10.1111/j.1432-1033.1994.00863.x.
[107] C. Englert, J.C. Brendel, T.C. Majdanski, T. Yildirim, S. Schubert, M. Gottschaldt, N. Windhab, U.S. Schubert, Pharmapolymers in the 21st century: synthetic polymers in drug delivery applications, Prog. Polym. Sci. 87 (2018) 107–164, https://doi.org/10.1016/j.progpolymsci.2018.07.005.
[108] J. Deng, H. Mei, W. Shi, Z.-Q. Pang, B. Zhang, T. Guo, H.-F. Wang, X.-G. Jiang, Y. Hu, Recombinant tissue plasminogen activator-conjugated nanoparticles effectively targets thrombolysis in a rat model of middle cerebral artery occlusion, Curr. Med. Sci. 38 (2018) 427–435, https://doi.org/10.1007/s11596-018-1896-z.
[109] Y. Pan, X. Wang, Z. Yin, Synthesis and evaluation of cationic polymeric micelles as carriers of lumbrokinase for targeted thrombolysis, Asian J. Pharm. Sci. 14 (2019) 144–153, https://doi.org/10.1016/j.ajps.2018.03.004.
[110] Y. Pan, X. Ren, S. Wang, X. Li, X. Luo, Z. Yin, Annexin V-conjugated mixed micelles as a potential drug delivery system for targeted thrombolysis, Biomacromolecules 18 (2017) 865–876, https://doi.org/10.1021/acs.biomac.6b01756.
[111] J.F. Tait, M.D. Cerqueira, T.A. Dewhurst, K. Fujikawa, J.L. Ritchie, J.R. Stratton, Evaluation of annexin V as a platelet-directed thrombus targeting agent, Thromb. Res. 75 (1994) 491–501, https://doi.org/10.1016/0049-3848(94)90224-0.
[112] L.I. Mukhametova, R.B. Aisina, E.M. Zakharyan, E.A. Karakhanov, K. B. Gershkovich, S.D. Varfolomeyev, Thrombolytic and fibrinogenolytic properties of bioconjugate streptokinase-polyamidoamine dendrimers in vitro, Thromb. Res. 154 (2017) 50–52, https://doi.org/10.1016/j.thromres.2017.04.008.
[113] M. Labieniec-Watala, C. Watala, PAMAM dendrimers: destined for success or doomed to fail? Plain and modified PAMAM dendrimers in the context of biomedical applications, J. Pharmacol. Sci. 104 (2015) 2–14, https://doi.org/10.1002/jps.24222.
[114] L.W.E. Starmans, D. Burdinski, N.P.M. Haex, R.P.M. Moonen, G.J. Strijkers, K. Nicolay, H. Grüll, Iron oxide nanoparticle-micelles (ION-micelles) for sensitive (molecular) magnetic particle imaging and magnetic resonance imaging, PloS One 8 (2013) 1–9, https://doi.org/10.1371/journal.pone.0057335.
[115] R. Cheng, W. Huang, L. Huang, B. Yang, L. Mao, K. Jin, Q. Zhuge, Y. Zhao, Acceleration of tissue plasminogen activator-mediated thrombolysis by magnetically powered nanomotors, ACS Nano 8 (2014) 7746–7754, https://doi.org/10.1021/nn5029955.
[116] H. Kempe, M. Kempe, The use of magnetite nanoparticles for implant-assisted magnetic drug targeting in thrombolytic therapy, Biomaterials 31 (2010) 9499–9510, https://doi.org/10.1016/j.biomaterials.2010.07.107.
[117] J.P. Chen, P.C. Yang, Y.H. Ma, S.J. Tu, Y.J. Lu, Targeted delivery of tissue plasminogen activator by binding to silica-coated magnetic nanoparticle, Int. J. Nanomed. 7 (2012) 5137–5149, https://doi.org/10.2147/IJN.S36197.
[118] M. Wang, J. Zhang, Z. Yuan, W. Yang, Q. Wu, H. Gu, Targeted thrombolysis by using of magnetic mesoporous silica nanoparticles, J. Biomed. Nanotechnol. 8 (2012) 624–632, https://doi.org/10.1166/jbn.2012.1416.
[119] B.L. Razzaboni, P. Bolsaitis, Evidence of an oxidative mechanism for the hemolytic activity of silica particles, Environ. Health Perspect. 87 (1990) 337–341, https://doi.org/10.1289/ehp.9087337.
[120] V. Murashov, M. Harper, E. Demchuk, Impact of silanol surface density on the toxicity of silica aerosols measured by erythrocyte haemolysis, J. Occup. Environ. Hyg. 3 (2006) 718–723, https://doi.org/10.1080/15459620601015950.
[121] T. Wu, M. Tang, Review of the effects of manufactured nanoparticles on mammalian target organs, J. Appl. Toxicol. 38 (2018) 25–40, https://doi.org/10.1002/jat.3499.
[122] J.P. Chen, P.C. Yang, Y.H. Ma, Y.J. Lu, Superparamagnetic iron oxide nanoparticles for delivery of tissue plasminogen activator, J. Nanosci. Nanotechnol. (2011) 11089–11094, https://doi.org/10.1166/jnn.2011.3953.
[123] J.P. Chen, C.H. Liu, H.L. Hsu, T. Wu, Y.J. Lu, Y.H. Ma, Magnetically controlled release of recombinant tissue plasminogen activator from chitosan nanocomposites for targeted thrombolysis, J. Mater. Chem. B. 4 (2016) 2578–2590, https://doi.org/10.1039/c5tb02579f.
[124] S. Heid, H. Unterweger, R. Tietze, R.P. Friedrich, B. Weigel, I. Cicha, D. Eberbeck, A.R. Boccaccini, C. Alexiou, S. Lyer, Synthesis and characterization of tissue plasminogen activator-functionalized superparamagnetic iron oxide nanoparticles for targeted fibrin clot dissolution, Int. J. Mol. Sci. 18 (2017), https://doi.org/10.3390/ijms18091837.
[125] M. Chang, Y.H. Lin, J.L. Gabayno, Q. Li, X. Liu, Thrombolysis based on magnetically-controlled surface-functionalized Fe3O4 nanoparticle, Bioengineered 8 (2017) 29–35, https://doi.org/10.1080/21655979.2016.1227145.
[126] A.Y. Prilepskii, A.F. Fakhardo, A.S. Drozdov, V.V. Vinogradov, I.P. Dudanov, A. A. Shtil, P.P. Bel'Tyukov, A.M. Shibeko, E.M. Koltsova, D.Y. Nechipurenko, V. V. Vinogradov, Urokinase-conjugated magnetite nanoparticles as a promising drug delivery system for targeted thrombolysis: synthesis and preclinical evaluation, ACS Appl. Mater. Interfaces 10 (2018) 36764–36775, https://doi.org/10.1021/acsami.8b14790.
[127] L. Huang, J. Wang, S. Huang, F. Siaw-Debrah, M. Nyanzu, Q. Zhuge, Polyacrylic acid-coated nanoparticles loaded with recombinant tissue plasminogen activator for the treatment of mice with ischemic stroke, Biochem. Biophys. Res. Commun. 516 (2019) 565–570, https://doi.org/10.1016/j.bbrc.2019.06.079.
[128] R.P. Friedrich, J. Zaloga, E. Schreiber, I.Y. Tóth, E. Tombácz, S. Lyer, C. Alexiou, Tissue plasminogen activator binding to superparamagnetic iron oxide nanoparticle-covalent versus adsorptive approach, Nanoscale Res. Lett. 11 (2016) 1, https://doi.org/10.1186/s11671-016-1521-7.
[129] H.W. Yang, M.Y. Hua, K.J. Lin, S.P. Wey, R.Y. Tsai, S.Y. Wu, Y.C. Lu, H.L. Liu, T. Wu, Y.H. Ma, Bioconjugation of recombinant tissue plasminogen activator to magnetic nanocarriers for targeted thrombolysis, Int. J. Nanomed. 7 (2012) 5159–5173, https://doi.org/10.2147/IJN.S32939.
[130] J.B. Vines, J.H. Yoon, N.E. Ryu, D.J. Lim, H. Park, Gold nanoparticles for photothermal cancer therapy, Front. Chem. 7 (2019) 1–16, https://doi.org/10.3389/fchem.2019.00167.
[131] D.E. Kim, J.Y. Kim, D. Schellingerhout, J.H. Ryu, S.K. Lee, S. Jeon, J.S. Lee, J. Kim, H.J. Jang, J.E. Park, E.J. Kim, I.C. Kwon, C.H. Ahn, M. Nahrendorf, K. Kim, Quantitative imaging of cerebral thromboemboli in vivo: the effects of tissue-type plasminogen activator, Stroke 48 (2017) 1376–1385, https://doi.org/10.1161/STROKEAHA.117.016511.
[132] S.P. Kwon, S. Jeon, S.H. Lee, H.Y. Yoon, J.H. Ryu, D. Choi, J.Y. Kim, J. Kim, J. H. Park, D.E. Kim, I.C. Kwon, K. Kim, C.H. Ahn, Thrombin-activatable fluorescent peptide incorporated gold nanoparticles for dual optical/computed tomography thrombus imaging, Biomaterials 150 (2018) 125–136, https://doi.org/10.1016/j.biomaterials.2017.10.017.
[133] A. Parodi, R. Molinaro, M. Sushnitha, M. Evangelopoulos, J.O. Martinez, N. Arrighetti, C. Corbo, E. Tasciotti, Bio-inspired engineering of cell- and virus-like nanoparticles for drug delivery, Biomaterials 147 (2017) 155–168, https://doi.org/10.1016/j.biomaterials.2017.09.020.
[134] S. Absar, Y.M. Kwon, F. Ahsan, Bio-responsive delivery of tissue plasminogen activator for localized thrombolysis, J. Contr. Release 177 (2014) 42–50, https://doi.org/10.1016/j.jconrel.2013.12.036.
[135] R.A. Petros, J.M. Desimone, Strategies in the design of nanoparticles for therapeutic applications, Nat. Rev. Drug Discov. 9 (2010) 615–627, https://doi.org/10.1038/nrd2591.
[136] R. Vankayala, S.R. Corber, J.T. Mac, M.P. Rao, M. Shafie, B. Anvari, Erythrocyte-derived nanoparticles as a theranostic agent for near-infrared fluorescence imaging and thrombolysis of blood clots, Macromol. Biosci. 18 (2018), https://doi.org/10.1002/mabi.201700379, 1700379–1700379.
[137] S. Nozohouri, A.E. Sifat, B. Vaidya, T.J. Abbruscato, Novel approaches for the delivery of therapeutics in ischemic stroke, Drug Discov. Today 25 (2020) 535–551, https://doi.org/10.1016/j.drudis.2020.01.007.
[138] J. Xu, X. Wang, H. Yin, X. Cao, Q. Hu, W. Lv, Q. Xu, Z. Gu, H. Xin, Sequentially site-specific delivery of thrombolytics and neuroprotectant for enhanced treatment of ischemic stroke, ACS Nano 13 (2019) 8577–8588, https://doi.org/10.1021/acsnano.9b01798.
[139] G. Camussi, M.C. Deregibus, S. Bruno, V. Cantaluppi, L. Biancone, Exosomes/microvesicles as a mechanism of cell-to-cell communication, Kidney Int. 78 (2010) 838–848, https://doi.org/10.1038/ki.2010.278.
[140] A.K.A. Silva, N. Luciani, F. Gazeau, K. Aubertin, S. Bonneau, C. Chauvierre, D. Letourneur, C. Wilhelm, Combining magnetic nanoparticles with cell derived

microvesicles for drug loading and targeting, Nanomed. Nanotechnol. Biol. Med. 11 (2015) 645–655, https://doi.org/10.1016/j.nano.2014.11.009.
[141] Y. Zhong, W.J. Gong, X.H. Gao, Y.N. Li, K. Liu, Y.G. Hu, J.S. Qi, Synthesis and evaluation of a novel nanoparticle carrying urokinase used in targeted thrombolysis, J. Biomed. Mater. Res. 108 (2019) 193–200, https://doi.org/10.1002/jbm.a.36803.
[142] K.J. Koudelka, A.S. Pitek, M. Manchester, N.F. Steinmetz, Virus-based nanoparticles as versatile nanomachines, Annu Rev Virol 2 (2015) 379–401, https://doi.org/10.1146/annurev-virology-100114-055141.
[143] A.S. Pitek, J. Park, Y. Wang, H. Gao, H. Hu, D.I. Simon, N.F. Steinmetz, Delivery of thrombolytic therapy using rod-shaped plant viral nanoparticles decreases the risk of hemorrhage, Nanoscale 10 (2018) 16547–16555, https://doi.org/10.1039/c8nr02861c.
[144] J.W. Yoo, D.J. Irvine, D.E. Discher, S. Mitragotri, Bio-inspired, bioengineered and biomimetic drug delivery carriers, Nat. Rev. Drug Discov. 10 (2011) 521–535, https://doi.org/10.1038/nrd3499.
[145] E.C. Unger, T. Porter, W. Culp, R. Labell, T. Matsunaga, R. Zutshi, Therapeutic applications of lipid-coated microbubbles, Adv. Drug Deliv. Rev. 56 (2004) 1291–1314, https://doi.org/10.1016/j.addr.2003.12.006.
[146] B. Li, R. Aid-Launais, M.N. Labour, A. Zenych, M. Juenet, C. Choqueux, V. Ollivier, O. Couture, D. Letourneur, C. Chauvierre, Functionalized polymer microbubbles as new molecular ultrasound contrast agent to target P-selectin in thrombus, Biomaterials 194 (2019) 139–150, https://doi.org/10.1016/j.biomaterials.2018.12.023.
[147] C.M. Moran, Ultrasonic contrast agents, Clin. Ultrasound. 1 (2011) 77–89, https://doi.org/10.1016/B978-0-7020-3131-1.00006-7.
[148] K.B. Bader, G. Bouchoux, C.K. Holland, Sonothrombolysis (2016), https://doi.org/10.1007/978-3-319-22536-4_19.
[149] Y. Sawaguchi, Z. Wang, Ultrasound acceleration of rt-PA thrombolysis depends on acoustic intensity, Biol. Pharm. Bull. 40 (2017) 97–103, https://doi.org/10.1248/bpb.b16-00702.
[150] A. Goyal, F.T.H. Yu, M.G. Tenwalde, X. Chen, A. Althouse, F.S. Villanueva, J. J. Pacella, Inertial cavitation ultrasound with microbubbles improves reperfusion efficacy when combined with tissue plasminogen activator in an in vitro model of microvascular obstruction, Ultrasound Med. Biol. 43 (2017) 1391–1400, https://doi.org/10.1016/j.ultrasmedbio.2017.02.013.
[151] T.R. Porter, The utilization of ultrasound and microbubbles for therapy in acute coronary syndromes, Cardiovasc, Res. 83 (2009) 636–642, https://doi.org/10.1093/cvr/cvp206.
[152] A. Agarwal, W.J. Ng, Y. Liu, Principle and applications of microbubble and nanobubble technology for water treatment, Chemosphere 84 (2011) 1175–1180, https://doi.org/10.1016/j.chemosphere.2011.05.054.
[153] K. Tachibana, S. Tachibana, Albumin microbubble echo-contrast material as an enhancer for ultrasound accelerated thrombolysis, Circulation 92 (1995) 1148–1150, https://doi.org/10.1161/01.CIR.92.5.1148.
[154] K.B. Bader, G. Bouchoux, T. Peng, M.E. Klegerman, D.D. McPherson, C. K. Holland, Thrombolytic efficacy and enzymatic activity of rt-PA-loaded echogenic liposomes, J. Thromb. Thrombolysis 40 (2015) 144–155, https://doi.org/10.1007/s11239-015-1204-8.
[155] H. Shekhar, K.B. Bader, S. Huang, T. Peng, S. Huang, D.D. McPherson, C. K. Holland, In vitro thrombolytic efficacy of echogenic liposomes loaded with tissue plasminogen activator and octafluoropropane gas, Phys. Med. Biol. 62 (2017) 517–538, https://doi.org/10.1088/1361-6560/62/2/517.
[156] S.T. Laing, M.R. Moody, H. Kim, B. Smulevitz, S.L. Huang, C.K. Holland, D. D. McPherson, M.E. Klegerman, Thrombolytic efficacy of tissue plasminogen activator-loaded echogenic liposomes in a rabbit thrombus model, Thromb. Res. 130 (2012) 629–635, https://doi.org/10.1016/j.thromres.2011.11.010.
[157] S.T. Laing, M. Moody, B. Smulevitz, H. Kim, P. Kee, S. Huang, C.K. Holland, D. D. McPherson, Ultrasound-enhanced thrombolytic effect of tissue plasminogen activator-loaded echogenic liposomes in an in vivo rabbit aorta thrombus model-brief report, Arterioscler. Thromb. Vasc. Biol. 31 (2011) 1357–1359, https://doi.org/10.1161/ATVBAHA.111.225938.
[158] M.A. Kandadai, P. Mukherjee, H. Shekhar, G.J. Shaw, I. Papautsky, C.K. Holland, Microfluidic manufacture of rt-PA -loaded echogenic liposomes, Biomed, Microdevices 18 (2016) 1–21, https://doi.org/10.1007/s10544-016-0072-0.
[159] W.C. Yan, Q.W. Chua, X.J. Ong, V.K. Sharma, Y.W. Tong, C.H. Wang, Fabrication of ultrasound-responsive microbubbles via coaxial electrohydrodynamic atomization for triggered release of tPA, J. Colloid Interface Sci. 501 (2017) 282–293, https://doi.org/10.1016/j.jcis.2017.04.073.
[160] D. Susan, Tiukinhoy-Laing, Ultrasound-facilitated thrombolysis using tissue-plasminogen activator-loaded echogenic liposomes, Bone 23 (2011) 1–7, https://doi.org/10.1161/CIRCULATIONAHA.110.956839.
[161] J.M. Correas, L. Bridal, A. Lesavre, A. Méjean, M. Claudon, O. Hélénon, Ultrasound contrast agents: properties, principles of action, tolerance, and artifacts, Eur. Radiol. 11 (2001) 1316–1328, https://doi.org/10.1007/s003300100940.
[162] T. Şen, O. Tüfekçioğlu, Y. Koza, Mechanical index, Anadolu Kardiyol. Derg. 15 (2015) 334–336, https://doi.org/10.5152/akd.2015.6061.
[163] Y. Zhu, L. Guan, Y. Mu, Combined low-frequency ultrasound and urokinase-containing microbubbles in treatment of femoral artery thrombosis in a rabbit model, PloS One 11 (2016) 1–13, https://doi.org/10.1371/journal.pone.0168909.
[164] X. Hua, L. Zhou, P. Liu, Y. He, K. Tan, Q. Chen, Y. Gao, Y. Gao, In vivo thrombolysis with targeted microbubbles loading tissue plasminogen activator in a rabbit femoral artery thrombus model, J. Thromb. Thrombolysis 38 (2014) 57–64, https://doi.org/10.1007/s11239-014-1071-8.
[165] X. Hua, P. Liu, Y.H. Gao, K. Bin Tan, L.N. Zhou, Z. Liu, X. Li, S.W. Zhou, Y.J. Gao, Construction of thrombus-targeted microbubbles carrying tissue plasminogen activator and their in vitro thrombolysis efficacy: a primary research, J. Thromb. Thrombolysis 30 (2010) 29–35, https://doi.org/10.1007/s11239-010-0450-z.
[166] J.H. Nederhoed, H.P. Ebben, J. Slikkerveer, A.W.J. Hoksbergen, O. Kamp, G. J. Tangelder, W. Wisselink, R.J.P. Musters, K.K. Yeung, Intravenous targeted microbubbles carrying urokinase versus urokinase alone in acute peripheral arterial thrombosis in a porcine model, Ann. Vasc. Surg. 44 (2017) 400–407, https://doi.org/10.1016/j.avsg.2017.05.011.
[167] C. Correa-Paz, M.F. Navarro Poupard, E. Polo, M. Rodríguez-Pérez, P. Taboada, R. Iglesias-Rey, P. Hervella, T. Sobrino, D. Vivien, J. Castillo, P. del Pino, F. Campos, B. Pelaz, In vivo ultrasound-activated delivery of recombinant tissue plasminogen activator from the cavity of sub-micrometric capsules, J. Contr. Release 308 (2019) 162–171, https://doi.org/10.1016/j.jconrel.2019.07.017.
[168] X. Wang, Y. Gkanatsas, J. Palasubramaniam, J.D. Hohmann, Y.C. Chen, B. Lim, C. E. Hagemeyer, K. Peter, Thrombus-targeted theranostic microbubbles: a new technology towards concurrent rapid ultrasound diagnosis and bleeding-free fibrinolytic treatment of thrombosis, Theranostics 6 (2016) 726–738, https://doi.org/10.7150/thno.14514.
[169] M. de Saint Victor, L.C. Barnsley, D. Carugo, J. Owen, C.C. Coussios, E. Stride, Sonothrombolysis with magnetically targeted microbubbles, Ultrasound Med. Biol. 45 (2019) 1151–1163, https://doi.org/10.1016/j.ultrasmedbio.2018.12.014.
[170] L. Auboire, C.A. Sennoga, J.M. Hyvelin, F. Ossant, J.M. Escoffre, F. Tranquart, A. Bouakaz, Microbubbles combined with ultrasound therapy in ischemic stroke: a systematic review of in-vivo preclinical studies, PloS One 13 (2018) 1–19, https://doi.org/10.1371/journal.pone.0191788.
[171] C.A. Sennoga, E. Kanbar, L. Auboire, P.A. Dujardin, D. Fouan, J.M. Escoffre, A. Bouakaz, Microbubble-mediated ultrasound drug-delivery and therapeutic monitoring, Expet Opin. Drug Deliv. 14 (2017) 1031–1043, https://doi.org/10.1080/17425247.2017.1266328.
[172] A. Moumouh, L. Barentin, F. Tranquart, S. Serrierre, I. Bonnaud, J.P. Tasu, Fibrinolytic effects of transparietal ultrasound associated with intravenous infusion of an ultrasound contrast agent: study of a rat model of acute cerebral stroke, Ultrasound Med. Biol. 36 (2010) 51–57, https://doi.org/10.1016/j.ultrasmedbio.2009.06.1103.
[173] R. Chen, D.G. Paeng, K.H. Lam, Q. Zhou, K.K. Shung, N. Matsuoka, M. S. Humayun, In vivo sonothrombolysis of ear marginal vein of rabbits monitored with high-frequency ultrasound needle transducer, J. Med. Biol. Eng. 33 (2013) 103–110, https://doi.org/10.5405/jmbe.1219.
[174] A.D. Barreto, A.V. Alexandrov, L. Shen, A. Sisson, A.W. Bursaw, P. Sahota, H. Peng, M. Ardjomand-Hessabi, R. Pandurengan, M.H. Rahbar, K. Barlinn, H. Indupuru, N.R. Gonzales, S.I. Savitz, J.C. Grotta, Clotbust-hands free: pilot safety study of a novel operator-independent ultrasound device in patients with acute ischemic stroke, Stroke 44 (2013) 3376–3381, https://doi.org/10.1161/STROKEAHA.113.002713.
[175] Jonathan T. Sutton, et al., Clot retraction affects the extent of ultrasound-enhanced thrombolysis in an ex vivo porcine thrombosis model Jonathan, Ultrasound Med. Biol. 23 (2013) 1–7, https://doi.org/10.1038/jid.2014.371.
[176] H. Soo Choi, W. Liu, P. Misra, E. Tanaka, J.P. Zimmer, B. Itty Ipe, M.G. Bawendi, J. V Frangioni, Renal clearance of quantum dots, Nat. Biotechnol. 25 (2007) 1165–1170, https://doi.org/10.1038/nbt1340.
[177] A.E. Nel, L. Mädler, D. Velegol, T. Xia, E.M.V. Hoek, P. Somasundaran, F. Klaessig, V. Castranova, M. Thompson, Understanding biophysicochemical interactions at the nano-bio interface, Nat. Mater. 8 (2009) 543–557, https://doi.org/10.1038/nmat2442.
[178] F. Alexis, E. Pridgen, L.K. Molnar, O.C. Farokhzad, Factors affecting the clearance and biodistribution of polymeric nanoparticles, Mol. Pharm. 5 (2008) 505–515, https://doi.org/10.1021/mp800051m.
[179] Y. Geng, P. Dalhaimer, S. Cai, R. Tsai, M. Tewari, T. Minko, D.E. Discher, Shape effects of filaments versus spherical particles in flow and drug delivery, Nat. Nanotechnol. 2 (2007) 249–255, https://doi.org/10.1038/nnano.2007.70.
[180] L. Zhang, Z. Cao, Y. Li, J.-R. Ella-Menye, T. Bai, S. Jiang, Softer zwitterionic nanogels for longer circulation and lower splenic accumulation, ACS Nano 6 (2012) 6681–6686, https://doi.org/10.1021/nn301159a.
[181] R. Palomba, A.L. Palange, I.F. Rizzuti, M. Ferreira, A. Cervadoro, M.G. Barbato, C. Canale, P. Decuzzi, Modulating phagocytic cell sequestration by tailoring nanoconstruct softness, ACS Nano 12 (2018) 1433–1444, https://doi.org/10.1021/acsnano.7b07797.
[182] N.Y. Lotosh, S.O. Aliaseva, I.K. Malashenkova, G.M. Sorokoumova, R.G. Vasilov, A.A. Selischeva, Cationic liposomes cause ROS generation and release of neutrophil extracellular traps, Biochem. Suppl. Ser. A Membr. Cell Biol. 13 (2019) 40–49, https://doi.org/10.1134/S1990747818040074.
[183] T.L. Hwang, I.A. Aljuffali, C.F. Hung, C.H. Chen, J.Y. Fang, The impact of cationic solid lipid nanoparticles on human neutrophil activation and formation of neutrophil extracellular traps (NETs), Chem. Biol. Interact. 235 (2015) 106–114, https://doi.org/10.1016/j.cbi.2015.04.011.
[184] T.L. Hwang, I.A. Aljuffali, C.F. Lin, Y.T. Chang, J.Y. Fang, Cationic additives in nanosystems activate cytotoxicity and inflammatory response of human neutrophils: lipid nanoparticles versus polymeric nanoparticles, Int. J. Nanomed. 10 (2015) 371–385, https://doi.org/10.2147/IJN.S73017.
[185] K. Knop, R. Hoogenboom, D. Fischer, U.S. Schubert, Poly(ethylene glycol) in drug delivery: pros and cons as well as potential alternatives, Angew. Chem. Int. Ed. 49 (2010) 6288–6308, https://doi.org/10.1002/anie.200902672.
[186] P.L. Rodriguez, T. Harada, D.A. Christian, D.A. Pantano, R.K. Tsai, D.E. Discher, Minimal "self" peptides that inhibit phagocytic clearance and enhance delivery of

nanoparticles, Science 339 (2013) 971–975, https://doi.org/10.1126/science.1229568.
[187] J. Saikia, R. Mohammadpour, M. Yazdimamaghani, H. Northrup, V. Hlady, H. Ghandehari, Silica nanoparticle-endothelial interaction: uptake and effect on platelet adhesion under flow conditions, ACS Appl. Bio Mater. 1 (2018) 1620–1627, https://doi.org/10.1021/acsabm.8b00466.
[188] J. Duan, S. Liang, Y. Yu, Y. Li, L. Wang, Z. Wu, Y. Chen, M.R. Miller, Z. Sun, Inflammation–coagulation response and thrombotic effects induced by silica nanoparticles in zebrafish embryos, Nanotoxicology 12 (2018) 470–484, https://doi.org/10.1080/17435390.2018.1461267.
[189] J. Jose Corbalan, C. Medina, A. Jacoby, T. Malinski, M.W. Radomski, Amorphous silica nanoparticles aggregate human platelets: potential implications for vascular homeostasis, Int. J. Nanomed. 7 (2012) 631–639, https://doi.org/10.2147/IJN.S28293.
[190] X.D. Zhang, H.Y. Wu, D. Wu, Y.Y. Wang, J.H. Chang, Z. Bin Zhai, A.M. Meng, P. X. Liu, L.A. Zhang, F.Y. Fan, Toxicologic effects of gold nanoparticles in vivo by different administration routes, Int. J. Nanomed. 5 (2010) 771–781, https://doi.org/10.2147/IJN.S8428.
[191] L. Shang, K. Nienhaus, G.U. Nienhaus, Engineered nanoparticles interacting with cells: size matters, J. Nanobiotechnol. 12 (2014) 1, https://doi.org/10.1186/1477-3155-12-5.
[192] Y. Pan, S. Neuss, A. Leifert, M. Fischler, F. Wen, U. Simon, G. Schmid, W. Brandau, W. Jahnen-Dechent, Size-dependent cytotoxicity of gold nanoparticles, Small 3 (2007) 1941–1949, https://doi.org/10.1002/smll.200700378.
[193] Z. He, J. Liu, L. Du, The unexpected effect of PEGylated gold nanoparticles on the primary function of erythrocytes, Nanoscale 6 (2014) 9017–9024, https://doi.org/10.1039/c4nr01857e.
[194] J. Feng, H. Liu, K.K. Bhakoo, L. Lu, Z. Chen, A metabonomic analysis of organ specific response to USPIO administration, Biomaterials 32 (2011) 6558–6569, https://doi.org/10.1016/j.biomaterials.2011.05.035.
[195] C. Lasagna-Reeves, D. Gonzalez-Romero, M.A. Barria, I. Olmedo, A. Clos, V. M. Sadagopa Ramanujam, A. Urayama, L. Vergara, M.J. Kogan, C. Soto, Bioaccumulation and toxicity of gold nanoparticles after repeated administration in mice, Biochem. Biophys. Res. Commun. 393 (2010) 649–655, https://doi.org/10.1016/j.bbrc.2010.02.046.
[196] K. Andrieux, P. Couvreur, Polyalkylcyanoacrylate nanoparticles for delivery of drugs across the blood-brain barrier 1, Wiley Interdiscip Rev Nanomed Nanobiotechnol, 2009, pp. 463–474, https://doi.org/10.1002/wnan.5.
[197] N.J. Siddiqi, M.A.K. Abdelhalim, A.K. El-Ansary, A.S. Alhomida, W.Y. Ong, Identification of potential biomarkers of gold nanoparticle toxicity in rat brains, J. Neuroinflammation 9 (2012) 1–7, https://doi.org/10.1186/1742-2094-9-123.
[198] R. Brouns, P.P. De Deyn, The complexity of neurobiological processes in acute ischemic stroke, Clin. Neurol. Neurosurg. 111 (2009) 483–495, https://doi.org/10.1016/j.clineuro.2009.04.001.
[199] D. Vivien, M. Gauberti, A. Montagne, G. Defer, E. Touzé, Impact of tissue plasminogen activator on the neurovascular unit: from clinical data to experimental evidence, J. Cerebr. Blood Flow Metabol. 31 (2011) 2119–2134, https://doi.org/10.1038/jcbfm.2011.127.
[200] M. Bartneck, T. Ritz, H.A. Keul, M. Wambach, J. Bornemann, U. Gbureck, J. Ehling, T. Lammers, F. Heymann, N. Gassler, T. Lüdde, C. Trautwein, J. Groll, F. Tacke, Peptide-functionalized gold nanorods increase liver injury in hepatitis, ACS Nano 6 (2012) 8767–8777, https://doi.org/10.1021/nn302502u.
[201] C.H. Fu, T.L. Liu, F.Q. Tang, D. Chen, L.L. Li, H.Y. Liu, X.M. Li, Acute toxicity and oxidative damage induced by silica nanorattle in vivo, Chin. Sci. Bull. 57 (2012) 2525–2532, https://doi.org/10.1007/s11434-012-5187-y.
[202] H. Nishimori, M. Kondoh, K. Isoda, S. ichi Tsunoda, Y. Tsutsumi, K. Yagi, Histological analysis of 70-nm silica particles-induced chronic toxicity in mice, Eur. J. Pharm. Biopharm. 72 (2009) 626–629, https://doi.org/10.1016/j.ejpb.2009.03.007.
[203] D. Couto, M. Freitas, V.M. Costa, R.C. Chisté, A. Almeida, M.A. Lopez-Quintela, J. Rivas, P. Freitas, P. Silva, F. Carvalho, E. Fernandes, Biodistribution of polyacrylic acid-coated iron oxide nanoparticles is associated with proinflammatory activation and liver toxicity, J. Appl. Toxicol. 36 (2016) 1321–1331, https://doi.org/10.1002/jat.3323.
[204] B. Zhao, X.Q. Wang, X.Y. Wang, H. Zhang, W.B. Dai, J. Wang, Z.L. Zhong, H. N. Wu, Q. Zhang, Nanotoxicity comparison of four amphiphilic polymeric micelles with similar hydrophilic or hydrophobic structure, Part, Fibre Toxicol 10 (2013) 1–16, https://doi.org/10.1186/1743-8977-10-47.
[205] X. Li, A. Radomski, O.I. Corrigan, L. Tajber, F. De Sousa Menezes, S. Endter, C. Medina, M.W. Radomski, Platelet compatibility of PLGA, chitosan and PLGA-chitosan nanoparticles, Nanomedicine 4 (2009) 735–746, https://doi.org/10.2217/nnm.09.65.
[206] Y. Zhao, D. Sultan, Y. Liu, Biodistribution, excretion, and toxicity of nanoparticles. Theranostic Bionanomaterials, Elsevier Inc., 2019, pp. 27–53, https://doi.org/10.1016/B978-0-12-815341-3.00002-X.
[207] K.D. Grieger, I. Linkov, S.F. Hansen, A. Baun, Environmental risk analysis for nanomaterials: review and evaluation of frameworks, Nanotoxicology 6 (2012) 196–212, https://doi.org/10.3109/17435390.2011.569095.
[208] E. Sadauskas, G. Danscher, M. Stoltenberg, U. Vogel, A. Larsen, H. Wallin, Protracted elimination of gold nanoparticles from mouse liver, Nanomed. Nanotechnol. Biol. Med. 5 (2009) 162–169, https://doi.org/10.1016/j.nano.2008.11.002.
[209] J. Feng, H. Liu, L. Zhang, K. Bhakoo, L. Lu, An insight into the metabolic responses of ultra-small superparamagnetic particles of iron oxide using metabonomic analysis of biofluids, Nanotechnology 21 (2010) 395101, https://doi.org/10.1088/0957-4484/21/39/395101.
[210] Q. Ran, Y. Xiang, Y. Liu, L. Xiang, F. Li, X. Deng, Y. Xiao, L. Chen, L. Chen, Z. Li, Eryptosis indices as a novel predictive parameter for biocompatibility of Fe3O4 magnetic nanoparticles on erythrocytes, Sci. Rep. 5 (2015) 16209, https://doi.org/10.1038/srep16209.
[211] K. de la Harpe, P. Kondiah, Y. Choonara, T. Marimuthu, L. du Toit, V. Pillay, The hemocompatibility of nanoparticles: a review of cell–nanoparticle interactions and hemostasis, Cells 8 (2019) 1209, https://doi.org/10.3390/cells8101209.
[212] S. Vrignaud, J.P. Benoit, P. Saulnier, Strategies for the nanoencapsulation of hydrophilic molecules in polymer-based nanoparticles, Biomaterials 32 (2011) 8593–8604, https://doi.org/10.1016/j.biomaterials.2011.07.057.
[213] M. Di Marco, K.A. Razak, A.A. Aziz, C. Devaux, E. Borghi, L. Levy, C. Sadun, Overview of the main methods used to combine proteins with nanosystems : absorption, bioconjugation, and encapsulation, Int. J. Nanomed. 5 (2010) 37–49.
[214] L. Arnfast, C.G. Madsen, L. Jorgensen, S. Baldursdottir, Design and processing of nanogels as delivery systems for peptides and proteins, Ther. Deliv. 5 (2014) 691–708, https://doi.org/10.4155/tde.14.38.
[215] S.R. Van Tomme, W.E. Hennink, Biodegradable dextran hydrogels for protein delivery applications, Expet Rev. Med. Dev. 4 (2007) 147–164, https://doi.org/10.1586/17434440.4.2.147.
[216] X. Xiong, F. Zhao, M. Shi, H. Yang, Y. Liu, Polymeric microbubbles for ultrasonic molecular imaging and targeted therapeutics, J. Biomater. Sci. Polym. Ed. 22 (2011) 417–428, https://doi.org/10.1163/092050610X540440.
[217] B. Li, R. Aid-Launais, M.-N. Labour, A. Zenych, M. Juenet, C. Choqueux, V. Ollivier, O. Couture, D. Letourneur, C. Chauvierre, Functionalized polymer microbubbles as new molecular ultrasound contrast agent to target P-selectin in thrombus, Biomaterials 194 (2019) 139–150, https://doi.org/10.1016/j.biomaterials.2018.12.023.
[218] C. Chauvierre, R. Aid-Launais, J. Aerts, M. Maire, L. Chollet, L. Rolland, R. Bonaf, S. Rossi, S. Bussi, C. Cabella, D. Laszlo, T. Fülöp, J. Szebeni, Y. Chahid, K. H. Zheng, E.S.G. Stroes, D. Le Guludec, F. Rouzet, D. Letourneur, Pharmaceutical development and safety evaluation of a GMP-grade fucoidan for molecular diagnosis of cardiovascular diseases, Mar. Drugs 17 (2019) 1–17, https://doi.org/10.3390/md17120699.
[219] K.H. Zheng, Y. Kaiser, E. Poel, H. Verberne, J. Aerts, F. Rouzet, E. Stroes, D. Letourneur, C. Chauvierre, 99Mtc-Fucoidan as diagnostic agent for P-selectin imaging: first-in-human evaluation (phase I), Atherosclerosis 287 (2019) e143, https://doi.org/10.1016/j.atherosclerosis.2019.06.425.
[220] J.C. Antunes, L. Benarroch, F.C. Moraes, M. Juenet, M.S. Gross, M. Aubart, C. Boileau, G. Caligiuri, A. Nicoletti, V. Ollivier, F. Chaubet, D. Letourneur, C. Chauvierre, Core-shell polymer-based nanoparticles deliver miR-155-5p to endothelial cells, Mol. Ther. Nucleic Acids 17 (2019) 210–222, https://doi.org/10.1016/j.omtn.2019.05.016.
[221] B. Ovbiagele, C.S. Kidwell, S. Starkman, J.L. Saver, Potential role of neuroprotective agents in the treatment of patients with acute ischemic stroke, Curr. Treat. Options Neurol. 5 (2003) 367–375, https://doi.org/10.1007/s11940-003-0027-7.
[222] R. Goulay, M. Naveau, T. Gaberel, D. Vivien, J. Parcq, Optimized tPA: a non-neurotoxic fibrinolytic agent for the drainage of intracerebral hemorrhages, J. Cerebr. Blood Flow Metabol. 38 (2018) 1180–1189, https://doi.org/10.1177/0271678X17719180.
[223] J. Matuszak, P. Dörfler, S. Lyer, H. Unterweger, M. Juenet, C. Chauvierre, A. Alaarg, D. Franke, G. Almer, I. Texier, J.M. Metselaar, R. Prassl, C. Alexiou, H. Mangge, D. Letourneur, I. Cicha, Comparative analysis of nanosystems' effects on human endothelial and monocytic cell functions, Nanotoxicology 12 (2018) 957–974, https://doi.org/10.1080/17435390.2018.1502375.
[224] I. Cicha, C. Chauvierre, I. Texier, C. Cabella, J.M. Metselaar, J. Szebeni, L. Dézsi, C. Alexiou, F. Rouzet, G. Storm, E. Stroes, D. Bruce, N. MacRitchie, P. Maffia, D. Letourneur, From design to the clinic: practical guidelines for translating cardiovascular nanomedicine, Cardiovasc. Res. 114 (2018) 1714–1727, https://doi.org/10.1093/cvr/cvy219.
[225] C. Chauvierre, D. Letourneur, The European project NanoAthero to fight cardiovascular diseases using nanotechnologies, Nanomedicine 10 (2015) 3391–3400, https://doi.org/10.2217/nnm.15.170.
[226] K.H. Zheng, J. Schoormans, L.C.A. Stiekema, C. Calcagno, I. Cicha, C. Alexiou, G. J. Strijkers, A.J. Nederveen, E.S.G. Stroes, B.F. Coolen, Plaque permeability assessed with DCE-MRI associates with USPIO uptake in patients with peripheral artery disease, JACC Cardiovasc. Imaging 12 (2019) 2081–2083, https://doi.org/10.1016/j.jcmg.2019.04.014.
[227] F.M. van der Valk, D.F. van Wijk, M.E. Lobatto, H.J. Verberne, G. Storm, M.C. M. Willems, D.A. Legemate, A.J. Nederveen, C. Calcagno, V. Mani, S. Ramachandran, M.P.M. Paridaans, M.J. Otten, G.M. Dallinga-Thie, Z.A. Fayad, M. Nieuwdorp, D.M. Schulte, J.M. Metselaar, W.J.M. Mulder, E.S. Stroes, Prednisolone-containing liposomes accumulate in human atherosclerotic macrophages upon intravenous administration, Nanomed. Nanotechnol. Biol. Med. 11 (2015) 1039–1046, https://doi.org/10.1016/j.nano.2015.02.021.
[228] K.H. Zheng, F.M. van der Valk, L.P. Smits, M. Sandberg, J.L. Dasseux, R. Baron, R. Barbaras, C. Keyserling, B.F. Coolen, A.J. Nederveen, H.J. Verberne, T.E. Nell, D.J. Vugts, R. Duivenvoorden, Z.A. Fayad, W.J.M. Mulder, G.A.M.S. van Dongen, E.S.G. Stroes, HDL mimetic CER-001 targets atherosclerotic plaques in patients, Atherosclerosis 251 (2016) 381–388, https://doi.org/10.1016/j.atherosclerosis.2016.05.038.